NOVEL ROLES OF THROMBOSPONDIN-1 IN VASCULAR PHYSIOLOGY AND DISEASE

by

Eileen M Bauer

B.S., University of California Los Angeles, 1997

Submitted to the Graduate Faculty of

the Graduate School of Public Health in partial fulfillment

of the requirements for the degree of

Doctor of Philosophy

University of Pittsburgh

2010

UNIVERSITY OF PITTSBURGH

GRADUATE SCHOOL OF PUBLIC HEALTH

This dissertation was presented

by

Eileen Bauer

It was defended on

April 7, 2010

and approved by

Claudette M. St. Croix, PhD, Assistant Professor, Department of Environmental and Occupational Health, Graduate School of Public Health, University of Pittsburgh

Aaron Barchowsky, PhD, Associate Professor, Department of Environmental and Occupational Health, Graduate School of Public Health, University of Pittsburgh

Chris O'Donnell, PhD, Professor, Department of Medicine, School of Medicine, University of Pittsburgh

Bruce Pitt, PhD, Professor and Chair, Department of Environmental and Occupational Health, Graduate School of Public Health, University of Pittsburgh

Dissertation Advisor: Jeff S. Isenberg, MD MPH, Associate Professor, Vascular Medicine Institute, School of Medicine, University of Pittsburgh

NOVEL ROLES OF THROMBOSPONDIN-1 IN VASCULAR PHYSIOLOGY AND DISEASE

Eileen M Bauer, PhD

University of Pittsburgh, 2010

Heart disease is the leading cause of death nationwide, killing one of every four Americans in all communities. The health care costs associated with heart disease have been estimated to surpass 300 billion dollars in 2010. Various preventative risk factors have been identified like obesity, diabetes, cigarette smoking, and air pollution. Pulmonary hypertension (PH) is a common secondary pathogenesis associated with cardiovascular disease. Understanding its exact physiological mechanisms will allow for better treatment options and better ways of preventing the disease.

The importance of nitric oxide (NO) in biology was recognized in 1998 when the Nobel Prize in Physiology or Medicine was awarded for its discovery as a physiologic signaling molecule and was validated again in 1992 by naming it "the molecule of the year". NO, produced in the endothelium by the enzyme nitric oxide synthase (eNOS), is critical in maintaining blood pressure by functioning as vasodilator. Its lack in the vascular system leads to problems, like heart disease and PH. As a critical signaling molecule, NO is likely to be important in transducing the effects of a broad variety of environmental stimuli on vasomotor regulation and studying the regulation of NO's biosynthetic capacity is of great public health importance.

Recent studies demonstrate that the glycoprotein thrombospondin-1 (TSP1) influences vascular responses by interfering with the NO-mediated vasodilatory pathway at downstream

targets. We hypothesized that TSP1 directly modulates eNOS activity and, thus, endothelium-dependent relaxation of blood vessels. Further, we were interested in how the inhibitory effects of TSP1 on eNOS would translate in a disease setting, specifically PH. This study demonstrates TSP1's negative role in the protective NO-mediated vasodilatory pathway and establishes a clear role for TSP1 in the development of PH. Despite the advent of several new drugs for the treatment of PH mortality remains high. Importantly, these drugs aim at increasing NO's bioavailability. The studies described herein suggest that increased TSP1 expression may limit the efficacy of these drugs. A deeper understanding of the role of TSP1 in physiology and disease will open new avenues in our fight to prevent heart disease.

TABLE OF CONTENTS

LIST OF TABLES

LIST OF FIGURES

ACKNOWLEDGEMENTS

I would like to thank Dr. Claudette St. Croix and Dr. Jeff Isenberg for being wonderful mentors and for guiding me through my graduate studies. I have learned a lot from both of them and would not be the scientist I am today without their support. I am especially thankful for Dr. St. Croix's suggestion and encouragement to take the human physiology class in the neuroscience department. Though it was the hardest class I had ever taken, I loved it and will always be passionate about keeping my research focused on the organism as a whole. I would like to thank the rest of my committee, Dr. Aaron Barchowsky, Dr. Chris O' Donnell, and Dr. Bruce Pitt. Their suggestions and criticism have helped me to stay focused and get through my project. In addition, I would like to thank the many that I have bugged throughout the years for reagents and for advice.

All of this, however, would have been impossible without the unwavering support of my husband Mike and the never doubting belief of our three children, that this is what mothers do. Though Mike and I are enthusiastic scientists, we are foremost parents and did not want to jeopardize our children's well being by me chasing my dream. To do this Mike endured a crazy live-in nanny, working a shift schedule, and spending long nights with me studying for physiology exams. To my family I most humbly say: thank you.

ABBREVIATIONS

ACh	acetylcholine
Akt	protein kinase B
AMPK	AMP-activated kinase
BH_4	tetrahydrobiopterin
Ca^{2+}	calcium
CD36	cluster of differentiation 36
CD47	cluster of differentiation 47
CO	carbon monoxide
COPD	chronic obstructive pulmonary disease
cAMP	cyclic adenosine monophosphate
cGMP	guanosine 3',5'-cyclic monophosphate
DAG	diacylglycerol
EDRF	endothelium derived relaxing factor
EGF	epidermal growth factor
eNOS	endothelial nitric oxide synthase
FAD	flavin adenine dinucleotide
FDA	food and drug administration
Fe^{2+}	ferrous
Fe^{3+}	ferric
FMN	flavin mononucleotide
GPCR	G-protein coupled receptors
Hb	hemoglobin
H_2O_2	hydrogen peroxide
HO1	heme oxignase 1
H_2S	hydrogen sulfide
HSP90	Heat shock protein 90
HUVEC	human umbilical cord endothelial cells
IAP	integrin associated protein
i.p.	intraperitoneal
IP_3	Inositol trisphosphate
i.v.	intravenous

iNOS	inducible nitric oxide synthase
LV	left ventricle
MAP	mean arterial pressure
NADPH	nicotinamide adenine dinucleotide phosphate
nNOS	neuronal nitric oxide synthase
NO	nitric oxide
NOS1	neuronal nitric oxide synthase
NOS2	inducible nitric oxide synthase
NOS3	endothelial nitric oxide synthase
O_2^-	superoxide
PAH	pulmonary arterial hypertension
PASMC	pulmonary artery smooth muscle cells
PDE	phospho-diesterase
PE	phenylephrine
PGI_2	prostacyclins
PH	pulmonary hypertension
PI3K	Phosphoinositide 3-kinases
PIP2	phosphatidyl inositol 4, 5-bisphosphate
PKA	cyclic AMP-dependent protein kinase
PKC	protein kinase C
PKG	cGMP-dependent kinase
PLC	phospholipase C
RV	right ventricle
SIRPα	signal regulatory protein alpha
sGC	guanylate cyclase
SOD	superoxide dismutase
TSP1	thrombospondin 1
VEGF	vascular endothelial growth factor
VEGFR2	vascular endothelial growth factor receptor 2
VSMC	vascular smooth muscle cells

1.0 INTRODUCTION

1.1 THROMBOSPONDIN OVERVIEW

The thrombospondin family consists of five proteins, thrombospondin (I-V)[1]. All isoforms contain a common structural "signature piece". While thrombospondin 1 (TSP1) and thrombospondin 2 (TPS2) are trimeric proteins, TSP3-5 are pentamers. Expression of TSP is tissue specific. TSP1 and TSP2 are both expressed by vascular cells, like smooth muscle and endothelial cells, but only TSP1 is expressed by the α-granules of platelets. Upon hemostasis and thrombin-induced platelet aggregation [2-3] TSP1 is released from platelets and constitutes the main source of soluble TSP in the blood. This thesis will only focus on TSP1. TSP3, 4, and 5 are expressed in bone and cartilage and, though having some homology with TSP1, their role in modulating cardiovascular events has not been yet defined.

TSP1, an adhesive glycoprotein, was first identified in 1971 by Nancy Baenziger. Exposure of intact platelets to thrombin led their group to observe the appearance of a large protein that they called "Thrombin-sensitive protein" [4] now called thrombospondin 1.

1.1.1 Structure of Thrombospondin

TSP1 is a 450 kDa trimeric glycoprotein composed of three identical 145 kDa polypeptide chains linked by disulfide bonds. Various structural domains have been identified on each monomer [5]:

1. a NH_2-terminal globular domain of the laminin G domain and concanavalin A-like lectin/glucanase superfamily; 2. an α-helical region that has been suggested to form a parallel homotrimeric coiled coil; 3. a von Willebrand factor type C module; and 4. three TSP type 1 repeats that are homologous to the globulin protein properdin and a malarial coat protein. Each repeat consists of a novel, antiparallel three-stranded fold. The monomer is further composed of a "signature" piece that encompasses three epidermal growth factor (EGF)–like TSP type 2 repeats and seven calcium- binding type 3 repeats. The last calcium binding repeat contains an arginine-glycine-aspartic acid (RGD) sequence. The COOH-terminal domain forms a lectin-like β-sandwich [1].

The overall three-dimensional structure is further determined by interactions of the "signature piece" which forms three structural regions termed the stalk, wire and globe. These are additionally stabilized by disulfide bonds and bound calcium [6-7].

1.1.2 Thrombospondin Signaling

Expression of TSP1 is widespread and in addition to its expression in platelets and megakaryocytes [8], TSP1 has been reported to be produced by endothelial cells [9-10], smooth muscle cells, glial cells, type II pneumocytes, fibroblasts, keratinocytes and macrophages [11]. Thrombospondin is abundantly expressed following injury in the extracellular matrix and can interact with fibronectin, heparin sulfate proteoglycans, heparin, collagen, laminin, as well as with plasma proteins like fibrinogen, plasminogen, and histidine rich glycoproteins [11]. In the absence of disease TSP1 occurs in only two locations in the vascular system – as a soluble protein in the blood and preformed in the alpha granules of platelets.

In the last several years it was shown that activation of CD47 by TSP1 leads to decreased production of cGMP in endothelial and smooth muscle cells and in platelets, followed by changes in vascular responses like blood flow and tissue survival [12-19]. These responses to TSP1 have been shown to be due to its interaction with two receptors, CD36 (cluster of differentiation 36) and CD47 (cluster of differentiation 47). CD36 belongs to the scavenger receptor family recognizing low-density lipoproteins and is involved in fatty acid and glucose metabolism as well as diseases associated with these, like atherosclerosis and inflammation [20]. Studies in mice lacking CD36 or CD47 showed that TSP1 only leads to changes in NO-mediated vascular responses via its interaction with CD36 in the presence of CD47. However, TSP1 elicits no response via CD36 activation in the absence of CD47 [15, 17]. Additionally, *in vitro* analysis has found that TSP1's inhibitory signal on NO-stimulated cGMP production is 100-1000 fold more sensitive when mediated via CD47 compared to CD36. For this reason the studies herein will only focus on CD47 and not CD36.

Though the exact mechanism of this TSP1-CD47 signaling pathway is not yet understood, parts of this thesis demonstrate that activation of CD47 by TSP1 leads to changes in enzyme activity of endothelial nitric oxide synthase and changed vascular reactivity downstream. Interestingly, patients with gray platelet syndrome lack α-granules as well as α-granule constituents, like TSP1, and aggregate poorly in response to thrombin [21]. Unfortunately there are no studies of these patients in regard to their vascular health.

It has been shown that TSP1's interaction with CD47, via its C-terminus, leads to platelet activation and, in culture, to platelet spreading[22-24]. TSP1 stimulated cell migration has also been shown to be pertussis toxin sensitive, thus blocking Gi and leading to increased accumulation of cAMP levels downstream. Accordingly, addition of TSP1 in the absence of pertussis toxin

results in decreased cAMP levels, due to active Gi [25]. Further, binding of TSP1 to CD47 has been reported to promote apoptosis in activated T-cells. Thus by reducing the number of activated T-cells TSP1 leads to a reduced inflammation [26].

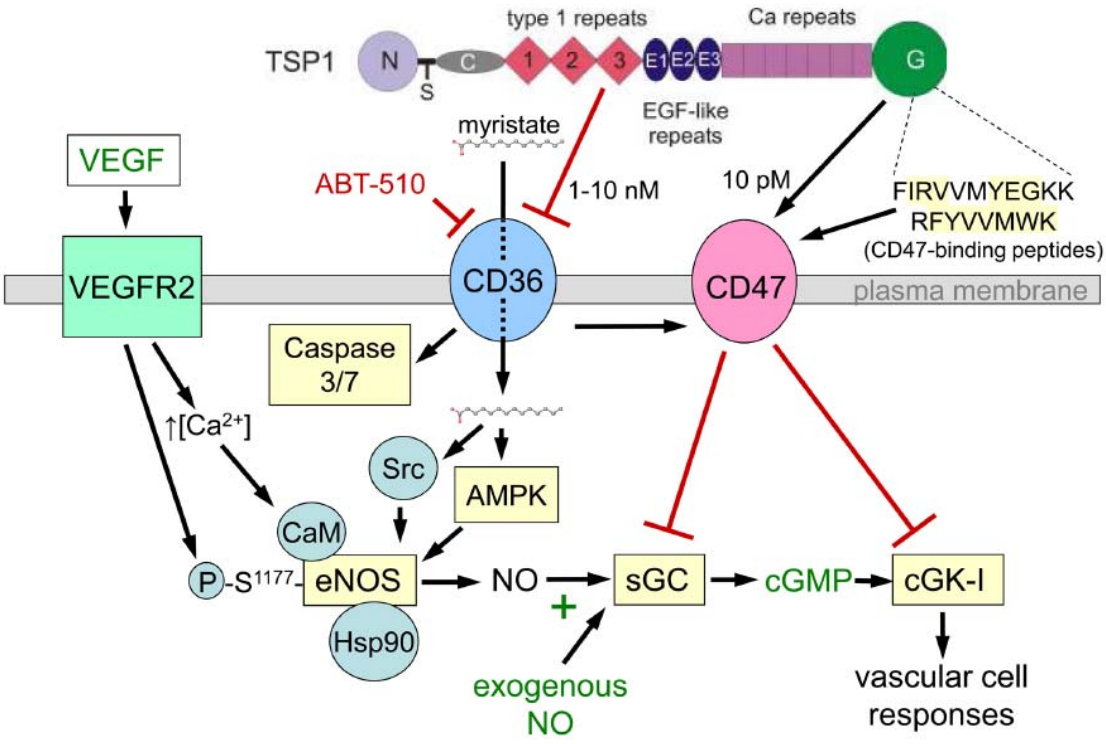

Figure 1. Domains of TSP1 and its interaction with CD47 and CD36 leading to inhibition of NO/cGMP signaling

This schematic illustrates the interaction of TPS1 with CD36 and CD47. Binding of TSP1 to CD47 results in decreased cGMP levels by interfering with the classic vasodilatory pathway of NO. Reprinted from Nature Reviews.Cancer 2009. Vol 9 No 3:182-94 with permission from Nature Publishing Group.

1.1.3 Structure and Ligands of CD47

Cluster of Differentiation 47 (CD47), also called Integrin-Associated Protein (IAP), is a 50 kDa membrane protein that belongs to the immunoglobulin superfamily. It consists of a single IgV-

like domain at its N-terminus, a hydrophobic stretch with five membrane-spanning segments and an alternatively spliced cytoplasmic C-terminus [27] (four splice variants). The length of the cytoplasmic tail can vary depending on tissue type. The most common cytoplasmic tail length observed is the second to shortest splice variant.

CD47 is ubiquitously expressed and was first discovered in copurification studies involving the integrins αvβ3 from leukocytes [27]. Further studies showed that CD47 interacts not only with αvβ3, but also with the integrins αIIbβ3 and α2β1 allowing it to interact with platelets, melanoma cells, ovarian carcinoma cells and smooth muscle cells [22, 28-30 31]. In addition CD47 has been shown to have complete homology to the cancer antigen, OV-3, further fueling research of its role in angiogenesis and cancer biology.

Attempts to identify additional Rhesus polypeptides on erythrocytes led to the discovery of Integrin-Associated-Protein as CD47 making the term "Integrin-Associated-Protein" a misnomer since erythrocytes lack integrins. In addition to its function in integrin signaling, two other ligands of the CD47 receptor have been identified, thrombospondin [32] and Signal–Regulatory Protein α (SIRPα)[33]. SIRPα is a transmembrane protein involved in cell to cell communications by recruiting specific tyrosine phosphatases (SHP-1, SHP-2)[34-36]. These in turn regulate binding of the protein superfamily Ras and of the "Ras-like" protein superfamily, Rho. SIRPα is thus involved in regulation of cell proliferation, migration and apoptosis. CD47-SIRPα signaling has also been shown to be important in the immune system[37-38]. Binding of macrophages that express SIRPα, to the CD47 receptor expressed on red blood cells, leads to inhibition of their phagocytosis [39-40].

1.1.4 Signaling of CD47

The various roles of CD47 activation include, but are not limited to, platelet activation, leukocyte motility, adhesion, migration, and phagocytosis [41]. For example, cells that lose CD47 expression, as happens during apoptosis, get cleared through phagocytosis[42]. In neurons and T-cells expression of CD47 has been shown to lead to caspase-independent apoptosis [42-43].

Original studies on CD47 focused on its role in integrin signaling[22, 30, 44]. Activation of integrins via activation of CD47 has been shown to lead to cross activation of other integrins and downstream signaling cascades resulting in changed cell migration [45].

CD47 signaling has also been reported to involve G-proteins, since activation of CD47 leads to pertussis toxin sensitive cellular responses establishing a role for G_i in the signaling cascade. Copurification studies were able to pull down G_i associated with CD47. It has been proposed that the integrin-CD47-Gαi complex resembles and functions as a heptahelical receptor (i.e. G protein coupled receptor) [45-46]. However, not all cellular responses that involve CD47 activation are G-protein mediated.

1.2 NITRIC OXIDE

1.2.1 Chemistry of Nitric Oxide

The gas nitric oxide (NO) is a free radical and a one electron oxidant. With nitrogen containing five valence electrons and oxygen six, NO has a total of eleven valence electrons (**:**N≡ ·O**:**). Since each orbital holds only two electrons with opposing spin, one electron is left over. This

unpaired electron weakens the triple bond between nitrogen and oxygen by one-half bond. The reason that two NO molecules don't combine to yield dinitrogen dioxide (O=N-N=O) lies in the weakness of the single bond holding both nitrogen molecules together. At room temperature this bond is broken by the thermal energies. As a free radical, NO does not easily react with organic molecules whose orbitals are already filled with two electrons of opposite spin. These reactions involve high activation energies and are generally slow, yielding an organic molecule with another left over electron. NO is much more likely to react with other radicals generating other highly reactive intermediates. Nitric oxide will readily react with oxygen which has two unpaired electrons of parallel spin ($^{\cdot}O\text{-}O^{\cdot}$) yielding a nitrosyldioxyl radical, peroxynitrite ($ONOO^{\cdot}$). The reaction of NO with superoxide to form peroxynitrite proceeds at a rate that is six times faster than superoxide dismutase's ability to quench superoxide. NO also reacts easily with transition metals and can react with the ferric (Fe^{3+}) as well as the ferrous (Fe^{2+}) form. These nitrosated compounds are called nitrosyl compounds.

Under physiologic, non-stress conditions NO acts as a signaling molecule at dilute concentrations of 10-400 nM with a short half-life and the ability to diffuse over 100 μm. As hydrophobic gas, NO crosses the cell membrane as easily as oxygen or carbon dioxide requiring neither channels nor receptors. In addition, NO has a higher diffusion coefficient than oxygen, carbon dioxide, or carbon monoxide and thus becomes an ideal messenger. It was originally thought that the reaction of NO with oxygen, generating the toxic nitrogen dioxide, was responsible for its short half-life. However, the rate of that reaction is too slow to account for this. The concentration of NO available in a biological system dictates what chemistry it will be able to participate in and these reactions differ a lot under conditions that produce cytotoxic levels of NO (i.e. mM concentration produced by iNOS)

This dissertation focuses on NO as signaling molecule and will address the reactions that are important in this context. Three key reactions of NO have been identified:

1) $Heme\text{-}Fe^{2+} + {}^{\cdot}NO \rightarrow heme\text{-}Fe^{2+}\text{-}NO$

This reaction describes the binding of NO to a ferrous heme iron in a protein and elucidates the mechanism of how guanylate cyclase is activated by NO. It has been reported that 10 nM of NO are able to activate guanylate cylase in smooth muscle initiating the classical pathway leading to vasodilation [47].

2) $Hb\text{-}Fe^{2+}\text{-}O_2 + {}^{\cdot}NO \rightarrow Hb\text{-}Fe^{2+}OONO \rightarrow Hb\text{-}Fe^{3+} + NO_3^-$

This reaction describes the irreversible destruction of NO. Nitric oxide reacts with oxyhemoglobin or oxymyoglobin to produce nitrate. Therefore, the NO produced in the endothelium that will diffuse into the lumen of the vessel will be destroyed by red blood cells.

3) ${}^{\cdot}NO + {}^{\cdot}O\text{-}O{:}^- \rightarrow ONOO^-$

In this irreversible and very fast reaction NO reacts with superoxide generating peroxynitrite. This reaction can easily explain the short half-life of NO.

Chemical experiments using NO gas on the lab bench can give us many insights into the kinetics and types of reactions possible for this gas. However, the study of NO chemistry can differ from its physiologic chemistry. Scientists have often published contradictory results when studying nitric oxide. They are foremost limited by the technology that exists to measure NO levels accurately. In addition, the exact location, timing and rate of production of NO in a physiologic setting have to be carefully considered.

1.2.2 Signaling Pathways of NO

Nitric oxide was first identified as mediator of endothelium-dependent vasodilation [48]. However, we now know that this "classic" NO-sGC-cGMP pathway is not only important in vascular relaxation, but also in neurotransmission as well as inhibition of platelet aggregation. As an initiator of this pathway NO binds to the ferrous state of the heme moiety in guanylate cyclase (sGC) forming a five coordinate ferrous nitrosyl complex [49]. This is followed by additional NO binding to a non-heme site leading to activation of the enzyme, and a subsequent increased production of guanosine 3',5'-cyclic monophosphate (cGMP) [50]. However, activation of sGC can also occur by NO-independent mechanisms [51]. The rise in cGMP leads to inactivation of myosin light chain kinase via its phosphorylation by cGMP-dependent protein kinase. This in turn leads to decreased phosphorylation of myosin light chain and as a result, stabilization of the inactive form of myosin and vasorelaxation [52-54].

Vasorelaxation is just one of the physiologic responses due to the activation of sGC. Increased levels of cGMP also modulate phototransduction as well as fluid and electrolyte homeostasis [55-56]. Binding of NO to sGC increases its activity by more than 200 fold. On the other hand, it is the enzymatic activity of phosphodiesterases that stops sGC activity by hydrolyzing cGMP to GMP [57].

1.2.3 Nitric Oxide and Disease

NO released by the endothelium functions to maintain vascular tone, blood viscosity (preventing the formation of abnormal blood clots) and has anti-inflammatory action. For these reasons the lack of NO or the lack of its bioavailability can give rise to many vascular diseases. The reaction

of NO with superoxide is one common reason for the reduction in bioavailable NO. Under healthy conditions, superoxide is eliminated by superoxide dismutases (SOD) [58]. However, the interaction of NO with O_2^- is six times faster than the reaction of O_2^- with SOD [59] and thus increased levels of $O2^-$ lead to increased production of peroxynitrite.

The protonation of peroxynitrite subsequently yields peroxynitrous acid which decomposes into nitrogen dioxide radical and hydroxyl radicals [59]. The nitrogen dioxide radical leads to the production of nitrophenols and further downstream to the formation of 3-nitrotyrosines at tyrosine residues, a marker of peroxynitrite formation. The source of O_2^- production is the result of enzymes like NADPH oxidases, xanthine oxidase, lipoxygenase and even uncoupled NOS [60-63]. During uncoupling eNOS, a homodimer, separates into its monomeric units while maintaining enzymatic activity. This leads to inefficient electron transfer resulting in the production of superoxide. Finally a range of cardiovascular and metabolic diseases in people have been associated with decreased NO production/bioavailability including peripheral vascular disease, diabetes, hypertension, stroke and myocardial infarction.

1.3 NITRIC OXIDE SYNTHASE

NO is produced endogenously by three enzymes, endothelial nitric oxide synthase (eNOS, NOS3), neuronal NOS (nNOS, NOS1), and inducible NOS (iNOS, NOS2)[64-66]. However, NO can also be produced enzyme independently [67-68]. While eNOS is constitutively expressed throughout the vasculature by endothelial cells [69-71](including cardiac myocytes, platelets, mast cells, leukocytes, erythrocytes, renal epithelium), nNOS is localized to the neuronal tissue. Activation of eNOS and nNOS lead to the production of pM amounts of NO that exert a range of

beneficial effects on the vasculature. This stands in contrast to iNOS which on induction by inflammatory stimuli is able to produce high levels of NO with cytotoxic effects (mM concentrations). This thesis will focus on eNOS [72-73], physiologic NO signaling and the downstream vasodilatory events mediated by this pathway.

1.3.1 Enzyme Structure

Endothelial nitric oxide synthase catalyzes the reaction from L-arginine to produce L-citrulline and NO with a Km for L-arginine of 2.9 μM [74]. Since L-arginine levels are 100 fold higher *in vivo* and tissue culture medium it does not easily become the rate limiting factor [75-76]. eNOS is a large dimer of about 140 kDa and both monomers are tightly linked through the heme domains. eNOS consists of two functional domains [77-78]. One is the catalytic domain at the N-terminal that binds the heme prosthetic group (iron protoporhyrin IX) and the permanently bound redox cofactor tetrahydrobiopterin (BH_4), the other domain is located at the C-terminal and binds FMN, FAD and NADPH [79]. BH_4 is indispensable for eNOS activity [80]. The crystal structure for eNOS is known and it has been reported that BH_4 stabilizes eNOS by binding to the dimer interface [81-84]. Further, the dimer interface contains a zinc ion that is tetrahedrally ligated by two Cys residues, one in each monomer, which are also responsible for the binding of BH_4 to the enzyme. Substrate binding occurs at the active heme site via extensive hydrogen bonding[81-84]. For NO production to occur eNOS requires oxygen and NADPH. Electron flow occurs from NADPH to FAD, to FMN and last to the heme [85].

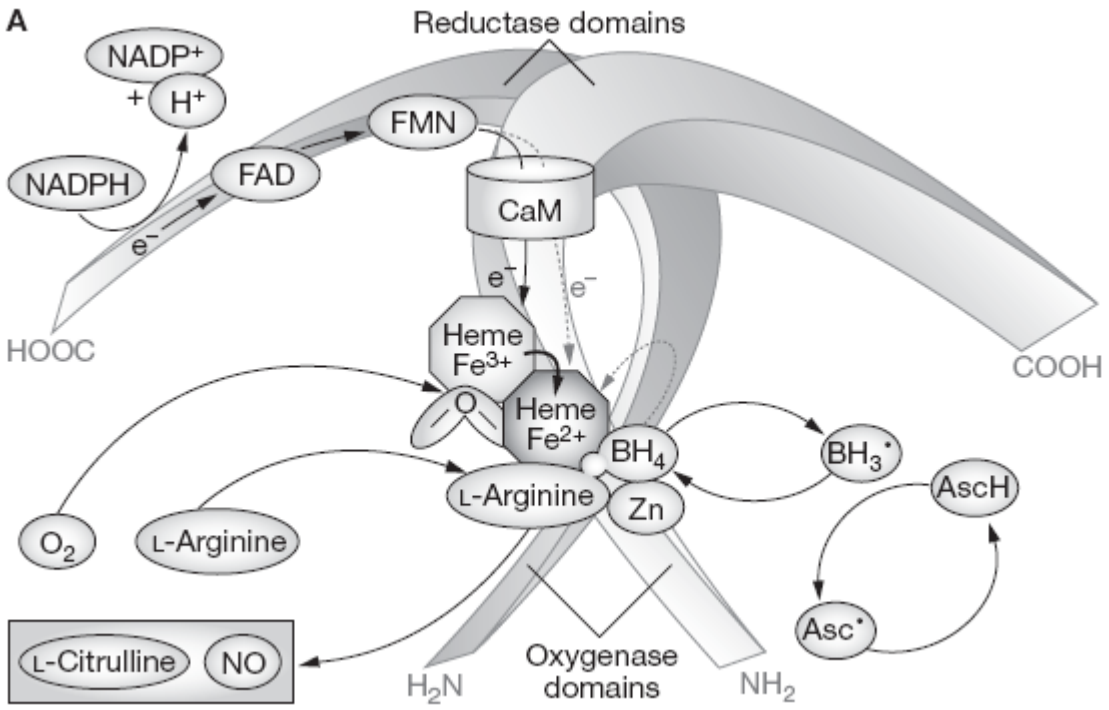

Figure 2. Schematic of factors required for endothelial nitric oxide synthase function

This schematic illustrates the various elements required for full endothelial nitric oxide synthase activity. Reprinted from Nature Cardiovascular Medicine 2008. Vol 5No 6:338-347 with permission from Nature Publishing Group.

1.3.2 Regulation of Enzyme Activity of eNOS

The regulation of eNOS's enzyme activity is complex occurring on a transcriptional, posttranscriptional as well as posttranslational level [86-87]. Since this thesis focuses only on acute changes in NO production and thus eNOS activation, transcriptional regulation will not be discussed here. Some posttranslational modifications include changes in phosphorylation state, interaction with a variety of factors, or even by self- nitrosylation of its own cysteine residues. Under unstimulated conditions eNOS is bound to caveolae in the cell membrane via acyl anchors produced by myristoylation and/or palmitoylation reaction of its N-terminus. Caveolae are important cellular regulatory sites where many multifunctional receptors, like G-protein-

like receptors, are sequestered and where signaling pathways converge via protein-protein interactions or protein-lipid interactions [88-91].

Binding of calmodulin to eNOS is one requirement to obtain full enzyme activity by allowing electron flow between its two catalytic domains. Calmodulin binding is dependent on changes in intracellular calcium levels. Stimuli, like bradykinin or acetylcholine, activate G-protein-dependent pathways leading to the production of diacylglycerol (DAG) via phospholipase C (PLC) and subsequent inositol 1,4,5,-triphosphate (IP_3) mediated calcium mobiliziation via ion channels [92].

In addition to calmodulin binding, eNOS activity is regulated by phosphorylation of specific serine and threonine residues (Ser1177, Ser635, Ser617 are stimulatory, Thr495, Ser 116 are inhibitory). Phosphorylation at Ser1177 has been shown to affect eNOS activity two-fold: 1. by increasing internal electron flow and 2. by inhibiting calmodulin dissociation. Adding complexity to the regulation of eNOS, various products of major signaling pathways can phosphorylate Ser1177, i.e. protein kinase B (akt), cyclic AMP-dependent protein kinase (PKA), AMP-activated protein kinase (AMPK), cGMP-dependent kinase (PKG), calcium/calmodulin-dependent protein kinase II [93-100]. It has been reported that PI3K recruits Akt to the membrane for phosphorylation, a requirement for subsequent phosphorylation of eNOS.

S-nitrosylation of eNOS has been shown to occur via its own NO production and subsequent inhibition [101-103]. During maximal NO production eNOS is denitrosylated. Nitrosylation or denitrosylation has been shown to depend on the cellular location of eNOS and several different mechanisms have been postulated to explain this inhibitory effect [101-103 104].

Caveolins are small membrane bound proteins. Caveolin 1 (cav-1) which is ubiquitously expressed in endothelial cells, leads to localization of eNOS to caveolae [105-109] and by direct protein interaction with eNOS sterically blocks the binding of calmodulin.

Endoglins are glycoproteins highly expressed in endothelial cell membranes, dominantly in caveolae. They stabilize eNOS by promoting its association with Heat shock protein 90 (HSP90) [110-113]. Partial loss of endoglin has been shown to cause a decrease in the half-life of eNOS protein, as well as a switch in production from NO to superoxide [110-113].

HSP90 is a protein involved in the folding and trafficking of other proteins. Binding of HSP90 to eNOS stimulates its activity by enhancing the affinity for calmodulin binding to eNOS and balances the production of NO over superoxide. In addition HSP90 affects eNOS activity indirectly by binding active and inactive Akt and is required for the interaction between Akt and eNOS. HSP90 also protects PI3K degradation and inhibits Akt deactivation. Interestingly HSP90 and Akt activate eNOS also in a calcium independent manner [114-118]. eNOS itself has been shown to have a negative feedback mechanism where the production of NO causes s-nitrosylation of a specific cysteine residue leading to eNOS-HSP90 disruption [119].

Another regulator of eNOS is shear stress [120]. This frictional force of blood flow has been shown to regulate eNOS activity. Flow rates of 10-15 dynes cm^{-2} in humans and between 30-35 dynes cm^{-2} in mice and rats are sufficient to increase eNOS activity and production. A shear stress-response element has been identified in the eNOS promoter region [121-122]. Within endothelial cells the cytoskeleton has also been identified as a factor of mechanotransductation and changes in flow and shear stress rapidly alter calcium flux and eNOS phosphorylation [123].

Additional regulation of eNOS activity is achieved by the action of phosphatases. Dephosphorylation of inhibitory or stimulatory residues can increase or decrease enzyme activity

respectively. Activity is also determined by subcellular localization of eNOS and as such various eNOS associated proteins have been identified that are involved in its trafficking like important interaction with cytoskeletal actin. The complexity of eNOS regulation is enormous and probably as such also a good indicator of its importance in our vasculature.

1.3.3 Agonist Dependent Activation of eNOS

Binding of a variety of agonists to the plasma-membrane leads to eNOS activation. This occurs mostly by activation of two downstream pathways that either activate Akt, or stimulate calcium release or do both. Vascular endothelial growth factor (VEGF) is one such physiologic agonist leading to rapid eNOS activation by binding the VEGF receptor 2 (VEGFR2, a tyrosine kinase). Subsequent activation of PLC in turn leads to IP_3 mediated eNOS activation and is described as "immediate" response. In parallel, eNOS activation via DAG and PKC is called "delayed" response. Binding to VEGFR2 also leads to increased downstream PI3K and Akt–mediated immediate eNOS activation [124-128].

Other agonists lead to eNOS activation via binding to G-protein coupled receptors (GPCR). For example, bradykinin binding to the GPCR bradykinin receptor B2 leads to calcium mediated eNOS activation. Another common pharmacologically used activator is acetylcholine (ACh), a neurotransmitter that binds the muscarinic M3 receptor followed by calcium dependent enzyme activation. Histamines, sphingosine-1-phosphate, as well as estrogen, are further examples of agonists binding to GPCRs and subsequent calcium mediated eNOS activation [129]. Natriuretic peptide will lead to eNOS activation by binding to its own receptor that has been shown to involve G-proteins and is also followed by downstream activation of calcium channels [130].

It has further been shown that low, though still physiologic, oxygen levels (i.e. PO_2 of 20-40 mmHg) can inhibit eNOS with subsequent reduced eNOS protein expression [131]. However, further research demonstrated the opposite effect and eNOS expression seems to be tissue specific [132-133].

1.3.4 Physiology and Biological Role of eNOS

eNOS functions to produce nitric oxide. The various effects of NO are discussed above (Nitric Oxide section). One main result of NO produced by eNOS is its control of vascular tone [134-137]. Diffusion of NO into the smooth muscle layer of the vessel wall leads to the activation of sGC and sGC increases conversion of GTP to cGMP. This increased cGMP production in turn starts a signal transduction cascade leading to smooth muscle relaxation (hypopolarization) [138-140].

Besides producing nitric oxide eNOS activity leads to the production of citrulline which is catalyzed in the urea cycle to argininosuccinate. Citrulline has also been shown to lead to posttranslational modifications, i.e. citrullination and is used as biomarker of autoimmune diseases, like rheumatoid arthritis [141].

1.3.5 eNOS in Disease

Vascular disease has been associated with a decrease in bioavailability of NO which is reported to be either the cause or the result of endothelial dysfunction. These diseases include atherosclerosis, diabetes and hypertension. Decreased NO is also associated with decreased angiogenesis and apoptosis. In atherosclerosis, peripheral vascular diseases, stroke and coronary heart disease, endothelial dysfunction is regarded as an initiator. Age-induced loss of normal

endothelial function, leads to loss of NO production from eNOS and under some conditions to upregulated NO production from iNOS [142]. For example, vessels of cholesterol fed animals have less vasoactive responses and administration of L-arginine, or tetrahydrobiopterin attenuates the formation of atherosclerotic lesions [143-149]. Regardless, the net effect is an overall decrease in physiologic (pM) levels of NO and suppression of the pro-flow and antithrombotic role endogenous NO exerts.

Diabetes mellitus is also characterized by endothelial dysfunction and the role of unbalanced bioavailability of NO has been well documented [150-151] [152-153]. For example, endothelial cells isolated from diabetic rats have reduced levels of tetrahydropterin leading to reduced NO but increased superoxide production [154-156].With its vasodilatory effect on the vasculature NO is crucial in blood pressure control [157]. In hypertension NO-mediated vasodilation is impaired. However, it is not clear if this is due to a reduction in NO synthesis or increased consumption of NO. In both animal and human studies blockade of eNOS activity with the competitive NOS inhibitor L-NAME uniformly results in increased blood pressure. Conversely, exogenous NO in the form of the commercial therapeutic Bidil has been found to significantly lower blood pressure in a subset of hypertensive patients. Efforts at enhancing physiologic (low level) NO production through increasing eNOS activity or stimulating cGC directly are areas of robust research.

1.4 PHYSIOLOGY OF VASCULAR TONE

1.4.1 Vessel Anatomy and Physiology

The anatomy of an artery is divided into three major structures, the tunica intima, the tunica media and the tunica adventitia [158]. The tunica intima is made up of endothelial cells lining the luminal area of the vessel, also called intima. On the side opposing the lumen endothelial cells are anchored to the basal lamina which is further composed of the internal elastic lamina. In larger animals, including humans, this sub-endothelial layer is made up of smooth muscle cells and aids in maintaining vascular integrity.

The tunica media mainly consists of smooth muscle cells and elastin. The elasticity of a vessel is mostly due to elastin which also allows for even stress distribution across the whole vessel wall onto collagen fibers [159-161].

The tunica adventitia makes up the outermost layer of the vessel wall and consists of collagen-rich extracellular matrix and fibroblasts. The high collagen content prevents the vessel wall from rupture at high pressures [162]. Small blood vessels, called the vaso vasorum, originate from the tunica adventitia and function as energy supply for the cells in the wall. Studies of injury models revealed in the last decade that the vaso vasorum contains progenitor cells that are able to differentiate into smooth muscle cells [163-164].

The circulatory system is divided into the pulmonary and the systemic circulation with the latter describing the blood supply to all tissues in the body except for the lungs. Pressures in the systemic circulation are high (120/80 mmHg in the human aorta) while pulmonary vascular pressures in the lung are low (14 mmHg at rest). Blood flow throughout the body occurs via a variety of vessels. Arteries are vessels with strong vascular walls that can withstand blood flow

under high pressure and high velocity. They are defined as carrying oxygenated blood from the lung to the rest of the body. It is the elasticity of the arteries that allows for large volume changes in the arterial branches with very little change in pressure. The aorta falls into the class of large arteries. These large vessels eventually lead to the smallest arterial branches, the arterioles. With their muscular walls the arterioles can dilate or constrict strongly and thus have the ability to control blood flow tremendously and in a very tissue specific fashion. Blood from the arterioles enters the capillaries (8 μm). These very thin walled and porous vessels function to exchange nutrients with tissue and interstitial fluid. The deoxygenated blood from the tissue then collects in the venules leading to larger vessels, the veins, leading back to the heart. Blood pressure in the venous system is low. Despite their thin walls these vessels are still able to dilate and constrict. This allows them to control blood volume by serving as an adaptable storage compartment. The heart then pumps the blood back into the lung for oxygenation [165].

Under conditions of laminar/streamlined flow the conductance of blood through the vessels is strongly affected by the fourth power of the vessel's diameter. This phenomenon is described by Poiseuille's Law: $F= \pi\Delta Pr^4/ 8\eta l$, where F is the rate of blood flow, ΔP is the pressure difference between the ends of the vessel, r is the radius of the vessel, l is the length of the vessel and η is the viscosity of the blood. Thus, because flow is directly proportional to the vessel radius to the fourth power, small changes in vessel diameter lead to large changes in blood flow [166].

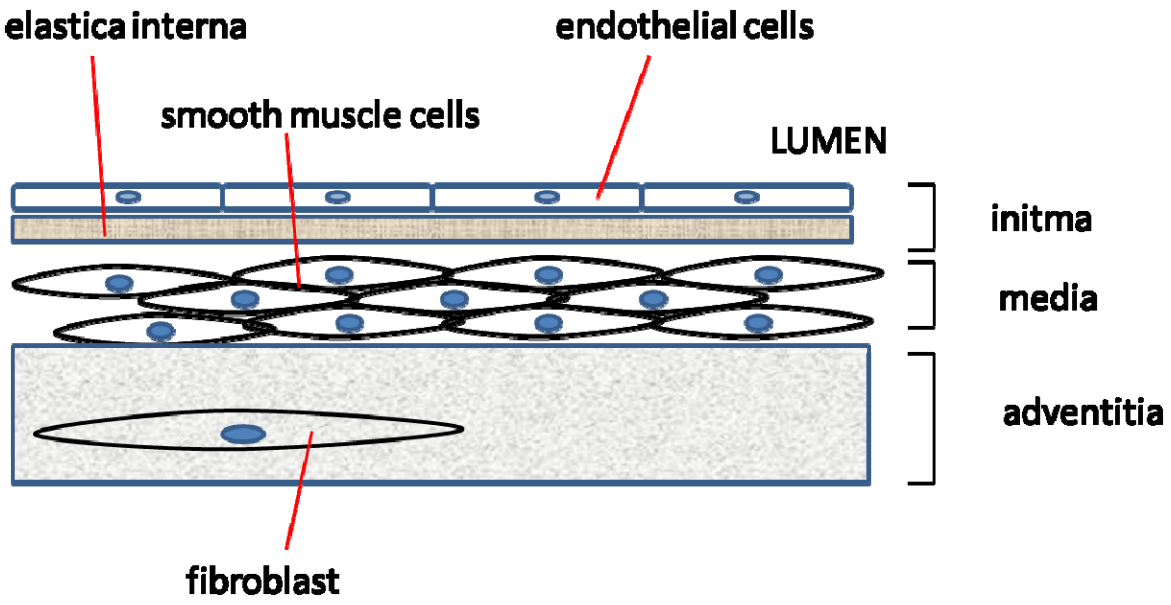

Figure 3. Simplified schematic demonstrating the cellular composition of blood vessels

Blood vessels are made up of three distinct layers; the adventitia, comprised mostly of fibroblasts; the media, made up of vascular smooth muscle; and the intima, comprised of a single layer of endothelial cells lining the lumen of the vessel.

1.4.2 Endothelial Dependent Relaxation

The endothelium functions to regulate angiogenesis, inflammatory responses, hemostasis, and permeability and is the key player in the control of vascular tone [167]. Its position in the vessel allows it to serve as an interface between the intravascular compartments (consisting of the blood) on one side and the underlying vascular smooth muscle cells on the other. The endothelium creates therefore the possibility to respond to physical stimuli of blood flow (i.e. shear stress, pressure) as well as to chemical agents in the blood (i.e. hormones) by either transmitting the signal to the smooth muscle layer via gap junctions, channels, other signal transduction cascades or by releasing its own compounds (i.e. nitric oxide) that can diffuse

across the layers. The effect on the smooth muscle layer to the endothelium is either hyperpolarization leading to relaxation or depolarization followed by contraction [168].

The release of nitric oxide as well as prostacyclins (PGI_2) is considered to be the main factor contributing to endothelium dependent vasodilation [169-170]. PGI_2 production is the result of cyclo-oxygenase mediated breakdown of arachidonic acid. Interestingly changes in vascular tone have also been reported in the presence of NOS and cyclo-oxygenase inhibitors, pointing to additional endothelial vasodilators. Various metabolites of endothelial cytochrome P450 have been reported to act as vasorelaxors (i.e. epoxyeicosatrienoic acids) or vasoconstrictors (i.e. 20-hydroxyeicosatetraenoic acid) [171-173]. Further, hydrogen peroxide (H_2O_2) can have either dilatory or constrictive endothelium-dependent effects. The production of superoxide, by nitric oxide synthases, cyclo-oxygenases, cytochrome P450 epoxygenases, NADPH oxidases as well as mitochondrial enzymes of the respiratory chain can lead to downstream H_2O_2 production in the endothelium[174-182]. Another endogenous vasodilator is CO that is produced by heme oxygenase 1(inducible) and 2 (constitutive). It has been shown that CO production can compensate for the loss in NO bioavailability [183], but, on the other hand, can also inhibit NOS function. The gas hydrogen sulfide (H_2S) which is produced enzymatically by cystathionine β-synthase and cystathionine γ-lyase, has been reported to have an endothelium-dependent vasorelaxant effect as well [184-185] though these studies used non-physiologic levels of H_2S (>150 μM). The complexity of endothelium-dependent vasodilation is further increased by reports showing different effects of agents mentioned above depending on the location of the vascular bed as well as gender. In addition to endogenously produced endothelium-dependent vasodilators exogenous anesthesia related agents like cannabinoids have also been shown to lead to endothelium dependent

relaxation [186] and need to be taken in consideration in the clinical setting as well as in animal research.

1.5 PULMONARY HYPERTENSION

1.5.1 The Disease and Etiology of Pulmonary Hypertension

Pulmonary arterial hypertension (PAH) is a disease/pathogenesis of the small pulmonary arteries that is characterized by vascular proliferation and remodeling [187-188]. PAH is identified histologically in patients by plexiform lesions as a result of endothelial cell proliferation. In addition, increased proliferation of smooth muscle cells and myofibroblasts leads to medial hypertrophy and adventitial hyperplasia [189-192]. Progressive vascular remodeling causes an increase in pulmonary vascular resistance. In humans PAH is defined by mean pulmonary artery pressures greater than 25 mmHg and a pulmonary-capillary wedge pressure of less than 15 mmHg. Over time this increase leads to further remodeling, right heart failure and ultimately death [193]. A diagnosis of idiopathic PAH is made when no known etiology is found [194 195]. The diagnosis for PAH is divided into 6 groups by the World Health Organization. In addition to inherited familial PAH, several diseases have been shown to lead to the development of PAH, such as congenital left-to-right cardiac shunts, hemoglobinopathies, human immunodeficiency virus infection, collagen vascular defects, significant left heart disease, chronic pulmonary thromboembolic diseases, and chronic lung disease and/or hypoxemia[195-196]. Recent studies have also unraveled the important clinical finding of PAH contributing to the pathogenesis and increased mortality in patients with sickle cell disease [187, 197].

Though various types of pulmonary hypertension arise from different etiologies, they share common pathophysiological features including remodeling of the pulmonary vessel wall, vasoconstriction, and thrombosis *in situ* [187]. Increased reactivity to vascoconstrictors and correspondingly decreased reactivity to vasodilators further emphasize the anatomical changes observed in the lung. As such impaired production of vasoactive NO or prostacyclins or over-expression of vasoconstrictors such as endothelin-1, can alter pulmonary vascular tone and lead to vascular remodeling. Alterations in these vasoactive molecules suggest that endothelial dysfunction plays a key role in the pathophysiology of PAH [198-202].

The cellular and molecular events underlying the evolution of these changes and those that occur in response to these changes are under investigation and continue to guide the development of therapeutics. A substantial number of molecules and molecular pathways have been implicated, but clearly the pathogenesis involves a multifactorial process [187-188, 200]. Treatment of PAH targets vasorelaxation and the blocking and reversal of cell proliferation (i.e. via induced apoptosis). Nonselective vasodilators are not useful due to their dilatory effect on the systemic vasculature and therefore the risk of hypotension. Inhibition of phosphodiesterase-5 is a common therapy used to treat moderate PAH and offers several advantages. First, its expression is not systemic but selective to the lung and penile tissue. Secondly, due to the function of phosphodiesterases to breakdown the production of cGMP, inhibition of these enzymes leads to increased cGMP levels and thus increased vasodilation. The PDE5 inhibitor sildenafil was approved by the FDA as treatment for moderate PAH in 2005. In addition to ongoing trials with PDE5 inhibitors, PAH can be treated by calcium channel blockers, as long as the patients responds to the acute administration of vasoactives. Other common drugs include prostacyclin

analogues as well as endothelin antagonists. However, despite 16 ongoing clinical trials showing a clear improvement in symptoms neither of these drugs have been shown to reduce mortality [203]. Another area of investigation is the role of potassium channels on the development of PAH. Decreased expression of voltage gated potassium channels as well as potassium channel depolarization has been associated with vasoconstriction and increased pulmonary artery smooth muscle cell (PASMC) proliferation[187-188, 204-208]. Likewise, manipulation of these molecules and pathways has been the basis for the development of drug therapy [200, 209-210].

Currently patients with PAH have a prognosis of 85% for a 1-year- survival rate in the US [211], up from 68% in the 1980s [193] and a median mortality rate of 5 years. The symptomatic outcome of PAH, independent of its cause, is on the rise worldwide [212]. With the harsh survival prognosis for PAH, with a rise of PAH worldwide, and with only a very limited number of drugs available for its treatment, research focusing on PAH is imperative to our understanding of the disease and thus our ability to find better therapies.

1.5.2 eNOS and Pulmonary Hypertension

While many of the mechanisms leading to PAH are still unknown it is well established that one of the key initiating events is endothelial dysfunction [213-215]. Importantly failure of NO mediated, endothelium dependent vasodilation has been well described both clinically and in experimental animal models of PAH [216-222]. Endothelial nitric oxide synthase is the NOS most prominently expressed in the vasculature under healthy conditions and thus of interest in the development of PAH [223]. Studies in eNOS null mice have shown a mild development of PAH in these mice exposed to room air that progresses to severe PAH when chronically exposed to mild hypoxia

[224-225]. eNOS is a tightly controlled enzyme on a transcriptional, postranscriptional, and posttranslational level. As such studies looking at endothelial impairment have focused on the regulatory factors involved in eNOS activation, including caveolin-1, heat shock protein 90, calcium as well as upstream regulators of eNOS activation, such as ion channels and AKT/protein kinase B [89, 226-230]. It has been reported in PAH animal models that eNOS is upregulated [231-232] while the lung shows impaired NO bioactivity. Interestingly it has also been shown that hypoxia induced PAH leads to tight interaction between eNOS and caveolin-1, thereby physically blocking the enzymes from other signaling molecules [233]. Others observed the loss of caveolin-1 and hemeoxygenase expression in severe PAH [234].

1.5.3 Animal Models of Pulmonary Hypertension

The newly updated classification system for PAH shows a broad range of parameters leading to its development [196]. Not surprisingly this diversity corresponds also to a variety of histological features observed in patients with PAH and therefore makes the study of PAH in animal models more complex [235]. One characteristic and defining feature distinguishing PAH from PH is the commonly described appearance of plexiform lesions during the late stage. However, even this hallmark is not always observed in all patients [236-237]. Others recently further described the heterogeneity observed in vascular lesions in PAH [238].

Additionally, death from PAH is due to right heart failure and also involves loss of elasticity in larger conduit vessels. This stiffening adds further complexity to the study of PAH in animal models.

The two most commonly used animal models of PH are the chronic hypoxic exposure model and the monocrotaline injury model. For chronic hypoxic exposures (10% for 3 weeks)

the investigator chooses between normobaric or hypobaric exposure with the latter resembling high altitude induced PAH. Chronic hypoxic exposure is commonly used in rodent models with reproducible outcomes. In this model rats initially demonstrate increased muscularization of small, previously non-muscular arterioles which leads to the progressive thickening and obliteration of muscularized precapillary arteries. In addition, inflammation, a rise in chemokines, fibrosis and stiffening of large conduit arteries have been observed in the hypoxic model. Interestingly rats develop right ventricular hypertrophy but not right ventricular heart failure.

Chronic hypoxic exposure in mice leads to increased pulmonary artery pressures but to less vascular remodeling than observed in rats. Differences in gene expression due to chronic hypoxic exposure have been reported between mice and rats [239]. However, there are also significant differences in response to chronic exposure between mouse strains [240]. Though vascular remodeling is less in mice exposed to chronic hypoxia they nonetheless do show changes as seen in rats, including muscularization of non-muscularized vessels, thickening of arteries, fibrosis and stiffening of the vessels [241-242]. PAH reversal has been observed in rodents by Stenmark (unpublished) when returned to normoxic conditions, which clearly differs from the human progression of PAH.

Monocrotaline injury requires either ingestion or subcutanous injection of this toxic pyrrolizidine alkaloid and is considered an acute damage model affecting also the peripheral vasculature. The compound requires enzymatic activation by the rat. Mice unfortunately lack that enzyme and have recently been injected with the activated compound. The exact mechanism of how monocrotaline induces PAH is not known, but increased vascular remodeling and a rise in pulmonary pressures is usually observed within 1-2 weeks after the initial dose. Interestingly

monocrotaline leads to sequestration of eNOS away from caveolae and thus causes a reduction of NO levels though eNOS protein levels stay unaffected [243]. Several groups suggest that adventitial inflammation contributes greater to the progression of PAH than the endothelium [164, 244-245]. Besides an effect on the lung vasculature, there have been reports on liver and kidney damage as well as changes in veins [244-246]. Interestingly there have been more than 30 compounds found that prevent and/or reverse monocrotaline-induced PAH.

In addition to these two classic models, investigators have used modifications to better recapitulate the human condition. Examples in rats include a combination of monocrotaline injection as well as pneumonectomy [247] resulting in the formation of neointima due to the changes in hemodynamics caused by the pneumonectomy [248]. Others have developed a severe model of PAH by inhibiting the VEGF receptor [249] with a pharmacological agent, Sugen 5416, in combination with chronic hypoxic exposures. They observed irreversible precapillary arterial endothelial proliferation in these rats. As with any model, none is perfect and investigators have to carefully consider their choice of model as well as the bias introduced into their results based on this choice. We have chosen the murine model of chronic hypoxic exposure (3 weeks at 10% Oxygen), since it is well established, produces reproducible results, and gives us the advantage to use transgenic animals.

1.6 STATEMENT OF HYPOTHESIS

In 1998 three scientists received the Nobel Prize in Physiology and Medicine for their discovery of NO as a signaling molecule in the cardiovascular system. Dr. Furchgott observed that relaxation of isolated vessels was endothelium dependent leading to the release of an Endothelium Derived Relaxing Factor (EDRF). Dr. Ignarro discovered that EDRF is NO, since exposure of NO or EDRF to hemoglobin resulted in an identical shift using spectral analysis and Dr. Murad had uncovered the mechanism of NO's dilatory action allowing for a whole new class of drug targets. Now we know that NO is produced by the endothelial enzyme nitric oxide synthase (eNOS) and that the lack of NO or the lack of its bioavailability is intimately involved in a wide range of diseases, like atherosclerosis, diabetes, hypertension or stroke. The initiating events of these vascular diseases are referred to as endothelial dysfunction.

Thrombospondin 1, an extracellular matrix protein released from platelets upon injury, has been studied in regard to tumor angiogenesis. Dr. Isenberg discovered that TSP1 antagonizes the NO-mediated-cGMP-dilatory pathway in smooth muscle and endothelial cells via the ubiquitous receptor CD47 leading to decreased levels of cGMP[12, 15-16]. In addition to its anti-angiogenic effects TSP1 was shown to modulate blood pressure as well as cardiac responses to vasoactive stress [14, 18]. Additionally, TSP null animals demonstrated enhanced shear-dependent blood flow compared to wild type animals. In the absence of disease TSP1 occurs in only two locations in the vascular system – as a soluble protein in the blood and preformed in the alpha granules of platelets. However, with a molecular weight of 450 kD TSP1 is too large to cross the subendothelial basement membrane of arteries and thus doesn't explain the observed differences in blood flow in the null animals.

We hypothesized that TSP1 directly modulates eNOS activity and, thus, endothelium-dependent relaxation of blood vessels. Further, we were interested in how the inhibitory effects of TSP1 on eNOS would translate in a disease setting, specifically pulmonary hypertension. Thus, we hypothesized that the lack of TSP1 would protect TSP1 null mice from the development of pulmonary hypertension. We used chronic hypoxic exposure of mice to model pulmonary hypertension. In addition, we were fortunate to have access to lung tissues from patients with or without PAH, that were compared to the results obtained in the hypoxic rodent model.

Understanding the role and mechanism of action of TSP1 in healthy and disease states will open up new routes for drug development and provide insight into the molecular mechanisms underlying the effects of current therapies targeting the NO/cGMP pathway.

2.0 MATERIALS AND METHODS

2.1 CELL CULTURE

2.1.1 Maintenance and Storage

Human umbilical cord endothelial cells (HUVEC) (Lonza, Walkersvile, MD) were grown in EGM2 basal media supplemented with various growth factors and fetal bovine serum (EGM-2 SingleQuots, Lonza). Cells were maintained under humidified conditions at 37°C and 5% CO_2 and medium was changed every 48 hrs.

To passage cells, they were rinsed with Hanks' Balanced Salt Solution (HBSS) (Invitrogen), followed by incubation in 2 ml trypsin/EDTA solution (Lonza, Walkersville, MD) for 3-4min per T75 flask. The enzyme was then neutralized by addition of 10 ml complete media. Cells were pelleted via centrifugation for 5 min at 4°C and 1200 rpm and reseeded at a ratio of 1:3. Cells were only used up to passage nine.

For long term storage pelleted cells were resuspended in complete media containing 10% dimethylsulfoxide (DMSO) (Sigma-Aldrich) and 10% additional fetal bovine serum (Lonza, Walkersvile, MD). One million cells were aliquoted per storage vial which was cooled for 24 hrs in -80 °C and then transferred to liquid nitrogen.

2.1.2 Common Experimental Treatments

For all endothelial cell experiments cells were serum starved in serum and growth factor free media containing 0.1% BSA for 24 hrs prior to treatment. Addition of TSP1 (2.2 nM) was always performed by preincubating cells or vessels for 15 min prior to other treatments.

2.2 CALCIUM IMAGING

2.2.1 Determination of Calcium Flux in Cells

Agonist-induced Ca^{2+} release was monitored in endothelial cells in the presence or absence of 2.2 nM TSP1 or other treatment agents using live cell imagining. For single-cell imaging, HUVEC were grown on gelatin-coated 35mm glass bottom dishes (MatTek Corp., MA) and serum starved with 0.1% BSA 24 hrs prior to experiments. Cells were loaded with 5 μmol/L Fluo-4AM ester (excitation at 488 nm, Molecular Probes, Invitrogen) for 30 min at 37°C in Hanks buffer solution (with 1.88 mmol/L fresh $CaCl_2$ and 20 mmol/L HEPES) followed by 2 washes with Hanks buffer and incubation at room temperature in the dark for an additional 20 min. Images were acquired every 3 sec on a Zeiss LSM 5 confocal microscope (Carl Zeiss, Thornwood, NY) at 20X with scan speed of 8.5 and a resolution of 256x256. Data were analyzed using software LSM Pascal 3.2 obtaining relative changes in fluorescence intensity compared to baseline. We added plain buffer 1 min prior to addition of the agonist ionomycin (3 μmol/L, Invitrogen). If cells showed changes in calcium flux due to buffer addition, they were excluded from the analysis.

2.2.2 Determination of Calcium Flux in Mouse Aorta

For en face calcium measurements 12 week old male C57Blk6 mice were euthanized by cervical dislocation. The abdominal vena cava was incised and the animal perfused via the heart using Krebs-buffer. The thoracic aorta was isolated and loaded for 1 hr with 5 μM Fluo-4AM (excitation at 488 nm, Molecular Probes, Invitrogen), followed by several washes in Hanks' buffer (plus 1.8 mM $CaCl_2$ and 20 mM HEPES at pH 7.4). Vessels were then opened lengthwise under a dissection microscope, secured face down onto MatTek dishes and incubated for 30 min in the dark. Aortic segments were transferred to the microscope stage on a Zeiss LSM 5 confocal microscope (Carl Zeiss, Thornwood, NY) and images were acquired every 3 sec at 10x magnification and a resolution of 512x512. Stimulation with 3 μmol/L ionomycin (Invitrogen) resulted in a fluorescence intensity wave traveling along the vessel. Therefore data were analyzed using the area under curve over time over several selected regions of interest on the vessels. Initial data analysis was performed using LSM Pascal 3.2 software and subsequent calculations were performed in Graphpad Prizm.

2.3 METHODS FOR THE STUDY OF PROTEIN EXPRESSION

Table 1. Buffers

Buffer	Protocol	Materials
SDS Electrophoresis Buffer	Western Blot	25mM Tris Base, 250mM Glycine (pH8.3), 0.1% SDS
Stacking Buffer	Western Blot	0.5M Tris Base, 0.4% SDS , pH 6.8
Resolving Buffer	Western Blot	1.5M Tris Base, 0.4% SDS, pH 8.8
Polyacrylamide Separating Gel 10%	Western Blot	2.5ml 30% Acrylamide, 1.875ml Resolving Buffer, 3.125ml H_2O, 50 µl 10% ammonium persulfate, 10 µl TEMED
Polyacrylamide Separating Gel 8%	Western Blot	2.0ml 30% Acrylamide, 1.875ml Resolving Buffer, 3.625ml H2O, 50 µl 10% ammonium persulfate, 10 µl TEMED
Polyacrylamide Stacking Gel	Western Blot	650µl 30% Acrylamide, 1.25 ml Stacking Buffer, 3 ml H_2O, 25µl 10% Ammonium Persulfate, 5µl TEMED
Transfer Buffer 10x	Western Blot	in 2L, 288 g Glycine, 60g Tris Base, fill with H2O
Laemmli Buffer 6x	Western Blot	7ml Stacking Buffer, 30% glycerol, 10% SDS, 0.6M DTT, 0.012% bromophenol blue, H_2O till 10ml final volume
Lysis Buffer	Western Blot	50mM tris, 1% NP-40, 1mM EDTA, 125mM NaCl, 2.54 mM Deoxycholic Acid
TBST Buffer	Western Blot	100mM Tris Base, 150mM NaCl, 0.1% Tween 20
IP-Lysis Buffer	Coimmunoprecipitation	50mM Tris HCl pH 7.5, 0.1mM EDTA, 0.1mM EGTA, 0.1%SDS, 0.1% Deoxycholic Acid, 1% NP-40
K-PSS Buffer	Myograph	4.7mM Sodium Chloride, 100mM Potassium Chloride, 1.18mM Potassium Phosphate, 1.17mM Magnesium Sulfate, 14.9mM Sodium Bicarbonate, 5.5mM Dextrose, 0.026 EDTA, 1.6mM Calcium Chloride, pH7.4
PSS Buffer	Myograph	130mM Sodium Chloride, 4.7mM Potassium Chloride, 1.18mM Potassium Phosphate, 1.17mM Magnesium Sulfate, 14.9mM Sodium Bicarbonate, 5.5mM Dextrose, 0.026 EDTA, 1.6mM Calcium Chloride, pH 7.4

2.3.1 Isolation of Total Proteins

Cells were rinsed once with cold HBSS, scraped in lysis buffer (Table1) supplemented with a protease inhibitor cocktail (Sigma), 20 mM sodium fluoride, 1 mM sodium pyruvate, 5 mM orthovanadate and collected in tubes. After rotating for 1h at 4°C, cell lysates were sonicated 3 times for 3 sec on ice and centrifuged for 15 min at 14,000 g. The supernatant was transferred to a new tube and total protein content was determined using the DC Protein Assay (BioRad) which included a BSA standard curve. Absorbance was read at 750 nm and protein content determined according to the Protein Assay's instructions.

For protein isolation from tissue either fresh or frozen samples were homogenized in lysis buffer (Table1) using an electric glass dounce homogenizer followed by 1h rotation at 4°C. The same protocol was then followed as described above for cells.

2.3.2 Western Blot Analysis

To determine the expression of one specific protein in cell or tissue lysates, samples of equal total protein content (30 µg) were suspended in Laemmlie Buffer (Table1), boiled for 5 min and resolved on a 10% SDS –PAGE (Mini-PROTEAN Tetra Cell, BioRad) at 100 V. The gel was allowed to equilibrate for 15 min in Transfer Buffer (Table1) and transferred onto nitrocellulose membrane (BioRad) in a Mini-Trans-Blot Electrophoretic Transfer Cell (BioRad) for 1.5 hrs at 4°C and 100 V. The membrane was blocked for 30min in blocking buffer to avoid non-specific binding (Odyssey, 927-40000) followed by addition of primary antibody (Table2) over night at 4°C. The membrane was washed three times for 5 min in TBST (Table1) and incubated for 1 h in infrared secondary antibody. The blot was visualized after 3 more 5 min washes in TBST

(Table1) using the Odyssey Infrared Imaging System (Licor). The intensity of the bands were either quantitated using the Odyssey software or Image J (rsbweb.nih.gove/ij)

Table 2. Antibodies

Antigen	Protocol	Primary Antibody Source/Dilution
Caveolin-1	Western	Rabbit anti-Caveolin-1 Santa Cruz, 1:5000, Cat.No. Sc-894
Hsp90	Western	Mouse anti-HSP90, BD Bioscience, 1:1000, Cat.No. H38220
Akt	Western	Rabbit anti-akt, Cell Signaling, 1:1000, Cat. No. 9272
Phospho-akt (Ser473)	Western	Rabbit anti-phospho-akt, Cell Signaling, 1:1000, Cat. No. 9271
actin	Western	Rabbit anti-β-Actin, Cell Signaling, 1:1000, Cat. No. 4967
Phospho-eNOS (pS1177)	Western	Mouse anti-Phospho-eNOS, BD Bioscience, 1:1000, Cat.No. 612392
eNOS	Western	Mouse anti-eNOS, Invitrogen, 1:1000, Cat.No. 33-4600
eNOS	Western	Rabbit anti-eNOS, Santa Cruz, 1:1000, Cat.No. sc-654
Thrombospondin	Western	Mouse anti-Thrombospondin, Abcam, 1:1000, Cat.No. ab1823
Nox4	Western	Mouse anti-nox4, Abcam, 1:1000, Cat.No. ab1823
Nitrotyrosine	DAB Staining	Rabbit anti-Nitrotyrosine, Millipore, 1:100, Cat.No.ab5411
4-Hydroxynonenal	DAB Staining	Goat anti-4-Hydroxynonenal, Abcam, 1:100, Cat.No. ab20953

2.3.3 Coimmunoprecipitation of Protein Complexes

Cells were lysed in IP lysis buffer (Table1) supplemented with a protease inhibitor cocktail (Sigma), 20 mM sodium fluoride, 1 mM sodium pyruvate, 5 mM orthovanadate, collected in tubes and treated as described in 2.3.1. above. 500 µg of total protein per sample were incubated with 4 µg total eNOS antibody (Table2) and rotated for 2 hrs at 4°C. Meanwhile protein A – Sepharose beads (Sigma) were washed 3 times in IP Lysis Buffer (Table1) to eliminate storage alcohol (50 µl bead-slurry per sample). After incubation in eNOS antibody 50 µl of bead-slurry was added to samples followed by rotation for 1hr at 4°C. Samples were centrifuged for 1min at 9000 rpm and resuspended in 500 µl IP-Lysis Buffer (Table1). After three 15 min washes samples were suspended in 2x Laemmli Buffer (Table1), boiled 5min and spun for 15 min at 14000 rpm.

The supernantant of each sample was then resolved on SDS-Page as described in 2.3.2 above and blotted for proteins of interest.

2.3.4 Determination of Monomer to Dimer Ratio of eNOS

Cell or tissue lysates were prepared as described above in 2.3.1. Samples of equal protein content were resuspended in Laemmli Buffer (Table1) and kept for 5 min at room temperature while one control sample was boiled to show monomer formation. Samples were then resolved on an 8% SDS-Page on ice and at 4°C at 100 V and transferred and probed against total eNOS as described under section 2.3.2.

2.3.5 Intracellular Cyclic Nucleotide Measurement

BAEC were starved overnight in endothelial basal medium plus 0.1% BSA prior to treatment. Intracellular cGMP levels were determined using an enzyme immunoassay (Amersham, GE Health Care, UK) as per the manufacturer's instructions. Data were normalized to total μg of protein with a BCA Assay kit (Pierce Biotechnology, Rockford, IL).

2.4 ENZYME ACTIVITY

BAEC were starved overnight in endothelial basal medium plus 0.1% BSA. On the day of treatment cells were incubated in assay incubation buffer (10 mmol/L HEPES, 145 mmol/L NaCl, 5 mmol/L KCl, 5 mmol/L $MgSO_4$, 10 mmol/L glucose, 1.5 mmol/L $CaCl_2$, 0.25% BSA, pH 7.4). Treatment agents were added for 15 min prior to cell stimulation using ACh (10 μM). Cells then received [^{3}H]-L-arginine (Perkins Elmer). The assay was terminated 3 min later by the addition of stop buffer (5 mmol/L L-arginine, 4 mmol/L EDTA, 4 mmol/L EGTA, 6 mmol/L L-citrulline in PBS). The cells were lysed with lysis buffer (5 mmol/L Tris-HCl (pH 7.4), 20 mmol/L EDTA, 0.5% Triton X-100), freeze-thawed twice, and the cell lysate was added to pre-equilibrated Dowex-50-H^+ columns. Equal volumes of eluent were mixed with 5 ml of scintillation cocktail, and ^{3}H-citrulline was quantified using a 1900CA Liquid Scintillation Analyzer (Packard). Lysate protein levels were determined using a BCA assay, and counts were normalized to protein levels. All conditions were assessed in triplicate, and all experiments were repeated at least three times. In other experiments cell lysates, prior to running through Dowex columns, were counted directly to measure L-arginine uptake.

2.5 ANIMAL STUDIES

2.5.1 Species and Maintenance

Wildtype C57BL/6, TPS1 null, and CD47 null male mice (Jackson Laboratories) were housed under pathogen-free conditions and had ad libitum access to filtered water and standard rat chow. All the investigations conformed to the Guide for the Care and Use of Laboratory Animals published by the US National Institute of Health (NIH Publications No.85-23, revised 1996), and were approved by the IACUC of the University of Pittsburgh and the Animal Care and Use Committee of the NCI, NIH.

2.5.2 Experiments of Vascular Reactivity

Adult male age matched C57BL/6 wild type, TSP1 and CD47 null or B6129SF2/J mice were euthanized by cervical dislocation, the vasculature was gently flushed with warm Krebs buffer via puncture of the left ventricle to remove blood and the thoracic and abdominal aorta cleaned of surrounding connective tissue *in situ* and then dissected free. Segments (3 mm in length) were mounted in a dual wire myograph system (Multi Myograph Model 610M). Vessels were allowed to equilibrate in standard PSS buffer (Table1) supplemented with 0.0031 M meclofenamate (cyclooxygenase inhibitor, IC50:0.6 μM, Sigma) and bubbled with 5% CO_2, 95% O_2 at 37°C. Passive tone of the arteries was set to 9.98 mN. Vessels were then allowed to equilibrate until baseline tension remained constant (30-60 min). Vessel viability was confirmed by a contractile response on addition of KCl buffer (Table1) supplemented with 0.0031 M meclofenamate, repeated twice for 5 min each. Concentration-response curves to phenylephrine (PE) were

carried out and a dose that produced 80% maximum contraction (EC_{80}) was chosen for establishing vascular tone prior to additional treatments. Vessels achieving at least 65% relaxation to 10^{-6} M ACh were considered to have intact endothelium. For treatment with TSP1 (2.2 nM, Athens Research) vessels were preincubated for 15 min in myograph chamber prior to PE constriction and ACh relaxation. For L-NAME (100 μM, Sigma) studies vessels were incubated prior to PE constriction for 30min to allow the competitive inhibitor to work.

2.5.3 Internal Blood Measurement via Telemetry

Mice were anesthetized using ketamine and xylazine (90 and 10 mg/kg, respectively). The telemeter catheter was inserted into the left carotid artery and advanced to reach the aortic arch, and the telemeter body (model TA11PA-C20, Data Sciences International, St. Paul, MN) was placed in a subcutaneous pocket. The telemeter signal was processed using a model RPC-1 receiver, a 20-channel data-exchange matrix, APR-1 ambient pressure monitor, and a Dataquest ART 2.3 acquisition system (Data Sciences International). The system was programmed to acquire data for 10 s every 2 min and to calculate 100 min averages of the mean, systolic, and diastolic blood pressure, pulse pressure, heart rate, and activity. Data represent the mean ± SD of 8 mice of each strain or treatment group.

2.5.4 Chronic Hypoxic Exposure as Model of PAH

Age matched male wild type, C57BL/6 and TSP1 null mice were placed in an airtight Plexiglass chamber and exposed to 10% O_2 for 21days under normobaric conditions. Mice from both strains were also maintained in room air and served as normoxic controls (n=8 for all groups).

2.5.5 Determination of Ventricular Hypertrophy and Ventricular Pressures

Mice were anesthetized i.p. with a 1:10 dilution of 1 μl/g body weight pentobarbital (Nembutal, sodium solution, 50 mg/ml). Following a tracheotomy mice were ventilated with a tidal volume 6-8 ml/kg and the thoracic cavity was opened. A calibrated Millar (Millar Instruments Inc, Houston, TX) catheter was then inserted into the right ventricle (RV) and RV systolic pressure was measured over a 30 sec interval using a PowerLab data acquisition system (AD Instruments, Colorado Springs, CO). For ventricular weight measurements, hearts were excised and atria were removed. The RV free wall was dissected, and each chamber was weighed. The ratio of RV weight to left ventricular (LV) weight plus septum (RV/LV+S) was used as an index of RV hypertrophy.

2.6 HUMAN SAMPLES

Ten human lung samples from patients not diagnosed with pulmonary hypertension were obtained from Joe Pilewski (University of Pittsburgh). Ten human lung samples from patients diagnosed with pulmonary hypertension were obtained from Hunter Champion (Johns Hopkins University).

2.7 HISTOLOGICAL STAINING

After hemodynamic measurements of the heart mouse lungs were perfused with PBS, fixed for 2 hrs with 4% paraformaldehyde (PFA at 4°C) and excised. Lungs were transferred into 30% sucrose (over night, 4°C), paraffin embedded and sectioned (10 μm). For pulmonary vascular morphometry studies images of peripheral arterioles were captured with a Nikon Eclipse 800 microscope. The diameter of measured vessels ranged between 30-70 μm. Twenty random vessels of comparable size per mouse were assessed from 4 mice per group.

2.7.1 Determination of Nitrotyrosine Formation in the Lung

Lung sections were de-paraffinized by heating sections for 30 min at 55°C and subsequent washes in xylene (2 times for 5 min) and gradual rehydration in ethanol (100% 2 times for 5 min, then 95%, 70%, 2 times for 2 min each) followed by one wash in PBS and water. Sections were then microwaved in 350 ml sodium citrate buffer for antigen retrieval (2.94 g sodium citrate/L pH 6, for 10 min) and allowed to cool for 45 min at room temperature. Sections were blocked and stained with a Rabbit anti-Nitrotyrosine antibody (Millipore) in combination with a Vectastain ABC kit (Vector laboratories, CA) and a metal enhanced DAB substrate kit (Thermo Scientific) following manufacturer's directions. Sections were counterstained for hematoxylin (Vector laboratories, CA), dehydrated in ethanol (70%, 95%, 100% and xylene) and coverslipped in mounting medium.

2.8 STATISTICS

All studies were performed a minimum of three independent times and significance was determined using the appropriate analysis with Graphpad Prizm software (San Diego, CA). Data were analyzed by 1-way ANOVA followed by Tukey test for multiple comparisons. For grouped analysis, data were analyzed by 2-way ANOVA followed by Bonferroni post hoc test.

The arterial reactivity studies were analyzed by performing a nonlinear regression on fitted curves. Significance between fitted curves was determined using a two-way ANOVA followed by the Bonferroni post test.

3.0 THROMBOSPONDIN-1 SUPPORTS BLOOD PRESSURE BY LIMITING ENDOTHELIAL NITRIC OXIDE SYNTHASE ACTIVATION AND ENDOTHELIAL DEPENDENT VASORELAXATION

Submitted for Publication

Eileen M. Bauer,[1] Yan Qin,[3] Thomas W. Miller, PhD,[5] Russell W. Bandle,[5] Gabor Csanyi, PhD, [1] Patrick J. Pagano, PhD,[1] Philip M. Bauer, PhD, [2] Jurgen Schnermann, PhD, [3] David D. Roberts, PhD, [5] Jeff S. Isenberg, MD, MPH [1*]

[1]Vascular Medicine Institute of the University of Pittsburgh and the Department of Medicine, University of Pittsburgh School of Medicine, the Department of Pharmacology and Chemical Biology, and the [2]Department of Surgery, University of Pittsburgh, Pittsburgh, PA and the [3]Kidney Diseases Branch, National Institute of Diabetes and Digestive and Kidney Diseases, and [5]Laboratory of Pathology, Center for Cancer Research, National Cancer Institute, National Institutes of Health, Bethesda, Maryland

This work was supported by NIH grant K22 CA128616 (J. S. I.) and Intramural Research Program of the NIH, NCI, Center for Cancer Research (D. D. R.) and NIDDK (J. S.).

Disclosure: J.S.I. is Chair of the Scientific Advisory Board of Vasculox, Inc. (St. Louis, MO).

3.1 ABSTRACT

Aims: Thrombospondin-1 (TSP1), via its necessary receptor CD47, inhibits nitric oxide (NO) stimulated soluble guanylate cyclase (sGC) activation in vascular smooth muscle cells, and TSP1 null mice have increased shear-dependent blood flow compared to wild type. However, circulating TSP1 is too large to traverse the endothelial basement membrane. These findings suggested that endothelial-dependent differences in blood flow in TSP1 null mice may be through direct modulation of eNOS activation by circulating TSP1. Herein we test the hypothesis that TSP1 inhibits eNOS activation and endothelial-dependent arterial relaxation.

Methods and Results: Acetylcholine-stimulated activation of eNOS and agonist-driven calcium transients in endothelial cells were inhibited by TSP1. TSP1 also inhibited eNOS phosphorylation at serine^{1177}. TSP1 treatment of the endothelium of wild type and TSP1 null, but not CD47 null arteries, inhibited acetylcholine-stimulated relaxation. TSP1 and CD47 null vessels demonstrated greater endothelial-dependent vasorelaxation compared to wild type. Conversely, null arteries demonstrated less vasoconstriction to phenylephrine compared to wild type, which was corrected by inhibition of eNOS with L-NAME. In TSP1 null mice, intravenous TSP1 blocked acetylcholine-stimulated decreases in blood pressure, and both TSP1 and a CD47 agonist antibody acutely elevated blood pressure on intravenous administration to mice.

Conclusions: TSP1, via CD47, inhibits eNOS activation and endothelial-dependent arterial relaxation and limits acetylcholine-driven decreases in blood pressure. Conversely, TSP1 and a CD47 antibody increase blood pressure. These findings suggest that circulating TSP1, by limiting endogenous NO production, functions as a pressor agent supporting blood pressure.

3.2 INTRODUCTION

The vascular endothelium is a critical regulator of blood vessel tone through its production of the bioactive gas nitric oxide (NO). NO is generated in the endothelium by the conversion of L-arginine to L-citrulline catalyzed by the NADPH-dependent enzyme endothelial nitric oxide synthase (eNOS), which requires Ca^{2+}/calmodulin, flavin adenine dinucleotide (FAD), flavin mononucleotide (FMN), and tetrahydrobiopterin (BH_4) as co-factors [72-73]. Constitutive production of NO by endothelial cells promotes blood flow by inhibiting vascular smooth muscle cell (VSMC) contracture and platelet aggregation[250]. NO-stimulated cGMP synthesis causes VSMC relaxation and decreases arterial vascular resistance by stimulating the dephosphorylation of myosin light chain-2 [251]. As such, endothelial NO is a central regulator of vascular health and blood pressure.

Recently we reported that the matricellular protein thrombospondin-1 (TSP1), via its necessary receptor CD47, limits NO signaling in vascular cells through inhibiting NO-stimulated cGMP production by soluble guanylate cyclase (sGC) [15-17]. TSP1 and CD47 null mice show increased shear-dependent changes in tissue blood flow and greater decreases in blood pressure to an NO challenge compared to wild type animals [12]. However, in the absence of disease or injury TSP1 is only found as a soluble circulating blood protein and in platelet alpha granules. With a mass of 450 kDa, TSP1 is too large to cross the endothelial basement membrane and thus, under normal conditions, cannot directly engage the vascular smooth muscle cell layer of resistance arteries. Thus it was not clear how circulating TSP1 limited tissue and blood flow responses unless it also limited primary eNOS activation and endogenous NO production.

To test the hypothesis that TSP1 regulates eNOS activation and hence endothelial-dependent relaxation we studied arterial relaxation in vessels from wild type, TSP1, and CD47

null animals. Wild type arteries demonstrated a dose-dependent relaxation to acetylcholine (ACh) which was significantly abrogated by pretreatment of the endothelium with physiologic concentrations of TSP1. TSP1 and CD47 null arteries demonstrated increased endothelium-dependent relaxation to acetylcholine compared to wild type arteries which exogenous TSP1 prevented in TSP1 null vessels only. TSP1 blocked agonist-stimulated eNOS activation and modulated calcium transients in endothelial cells. Finally administration of intravenous TSP1 and a CD47 antibody significantly elevated blood pressure in both wild type and TSP1 null mice. These results suggest that circulating TSP1, by limiting eNOS activation and endothelial-dependent arterial relaxation, functions as a pressor to support arterial tone and blood pressure.

3.3 RESULTS

3.3.1 TSP1 limits eNOS activity

The ability of TSP1 to inhibit NO-stimulated cGMP accumulation and functional responses in cultured vascular cells can be explained by CD47-dependent inhibition of the downstream target sGC [15-16, 252]. Higher basal levels of intracellular cGMP in TSP1 and CD47 null compared to wild type vascular endothelial cells [15-16] are also consistent with sGC regulation via CD47, but upstream inhibition of eNOS activation could also contribute to these results and has not been explored. To examine the ability of TSP1 to regulate basal eNOS activity, endothelial cells were treated with TSP1 for 15 min, and eNOS activity was assessed by conversion of [^{3}H]-L-arginine to [^{3}H]-L-citrulline (Fig. 4A). TSP1 inhibited basal eNOS activity at concentrations of 0.022

nmol/L. Thus, basal eNOS activity is inhibited by TSP1 concentrations equivalent to normal circulating plasma levels [253-254].

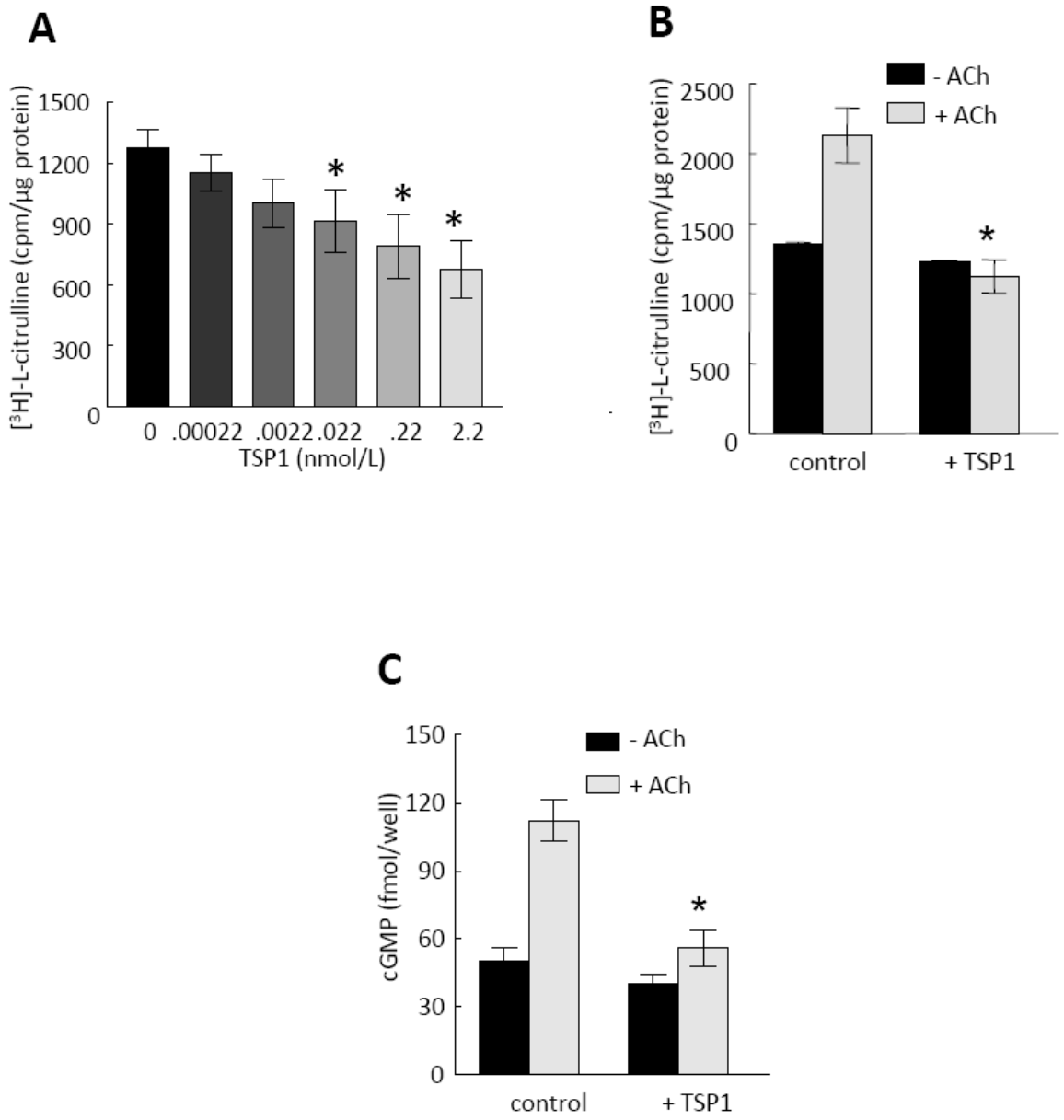

Figure 4. TSP1 inhibits basal and agonist-stimulated eNOS activity

BAEC (5 x 10^5 cells/well) were serum starved over 24 h and incubated with the indicated amounts of TSP1 (A) or TSP1 (2.2 nmol/L) followed by acetylcholine (10 µmol/L) (B) in L-arginine free minimal medium prior to adding

[3H]-L-arginine. [3H]-L-citrulline synthesis was determined as described and is presented normalized to total protein. Treatments were done in triplicate and repeated three times. $p < 0.05$ compared to untreated (A) or ACh alone (B). HUVEC (5×10^5 cells/well) were serum starved over 48 h and incubated in serum/additive free medium + 0.1% BSA and ACh (10 µmol/L) ± TSP1 (2.2 nmol/L). Intracellular cGMP levels were determined using an enzyme immunoassay.

3.3.2 TSP1 blocks eNOS activation by acetylcholine

Acetylcholine is a physiological activator of eNOS [255-256]. Endothelial cells treated with ACh demonstrated increased L-citrulline production, and this was blocked by pretreatment with 2.2 nmol/L TSP1 (Fig. 4B). Acetylcholine stimulates increases in intracellular cGMP in endothelial cells [257] and rat aorta [258]. TSP1 also completely blocked ACh-stimulated increases in cGMP levels (Fig. 4C).

3.3.3 TSP1-mediated inhibition of eNOS activation does not occur through substrate limitation

Post-translational regulation of eNOS occurs through multiple mechanisms including control of its substrates and co-factors [72, 259]. To exclude one explanation of the observed inhibition of eNOS activation we examined whether TSP1 inhibits the carrier-mediated uptake of L-arginine into endothelial cells. Pretreatment of endothelial cells with TSP1 did not significantly inhibit L-arginine uptake under conditions in which citrulline synthesis was inhibited (data not shown).

3.3.4 TSP1 modulates agonist-stimulated calcium transients in endothelial cells and murine aortas

Acetylcholine and ionomycin both activate eNOS in a calcium-dependent manner [260-262]. HUVEC showed a sustained rise in intracellular calcium in response to ionomycin. However, agonist driven calcium transients showed modulation in the plateau phase in cells treated with TSP1 compared to control cells (Fig. 5A, B). E*n face* confocal imaging of the endothelium in wild type arteries further demonstrated that TSP1 applied to the endothelial layer significantly attenuated agonist-driven calcium waves (Fig. 5C).

A

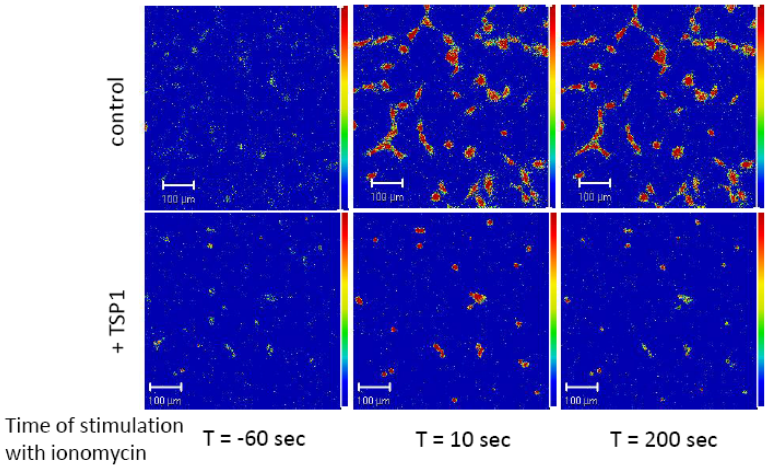

B

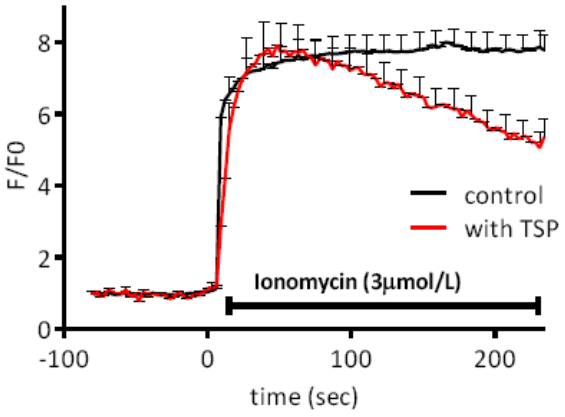

C

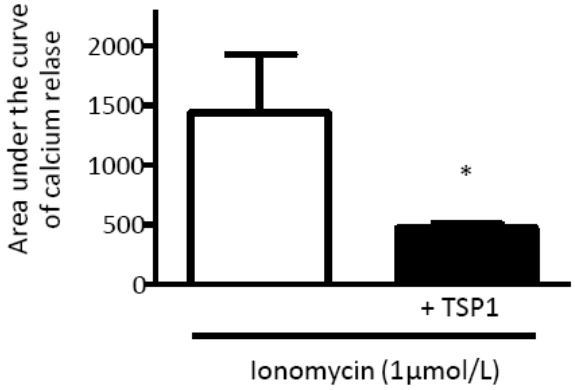

Figure 5. TSP1 modulates calcium transients

HUVEC cells were serum starved in basal medium overnight, loaded with fluo-4-AM and then pretreated with/without TSP1 (2.2 nmol/L) followed by stimulation with ionomycin (3 µmol/L). Images were acquired every 3 sec (20X, 259x259). Data analysis was performed using Pascal 3.2 software (LSM5 Pascal Zeiss) **(A)** Color Images are representative of quantification in (B) (fluorescence intensity bar on right) **(B)** Analyzed relative changes in fluorescence intensity over time (F/F0) as the result of 3 independent experiments. (untreated cells n = 113, TSP1 treated cells n = 64, +SD) **(C)** Measurement of the [Ca2+]i flux *in situ* in fresh aortic segments from wild type mice was performed using fluo-4-AM following treatment with/without TSP1 (2.2 nmol/L 15 min) followed by ionomycin. Results expressed as the change in area under the curve. Results are the mean ± SD of 6 vessels treated with ionomycin and 4 vessels treated with ionomycin + TSP1. $p < 0.05$ compared to ionomycin alone.

3.3.5 TSP1 inhibits agonist-stimulated phosphorylation of eNOS

eNOS activation by ACh and ionomycin is associated with increased phosphorylation at residue serine^{1177} in the human enzyme [263]. Treatment of HUVEC with TSP1 blocked both ACh- and ionomycin-stimulated eNOS phosphorylation at serine^{1177} (Fig. 6A, B). Findings in cultured cells

paralleled changes in whole vessels. Aortic segments from wild type mice treated with ACh showed enhanced eNOS phosphorylation at serine[1177] which was blocked by endothelial treatment with TSP1 (Fig. 6C).

3.3.6 TSP1 inhibits agonist-stimulated interactions between eNOS and Hsp90

Optimal eNOS activation requires specific protein-protein associations. Hsp90 is a chaperone protein that associates with eNOS and functions to promote correct folding and activation of the enzyme [264]. Consistent with its ability to limit eNOS activation and modulate calcium transients we found on co-immunoprecipitation that TSP1 inhibited ACh-stimulated association of eNOS with Hsp90 (Fig. 6D).

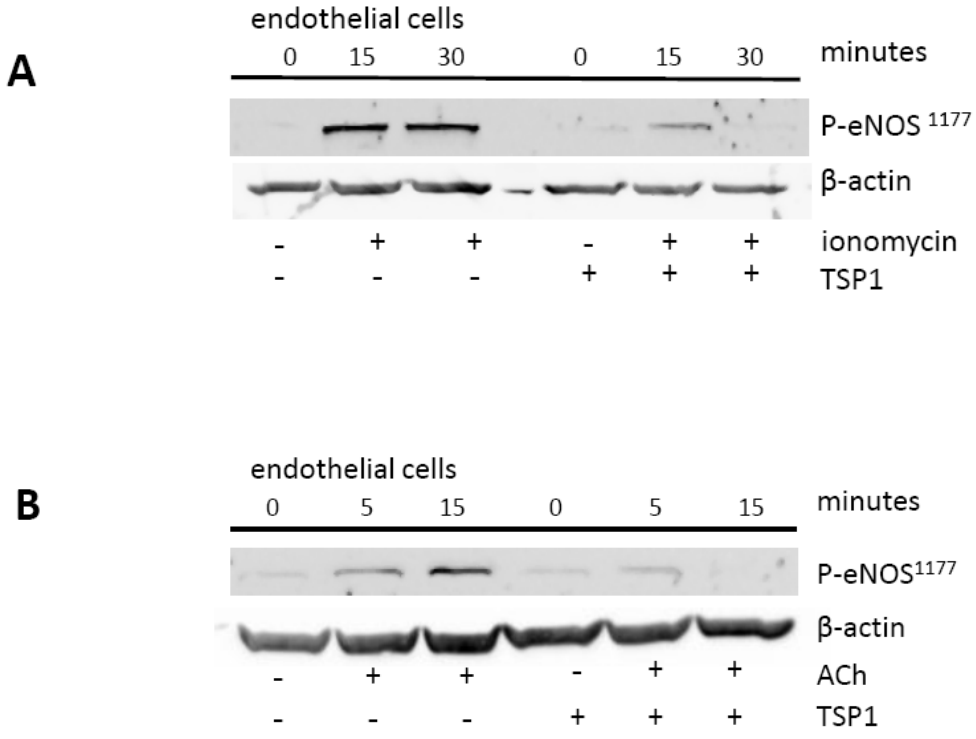

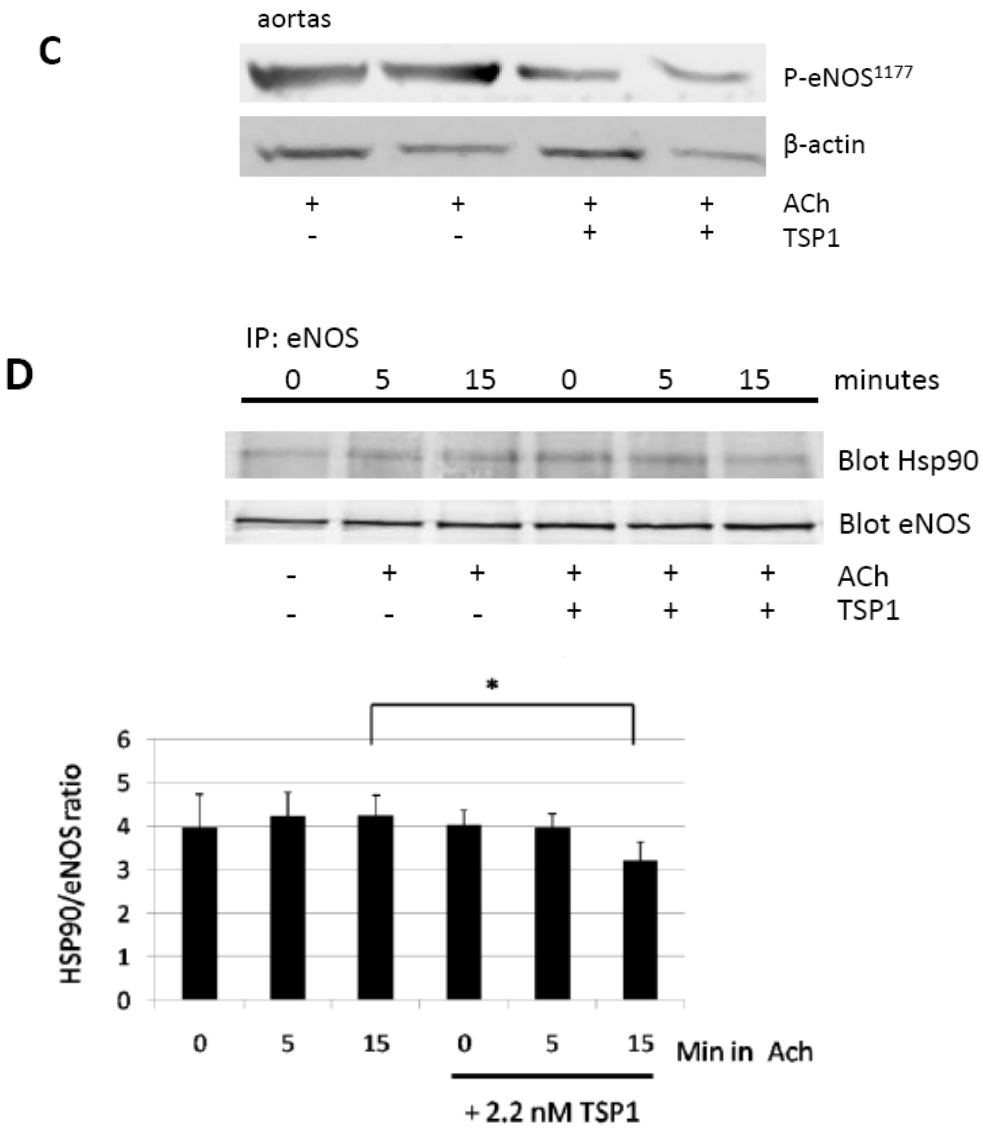

Figure 6. TSP1 inhibits agonist-stimulated phosphorylation of eNOS

HUVEC were serum starved over night and pretreated with TSP1 (2.2 nmol/L for15 min) followed by addition of ionomycin (3 µmol/L) (**A**) or ACh (10 µmol/L) for the times indicated (**B**). Lysates were prepared and Western blot analysis of eNOS phosphorylation at serine^{1177} determined. A representative blot of three experiments for each treatment is shown. Arterial segments from wild type mice were pretreated with TSP1 (2.2 nmol/L 15min) followed by ACh (10 µmol/L) and lysates blotted against eNOS phosphorylation at serine^{1177} (**C**). A representative blot of 3 separate experiments is presented. HUVEC were serum starved and pretreated with TSP1 (2.2 nmol/L for 15 min) followed by ACh (10 µmol/L) for the indicated times. eNOS was immunoprecipitated and then Western blotted against Hsp90 and quantitated using Image J (**D**). A representative blot of 3 separate experiments is presented.

3.3.7 Soluble TSP1 inhibits eNOS-dependent arterial relaxation

To test if soluble TSP1 can inhibit endothelium-dependent relaxation of blood vessels we studied *ex vivo* arterial contraction and relaxation with myography. Arterial relaxation to ACh in wild type vessels was inhibited following endothelial treatment with physiologic levels of TSP1 (0.22 nmol/L) (Fig. 7A) while higher concentrations (2.2 nmol/L) further shifted the response curve to ACh and decreased the maximum vasorelaxation response. The signature domain of TSP1, E123CaG1, that specifically engages CD47, also inhibited ACh-stimulated vasorelaxation (Fig. 7B). Thus, luminal TSP1, while not completely preventing eNOS dependent vasodilation by ACh, significantly attenuates this response. Ionomycin through activating eNOS also stimulates arterial relaxation [265]. Since TSP1 modulates ionomycin-stimulated calcium transients in endothelial cells and whole arteries, we treated wild type aortic segments with ionomycin. Importantly, TSP1 inhibited ionomycin stimulated vasorelaxation (Fig. 7C).

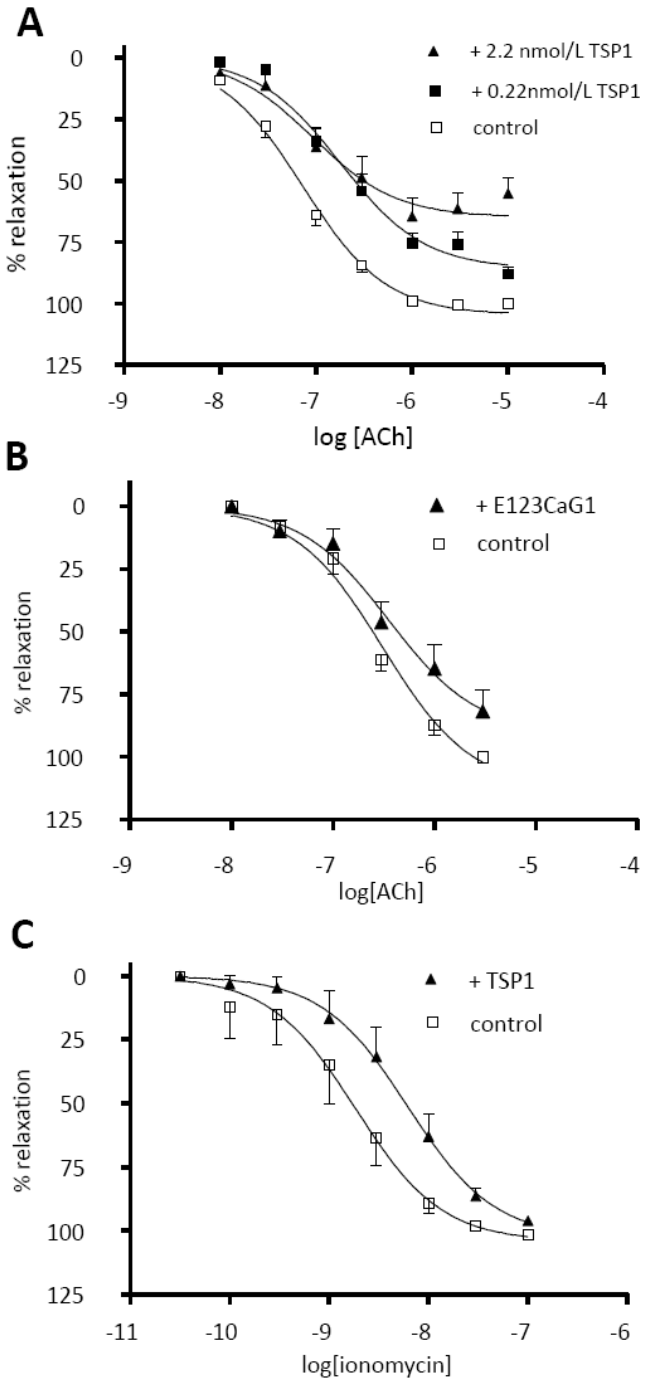

Figure 7. **TSP1 limits agonist-stimulated vasorelaxation**

Vasorelaxation of pre-contracted aortic segments from wild type male mice was determined in the presence of ACh alone. The luminal endothelium of the vessels was then pretreated with exogenous TSP1 (0.22 and 2.2 nmol/L, **A**) or a recombinant domain of TSP1 (E123CaG1, 2.2 nmol/L, **B**) for 15 minutes and vasorelaxation to ACh

determined. Results are the mean ± SD of 16 control vessels, 10 TSP1 (2.2 nmol/L) treated vessels, 6 TSP1 (0.22 nmol/L) treated vessels and 5 E123CaG1 domain (2.2 nmol/L) treated vessels. $p < 0.0001$ for both doses of TSP1 and $p < 0.0063$ for recombinant domain compared to untreated. Vasorelaxation of pre-contracted aortic segments from wild type mice was determined in the presence of ionomycin (3 μmol/L) ± TSP1 (2.2 nmol/L) (**C**). Results are the mean ± SD of 5 vessels per treatment group, $p < 0.0008$ compared to untreated. All control vessels were set to 100% relaxation and treated vessels normalized to untreated. All fitted curves were analyzed by two-way ANOVA followed by the Bonferroni post test.

3.3.8 CD47 is necessary for TSP1 inhibition of endothelial dependent vasorelaxation

eNOS-dependent arterial relaxation is enhanced in TSP1 null vessels compared to wild type (Fig. 8A). Conversely, treatment of the endothelial lining of TSP1 null vessels (which express CD47) with TSP1 inhibited ACh-stimulated vasorelaxation (Fig. 8B). However, endothelial-dependent vasorelaxation to ACh was not inhibited by treating the endothelium of CD47 null arteries with TSP1 (Fig. 8C), demonstrating that CD47 is necessary for this process.

To be certain that these responses in the null vessels are not artifacts resulting from differences in eNOS protein, we performed Western analysis of arterial segments and skeletal muscle samples from wild type and null mice. No significant differences were found in eNOS protein levels in arterial segments or skeletal muscle biopsies (Fig. 8D). Increased responsiveness in null vessels to ACh could also arise from increased sGC protein. However, no difference in sGC protein levels were found by Western blotting of lung tissue (Fig. 8E) or skeletal muscle samples (data not shown) from null mice as compared to wild type.

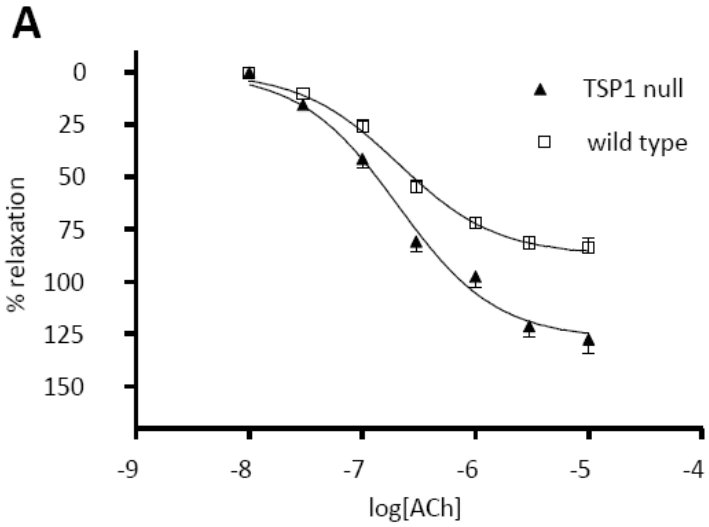
A
0
25
50
75
100
125
150
% relaxation
TSP1 null
wild type
-9
-8
-7
-6
-5
-4
log[ACh]

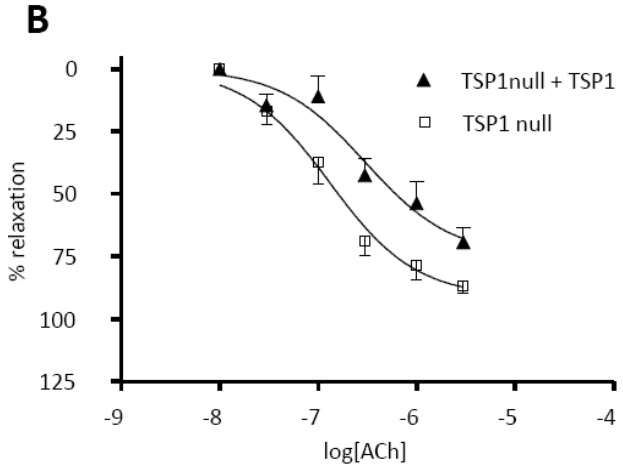
B
0
25
50
75
100
125
% relaxation
TSP1null + TSP1
TSP1 null
-9
-8
-7
-6
-5
-4
log[ACh]

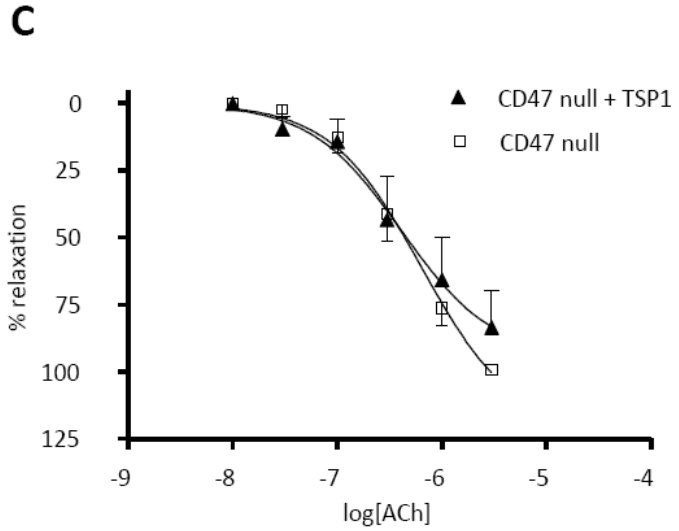
C
0
25
50
75
100
125
% relaxation
CD47 null + TSP1
CD47 null
-9
-8
-7
-6
-5
-4
log[ACh]

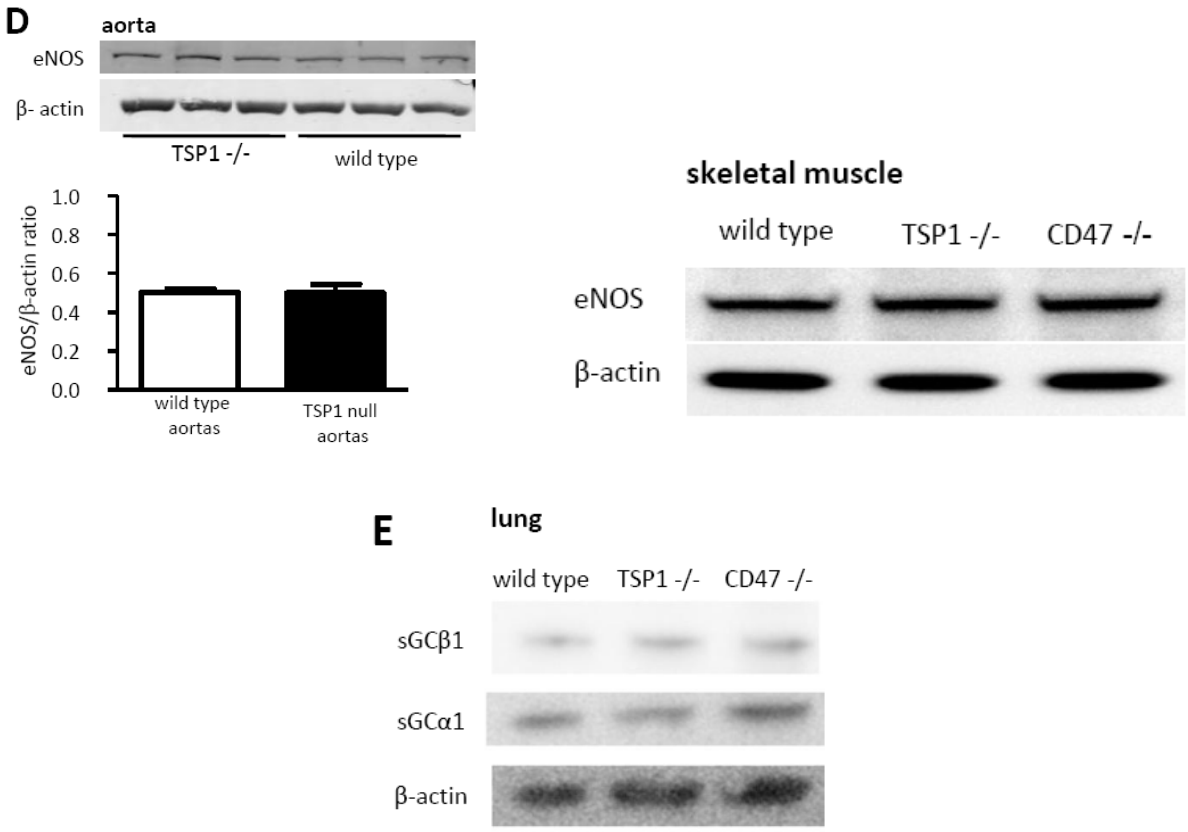

Figure 8. Inhibition of endothelial-dependent arterial relaxation by TSP1 requires CD47

Vasorelaxation dose-response curves of wild type and TSP1 null were determined to ACh (**A**). Data represent the mean ± SD of 6 TSP1 null and 4 control vessels. $p < 0.001$ TSP1 null compared to wild type on two-way ANOVA and Bonferroni post test. Vasorelaxation to ACh was determined in TSP1 (**B**) and CD47 null (**C**) aortic segments before and after treatment of the luminal endothelium with soluble TSP1 (2.2 nmol/L). Data represent the mean ± SD of 4 TSP1 null and 5 CD47 null mice. Two-way ANOVA analysis and Bonferroni post test of the significance of TSP1 treatment of TSP1 null arteries on ACh-stimulated vasorelaxation showed $p < 0.0028$ compared to untreated TSP1 null arteries. Lysates from thoracic aortic segments (n = 3 vessels per strain) and vastus medialis muscle biopsies from age and sex matched wild type and null mice were probed by Western analysis for total eNOS and quantified using Image J (**D**). For each tissue type representative blots of three experiments are presented. Lung tissue from age and sex matched wild type, TSP1 and CD47 null mice was processed for Western analysis of sGC subunits α1 and β1 (**E**). A representative blot of three experiments is presented.

3.3.9 TSP1 potentiates arterial vasoconstriction

Arterial tone represents a balance between vasorelaxation and vasoconstriction [266]. Consistent with their enhanced endothelial-dependent vasorelaxation, TSP1 and CD47 null arteries demonstrated decreased vasoconstriction to phenylephrine compared to wild type vessels (Fig. 9A, B). Inhibition of eNOS with L-NAME corrected the resistance to phenylephrine-stimulated vasoconstriction in TSP1 null arteries (Fig. 9C), providing additional evidence for increased eNOS activity in null vessels and confirming *ex vivo* our *in vivo* findings of enhanced shear-dependent perfusion in TSP1 null mice that was eliminated with L-NAME [12]. Consistent with the ability of TSP1 to limit eNOS-dependent vasorelaxation, treatment of the endothelium of wild type arteries with TSP1 more than doubled the vasoconstriction induced by phenylephrine (Fig. 9D) a response that was mimicked by the CD47-binding domain of TSP1, E123CaG1 (Fig. 9E).

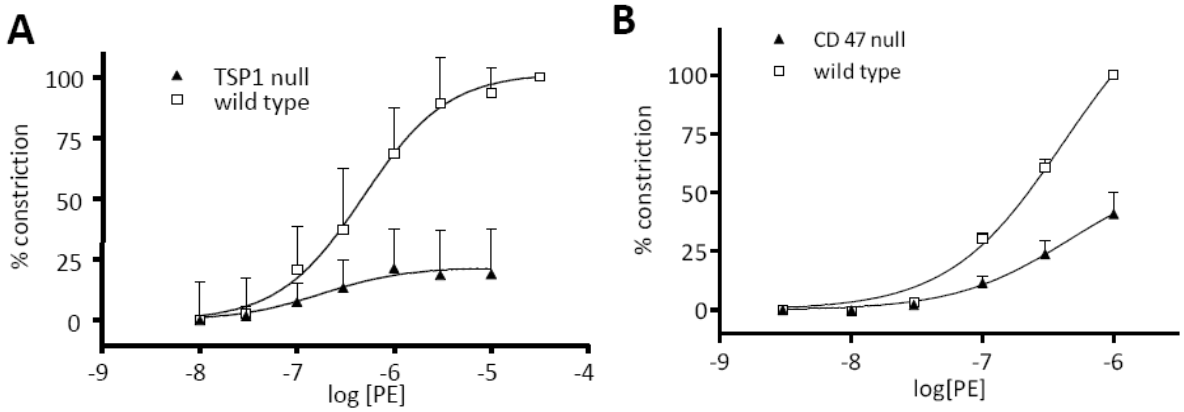

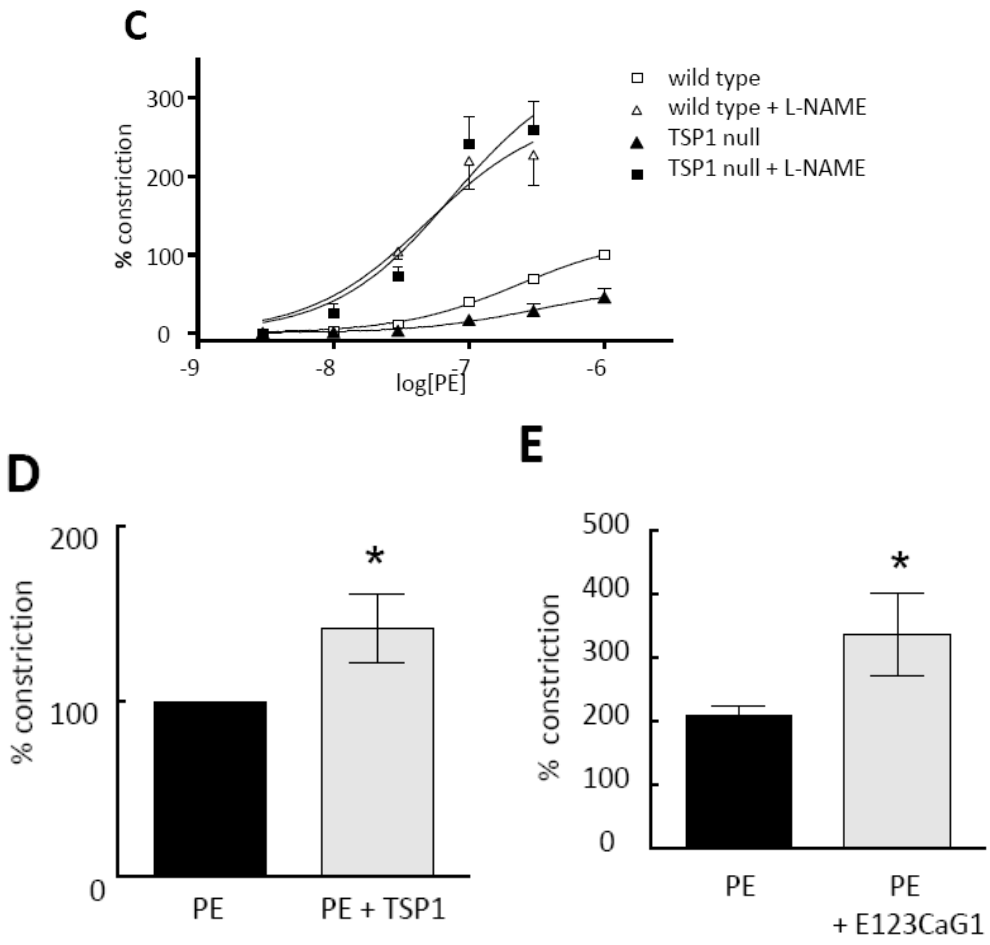

Figure 9. TSP1 potentiates phenylephrine-stimulated vasoconstriction

Vasoconstriction to PE to was determined in wild type and TSP1 null arteries (**A**) or wild type and CD47 null arteries (**B)**. Data represent the mean ± SD of 8 vessels from each strain (A) and 12 vessels from each strain (B). Two-way ANOVA analysis and Bonferroni post test of significance of PE-stimulated vasoconstriction in wild type versus TSP1 and CD47 null arteries showed $p < 0.0001$. Vasoconstriction to PE ± L-NAME (100 μmol/L) was determined in wild type and TSP1 null arteries (**C**). Data represents the mean ± SD of 5 vessels of each strain. Two-way ANOVA analysis and Bonferroni post test of significance of PE-stimulated vasoconstriction in wild type versus TSP1 null vessels showed $p < 0.0001$ compared to no difference in significance in vasoconstriction in wild type and null vessels treated with PE + L-NAME. Vasoconstriction of wild type arteries was determined in response to an EC80 dose of PE ± TSP1 (2.2 nmol/L) (**D**) or a recombinant fragment of the signature domain of TSP1 (E123CaG1, 2.2 nmol/L) (**E**). Data represent the mean ± SD of 4 vessels in each treatment group. $p < 0.05$ compared to PE alone (D, E).

3.3.10 Circulating TSP1 limits acetylcholine-stimulated changes in mean arterial pressure

To assess the *in vivo* role of circulating TSP1 in regulating eNOS-dependent vasorelaxation and blood pressure, age matched male wild type and TSP1 null mice bearing telemetric pressure transducers were treated with ACh (0.08 μg/gram weight i.v.) and mean arterial pressure (MAP) measured (Fig. 10A). TSP1 null mice demonstrated a significant decrease in MAP following ACh treatment. A similar dose of ACh in wild type animals did not result in a significant change in MAP, suggesting that circulating levels of TSP1 in the blood are sufficient to limit eNOS activation by ACh. The administered dose of ACh minimally altered heart rate in either strain of animals (data not shown), suggesting that the hypotensive effects demonstrated in TSP1 null animals were due to endothelial-dependent vasorelaxation and not secondary to acetylcholine-stimulated bradychardia. Importantly, pre-treating TSP1 null mice with intravenous TSP1 (11 pmol/L/gram weight), which was previously shown to significantly elevate circulating plasma TSP1 levels for over 6 h [267], blocked the ACh-stimulated decrease in blood pressure recapitulating the wild type response in null mice (Fig. 10B).

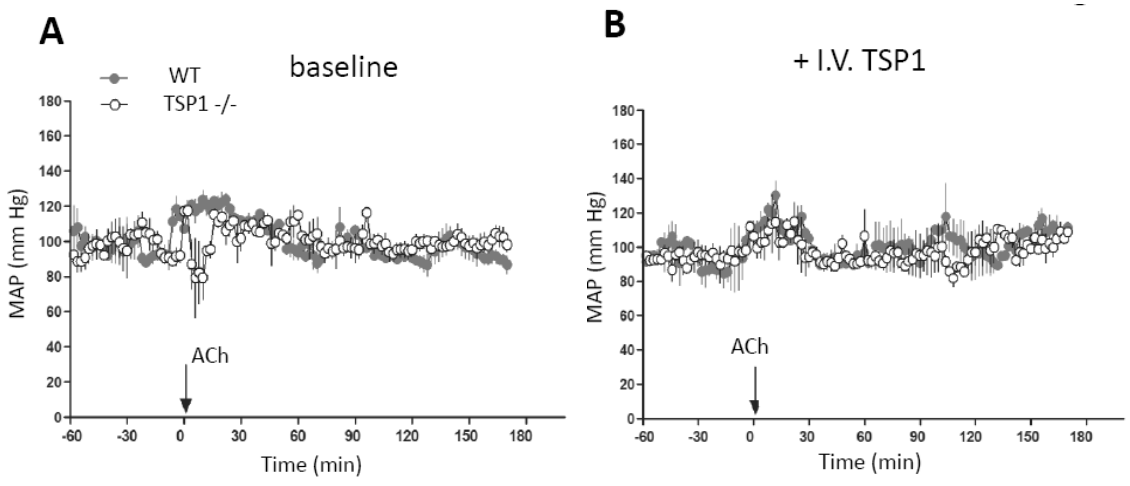

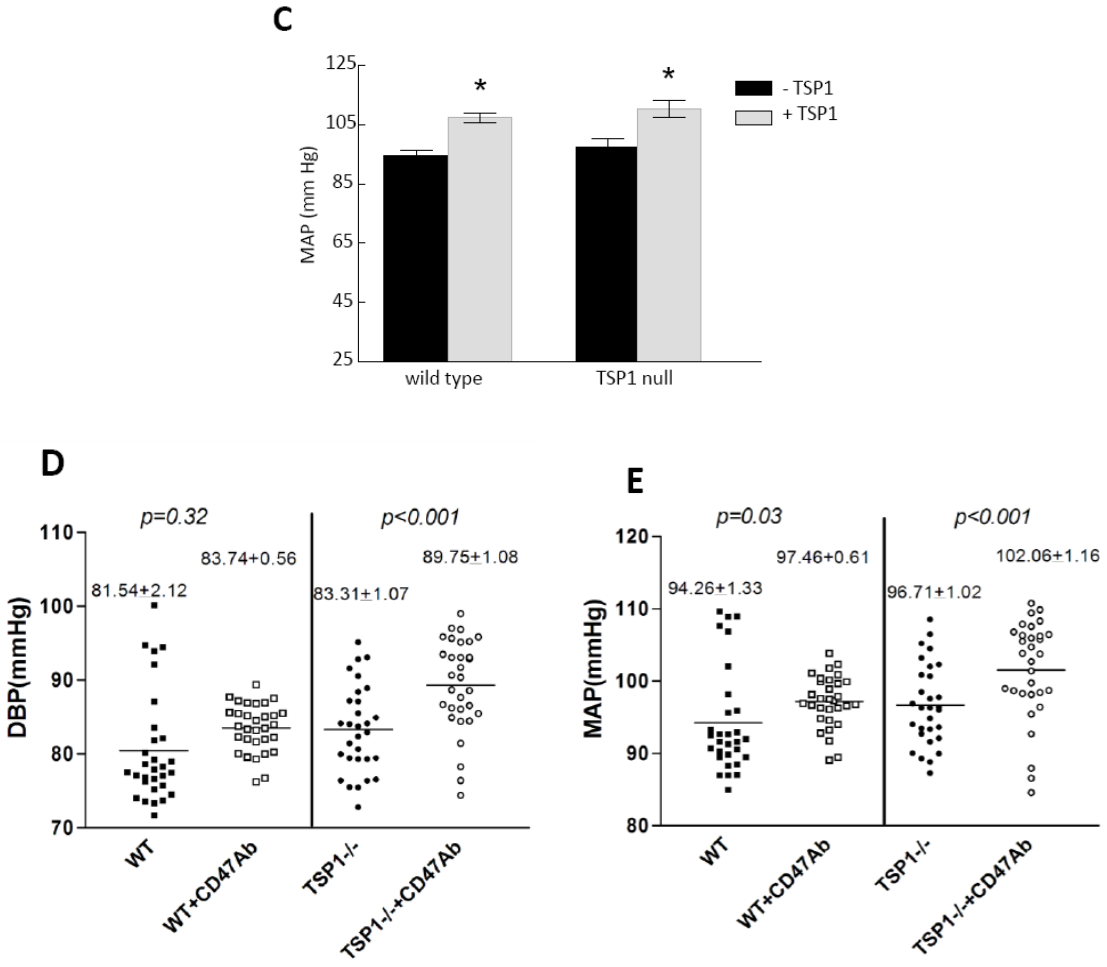

Figure 10. Circulating TSP1 limits endothelial dependent changes in blood pressure and is a hypertensive on acute administration

Age matched male wild type and TSP1 null mice bearing telemetric pressure transducers were treated with i.v. ACh (0.08 µg/gram weight) and MAP (**A**) determined. TSP1 null mice were pretreated with intravenous TSP1 (11 pmol/L/gram body weight) and followed 3 hrs later by i.v. ACh challenge and MAP determined (**B**). Age matched male wild type and TSP1 null mice were treated with intravenous TSP1 (22 pmol/L/gram body weight) and MAP determined via telemetry transducer (**C**). Results represent the mean ± SD over a 2 h time interval post-administration of 4 animals of each strain. $p < 0.05$ compared to untreated. Age matched wild type and TSP1 null male mice received a CD47 antibody (clone 301, 4 µg/gram weight) or vehicle (normal saline) and the change in MAP and diastolic blood pressure determined via telemetric transducer (**D, E**). Results represent the mean ± SD over a 2 h time interval post-administration of 8 animals of each strain (exp. in this figure were performed by Dr. Isenberg).

3.3.11 Systemic administration of TSP1 increases blood pressure in mice

Circulating levels of TSP1 have been found to be significantly elevated in several conditions associated with decreased tissue blood flow and elevated blood pressure including type I diabetes [268], dermatomyositis [269], systemic sclerosis [270] and sickle cell disease [271]. We treated telemetric transducer bearing wild type and TSP1 null mice with intravenous TSP1 (22 pmol/L/gram body weight) and followed blood pressure for 2 h. Consistent with its inhibition of endothelial-dependent vasorelaxation and enhancement of phenylephrine-stimulated vasoconstriction, intravenous TSP1 elevated MAP in wild type and TSP1 null mice ($p < 0.05$, Fig. 10C).

3.3.12 A CD47 antibody alters blood pressure in wild type and TSP1 null mice

To further explore the role of TSP1-CD47 signaling on blood pressure we studied the acute effects of a CD47 targeting monoclonal antibody on blood pressure. Wild type and TSP1 null mice were treated with CD47 antibody (clone 301) and blood pressure measured via telemetric transducer. Mimicking intravenous TSP1, engagement of CD47 with this antibody increased mean and diastolic blood pressure significantly in TSP1 null mice and mean arterial pressure in wild type mice (Fig. 10D, E). An isotype-matched control antibody did not change blood pressure (data not shown).

3.4 DISCUSSION

TSP1, via its receptor CD47, limits NO signaling in isolated endothelial cells, VSMC, and platelets by inhibiting NO-stimulated cGMP production by soluble guanylate cyclase [15-17]. Based on its mass of 450 kDa, TSP1 is unable to cross the subendothelial basement membrane in normal physiologic states. Therefore, circulating TSP1 cannot directly influence VSMC NO/cGMP signaling in intact vessels and yet TSP1 and CD47 null mice demonstrate enhanced shear-dependent changes in blood flow. We demonstrate herein that circulating TSP1 *in vivo* blocks endothelial-dependent decreases in blood pressure. Equally significant, intravenous TSP1 elevates blood pressure. This can be explained by our finding that TSP1-CD47 signaling inhibits eNOS activation in endothelial cells. Thus, TSP1 limits production of the diffusible vasodilator NO. This mechanism is consistent with our observations that addition of TSP1 to the luminal compartment in wild type and TSP1 null, but not in CD47 null arteries, decreases ACh-stimulated vasodilation. Further, treatment of the endothelium of wild type arterial segments with TSP1, and a recombinant domain of TSP1 that binds to CD47, by limiting NO production, potentiates phenylephrine-stimulated vasoconstriction.

In endothelial cells, TSP1 inhibits basal eNOS function as well as ACh-stimulated eNOS activation as measured by L-citrulline production. Importantly from a physiologic perspective exceedingly low levels of TSP1 (0.022 nmol/L) inhibited eNOS indicating that circulating levels of TSP1 are sufficient to limit both background and activated eNOS production of NO. Acetylcholine and ionomycin stimulation of endothelial cells is associated with activation of the PLC-IP_3 pathway, leading to Ca^{2+}-dependent eNOS activation and NO production [272-274]. TSP1 modulates Ca^{2+} transients in endothelial cells and blocks phosphorylation of eNOS at serine^{1177}. Thus,TSP1 modifies eNOS activity and endogenous NO production through altering cellular

calcium signaling, protein phosphorylation and protein-protein association. Acetylcholine interacts with M1 and M3 receptors on endothelial cells and through the heterotrimeric protein $G\alpha_q$ elevates IP3 and intracellular Ca^{2+} [46]. CD47 in complex with several integrins is believed to function as an atypical G-coupled protein receptor [31] In endothelial cells a CD47 antibody that blocked neutrophil activation also inhibited fibronectin-stimulated changes in cellular calcium [275]. Expanding upon these findings, our results support a novel role for TSP1 in regulating calcium in endothelial cells.

Interestingly inhibited Ca^{2+} transients in endothelial cells stimulated by ionomycin, but ionomycin does not act merely as a simple ionophore at the plasma membrane [276]. Rather, ionomycin also increases Ca^{2+} release from internal stores. Furthermore, thrombin has been shown to inhibit ionomycin-stimulated flux in HUVEC [277], indicating that physiological inhibition of this flux is possible.

Shear stress also induces a primary Ca^{2+} flux in endothelial cells and eNOS activation [278] and calcium signaling changes in isolated vascular cells are known to differ from changes in endothelium response in intact vessels[279]. *En face* analysis of arterial segments demonstrated that exogenous TSP1, on engaging the luminal endothelium, attenuated agonist-induced calcium waves on the intact endothelium. Recently pro-atherogenic turbulent flow conditions were linked to increased TSP1 expression [280]. Increased TSP1 under such conditions may account in part for the decreased NO bioavailability found in atherosclerotic arteries through modulating local Ca^{2+} transients in endothelial cells and secondary eNOS activation.

Blood pressure is determined by several factors including arterial tone [281-282]. NO is produced at low physiologic levels by the vascular endothelium at all times. Blockade of NO production using the NOS inhibitor L-NAME leads to hypertension in animals and people [283-284].

Hypertension in eNOS null mice, has been associated with increased TSP1 expression [285]. Conversely a recent clinical series noted an association between patients with hypotension and abnormally low levels of circulating TSP1 [286]. Consistent with the ability of circulating TSP1 to inhibit eNOS activation and endothelial-dependent vasorelaxation, TSP1 null animals treated with ACh demonstrated a significant decrease in MAP compared to wild type mice. Intravenous replacement of TSP1 in null mice blocked the ACh-stimulated drop in blood pressure, and in wild type and null mice intravenous TSP1 and a CD47 antibody elevated blood pressure. These new results explain in part published findings that TSP1 null mice demonstrate a greater decrease in MAP after partial sympathetic blockade compared to wild type mice [18]. Taken together, the results presented herein suggest that circulating TSP1 provides a rheostat to limit eNOS activation and NO production and in doing so exerts a pressor activity upon blood pressure.

4.0 THROMBOSPONDIN-1 IS UPREGULATED IN AND CONTRIBUTES TO PULMONARY HYPERTENSION

Eileen M. Bauer[1,3,*], Philip M. Bauer[2,3,*,§], Joesph M. Pileski[4], Hunter C. Champion[3,4], Jeff S. Isenberg, MD[3,4, §].

From the Department of Environmental and Occupational Health[1], University of Pittsburgh School of Public Health, Department of Surgery[2], Vascular Medicine Institute[3], and the Division of Pulmonary, Allergy and Critical Care Medicine[4], University of Pittsburgh School of Medicine, Pittsburgh, PA.

***Contributed equally to this work.**

This work was supported by NIH grant K22 CA128616 (J. S. I.) and NIH grant RO1 HL085134(P. M. B.)

Disclosure: J.S.I. is Chair of the Scientific Advisory Board of Vasculox, Inc. (St. Louis, MO).

4.1 ABSTRACT

Pulmonary hypertension (PH) is a fatal lung disease characterized by pulmonary vascular remodeling leading to increased pulmonary vascular resistance and right heart failure. Endothelial dysfunction is described as an initiating event leading to PH. Recently, thrombospondin-1 (TSP1) was reported to inhibit NO signaling by preventing activation of soluble guanylate cyclase and cGMP-dependent protein kinase. We thus hypothesized that TSP1 plays an important role in the pathogenesis of PH. Increased TSP1 expression was noted in humans with PH and corresponded to dysregulation of eNOS. In a mouse model of PH, TSP1-/- mice displayed minimal increases in right ventricular pressure and hypertrophy and decreased evidence of muscularized arterioles compared to WT mice. Under normoxic conditions eNOS phosphorylation was increased in lungs from TSP1-/- mice. Following hypoxia eNOS phosphorylation remained unchanged in WT lungs and was decreased in TSP1-/- lungs. Akt phosphorylation was significantly increased in WT hypoxic lungs but not TSP1-/- lungs. Alternatively, TSP-1 null hypoxic lungs exhibited a doubling of caveolin-1 expression. eNOS monomer was increased in WT and TSP1-/- hypoxic lungs but only WT mice showed evidence of increased oxidative stress. This suggests that these conditions, leading to suppression of eNOS activity in the TSP1-/- hypoxic lungs, may be protective. This hypothesis is supported by recent studies implicating overactive eNOS as the cause of PH in caveolin-1 null mice. These findings imply a dual role for TSP1 in PH. Initially, by suppressing eNOS activation and NO signaling, and later by promoting eNOS-derived reactive oxygen species.

4.2 INTRODUCTION

Pulmonary hypertension (PH) is a disease of the small pulmonary arteries marked by a progressive increase in pulmonary vascular resistance leading to uncompensated right heart failure and ultimately death [188, 193, 200]. While idiopathic PH occurs in the absence of any known insult, secondary PH results from chronic obstructive or interstitial lung diseases, scleroderma, heart disease, sleep apnea, and sickle cell disease [195, 287]. Independent of its etiology PH is characterized by remodeling of the pulmonary vasculature, vasoconstriction, and thrombosis *in situ* [193].

One of the key initiating events leading to PH is endothelial dysfunction characterized by uncoupling of endothelial nitric oxide synthase and an associated lack of bioavailable nitric oxide (NO) [288-290]. NO plays an important role in vascular homeostasis by causing vasodilation [291-292] and by suppressing VSMC proliferation [293-294], inflammation [295] and subsequent vascular remodeling. Thus it is not surprising that eNOS null mice are more susceptible to the development of PH. Regulation of eNOS activity is complex depending on phosphorylation, protein-protein interactions, and localization to specialized areas of the cell membrane. The serine threonine kinase Akt phosphorylates eNOS leading to its activation whereas Caveolin-1 (Cav-1) limits eNOS activity via direct association. Disassociation or loss of Cav-1 leads to enhanced eNOS activity and increased NO production. Paradoxically, Cav-1 null mice spontaneously develop pulmonary hypertension which is ameliorated by re-expression of caveolin-1 in the endothelium or eNOS inhibition.

Recent work by this group has found that the matrix cellular protein thrombospondin-1 (TSP1), through binding its receptor CD47, blocks physiologic NO responses in vascular cells [16-17]. Primary lung vascular cells from TSP1 and CD47 null mice demonstrate elevated levels of

cGMP indicating that endogenous TSP1 constantly limits NO/cGMP signaling. Additionally we have previously shown that TSP1 directly inhibits activation of soluble guanylate cyclase (sGC), thus cGMP production as well as activity of cGMP-dependent protein kinase [15-17]. Importantly, targeting TSP1 will maximize physiologic NO signaling, increase tissue perfusion and blood flow while minimizing inflammation and thrombosis [252, 296-298]. Thus its inhibition may offer therapeutic benefits in vascular disease.

We, therefore, hypothesized that TSP1 contributes to the development of PH in humans and that the lack of TSP1 in null mice is protective in a PH model of chronic hypoxia. Interestingly, we observed a marked increase in TSP1 expression in a cohort of patients diagnosed with primary and secondary PH. These findings in human PH were recapitulated in wild type mice with hypoxia-induced PH. Importantly, TSP1-null mice were significantly protected from the development of PH in this model in part through a decrease in oxidative/nitrosative stress and concurrent suppression of uncoupled eNOS activity.

4.3 RESULTS

4.3.1 TSP1 expression is increased in primary and secondary pulmonary hypertension

Several reports suggest that TSP1 expression is increased in cardiovascular disease [299-300]. However, there are no data on the role of TSP1 in pulmonary hypertension. Fig 11A shows a representative Western blot of lung specimens from non-PH patients, scleroderma-associated PH patients (SCD), and patients with iodpathic PH (IPAH). Densitometry of Western blots from the total cohort of 10 non-PH patients, and 10 PH patients (5 SCD and 5 IPAH) reveals a significant

increase in TSP1 protein expression in both SCD and IPAH compared to samples from patients without PH.

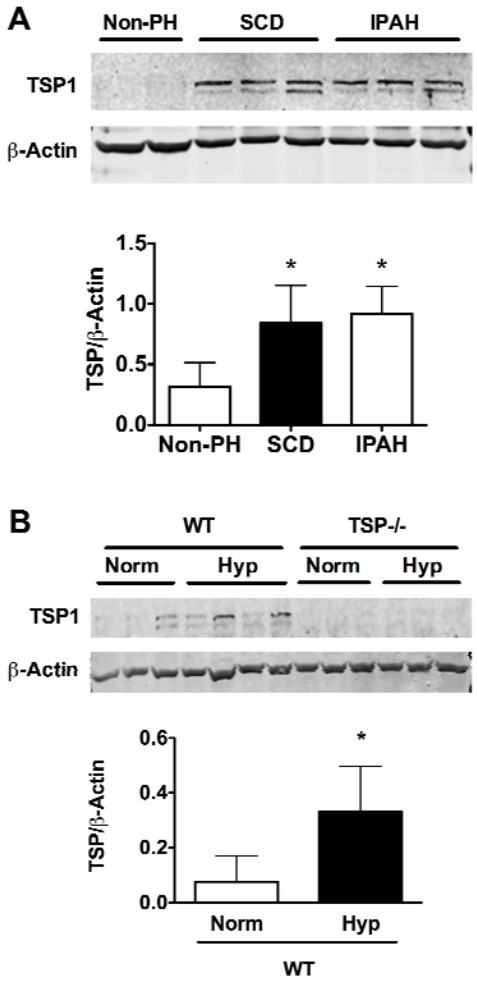

Figure 11. TSP1 expression is increased in patients with pulmonary hypertension.

(A) Lung tissue from non-PH, idiopathic PH or scleroderma associated PH patients was probed by Western blot for TSP1 and β-actin. Western blot is only representative. Densitometry below is the result of 10 non-PH patients, 5 SCD patients, 5 IPAH patients and is presented as mean ratio of TSP1 to β-actin (± S.D). * = statistically significant ($p < 0.05$) compared to non PH patients. **(B)** Representative Western blot of lung tissue from normoxic and chronic hypoxic WT and TSP1 null mice probed against TSP1 and β-actin. Densitometry is presented as mean ratio of TSP1 to β-actin (± S.D) * = statistically significant ($p < 0.05$) compared to normoxic mice and is based on analysis of 4 mice per group.

4.3.2 TSP1 exacerbates cardiovascular hemodynamics in hypoxia-driven PH

Based on the findings in the human patient samples we wished to determine whether TSP1 plays a role in the development of PH. In order to induce PH, WT or TSP1 null mice were subjected to three weeks chronic hypoxia (FIO_2 = 0.10) with animals maintained in room air serving as controls. As with the human patient population, induction of pulmonary hypertension in WT mice led to significantly increased TSP1 expression compared to normoxic controls (Fig 11B).

There was no difference in baseline RV pressures or hypertrophy in WT vs. TSP1-/- mice (Fig 12A, 12B). As expected chronic hypoxia led to a significant rise in RV pressure with associated RV hypertrophy in WT mice (n=8). However, after chronic hypoxia the loss of TSP significantly attenuated the rise in RV pressure and RV hypertrophy compared to WT animals.

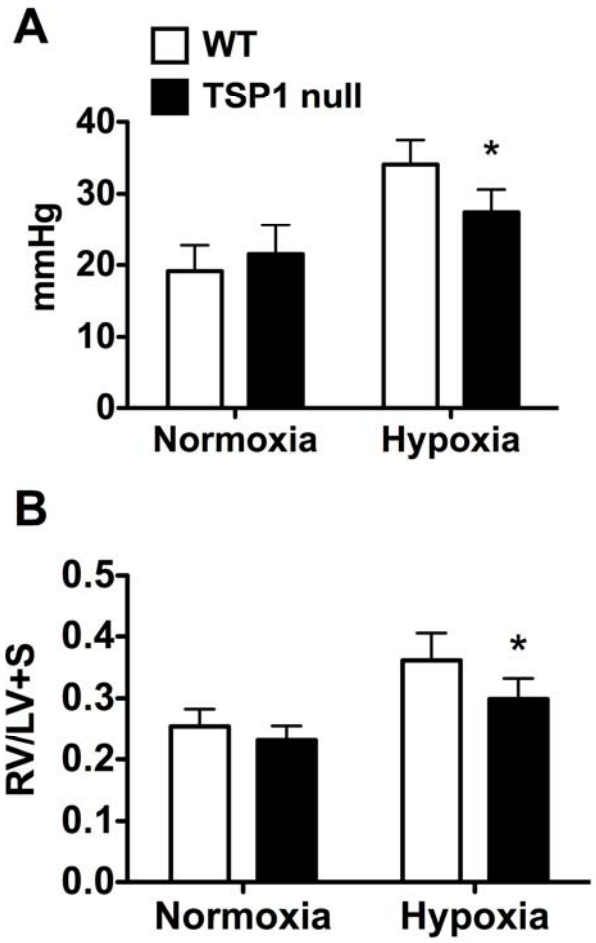

Figure 12. Loss of TSP1 protects mice from hypoxia-induced PH

WT type and TSP1 null mice were exposed to 21 days chronic hypoxia or room air. At the end of the exposure period, (A) right ventricular systolic pressure, and (B) right ventricular hypertrophy (Fulton Index) were determined. Data represent mean ± S.D. (n = 8 per group). *=statistical significance ($p<0.05$) compared to WT hypoxic.

4.3.3 TSP1 null lungs demonstrate decreased numbers of hypertrophied arterioles following chronic hypoxic challenge

A histological hall mark of pulmonary hypertension is vascular remodeling manifested as the increased presence of muscularized arterioles in the lung parenchyma [188]. Histological analysis

of tissue sections of lungs from wild type (n=4) and TSP1 null mice (n=4) subjected to 3 weeks of hypoxia was performed by an observer blinded to the genetic background of the tissue. Fig. 13B shows a representative image of H&E stained pulmonary arterioles from each treatment group. Sections of TSP1 null lungs demonstrated significantly fewer muscularized arterioles compared to lungs from wild type mice. Quantitation was based on 20 randomly picked arterioles per mouse (Fig. 13 A).

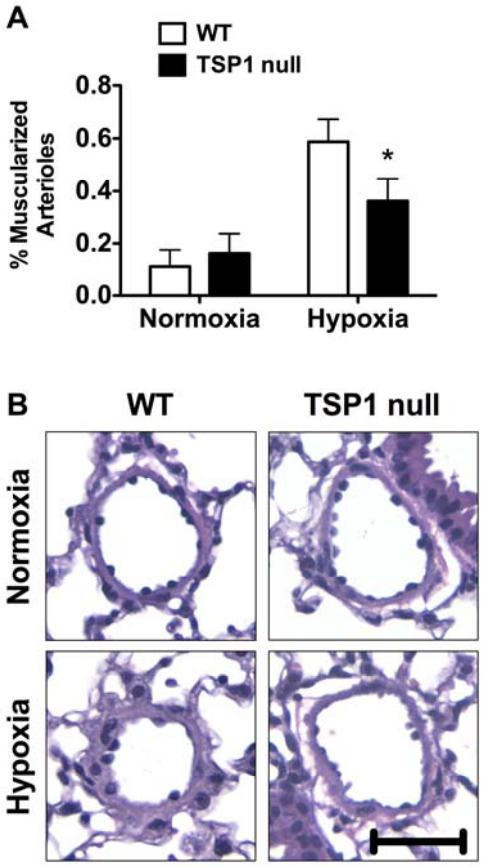

Figure 13. TSP1 null mice exhibit less arteriolar muscularization after chronic hypoxic exposure

(A) Representative images of H&E stained pulmonary arterioles from normoxic and hypoxic WT and and TSP1 null mice. Scale bar represents 50μm. **(B)** Sections of lungs were analyzed for muscularization of arterioles by a blinded observer. TSP null mice exposed to chronic hypoxia showed less muscularization than WT mice exposed to chronic hypoxia (n = 4 mice per group, analysis is the result of 20 vessels per section). * = statistical significance ($p<0.05$) compared to corresponding normoxic control.

4.3.4 eNOS phosphorylation is altered in lungs of TSP1 null mice exposed to chronic hypoxia

Fig. 14A shows a representative Western blot of WT and TSP1 null mice exposed to normoxia or hypoxia probed against, eNOS, phospho-serine 1176 eNOS or β-actin. Densitometry of protein expression was based on 4 mice per group. As previously reported, WT mice demonstrated a significant increase in total eNOS protein expression when exposed to chronic hypoxia, which was also observed in TSP-1 null mice (Fig 14B).

Maximum endothelial nitric oxide synthase (eNOS) activity and NO production are associated with phosphorylation of eNOS at serine 1176 (serine 1177 in human). WT mice exposed to hypoxia showed no change in eNOS phosphorylation compared to WT normoxic mice (Fig. 14C). Interestingly, lungs of normoxic TSP1 null mice demonstrated a significant increase in eNOS phosphorylation compared to normoxic WT mice (Fig. 14C) suggesting that TSP1 limits eNOS activity under normal physiology. In contrast, TSP1 null mice exposed to chronic hypoxia displayed a significant decrease in the ratio of phospho- to total eNOS compared to both WT and TSP1 null normoxic mice (Fig. 14C).

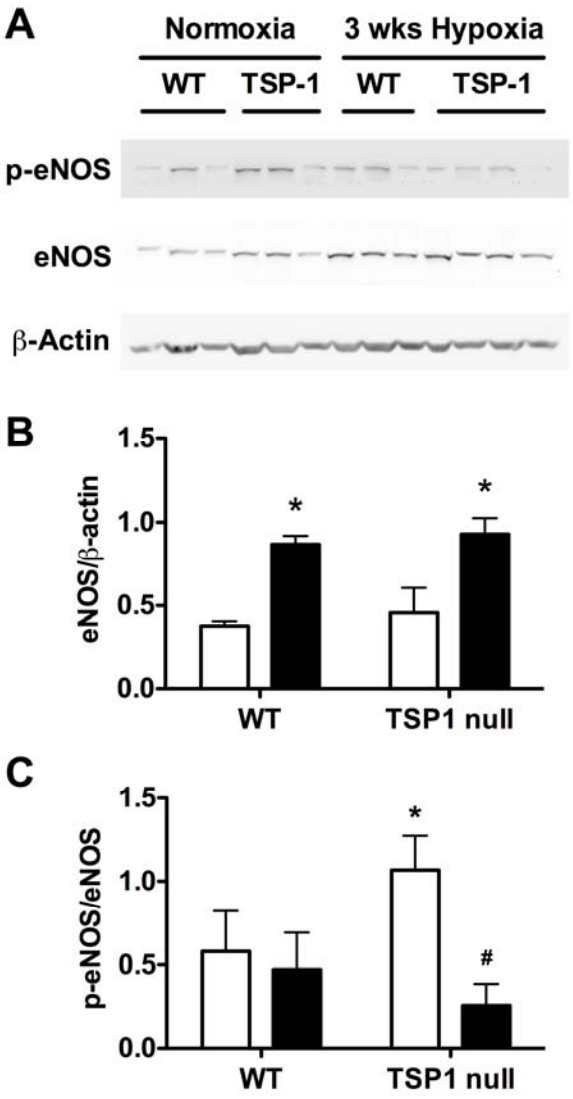

Figure 14. TSP1 changes eNOS regulation in hypoxic pulmonary hypertension

(A) Representative Western blot of lung tissue from WT and TSP1 null mice exposed to hypoxia or room air probed against total eNOS protein, eNOS phosphorylation at serine-1177, and β-actin. **(B)** Densitometry is based on 4 mice per group presented as mean ratio of total eNOS to β-actin (± S.D) **(C)** Densitometry is based on 4 mice per group presented as mean ratio of phosphorylation at Ser1177 to total eNOS (± S.D) * = statistically significant increase compared to WT normoxic ($p < 0.05$). # = statistically significant decrease compared to WT normoxic ($p < 0.05$).

4.3.5 Hypoxia-driven ROS is decreased in the absence of TSP1

Oxidative stress is known to contribute substantially to chronic vasculopathy including pulmonary hypertension. One source of oxidative stress in the blood vessel wall is uncoupled eNOS characterized by a loss of eNOS dimer (and a concomitant increase in monomer). Interestingly, both wild type and TSP1 null lungs showed a rise in eNOS monomer to dimer ratio after hypoxic challenge as shown in the representative native Western blot (Fig. 15A). Densitometry was based on 4 animals per group and showed a significant increase in eNOS monomer to dimer ratio in both WT and TSP1 null hypoxic lungs (Fig. 15B).

Nitrotyrosine is a common marker of oxidative and nitrosative stress such as that produced by uncoupled eNOS. Immunostaining of normoxic and hypoxic WT or TSP1 null mice revealed increased nitrotyrosine staining in the lungs of hypoxic WT mice (Fig 15C). In contrast, nitrotyrosine staining was unchanged in hypoxic TSP1 null mice compared to normoxic WT or TSP1 null animals.

.

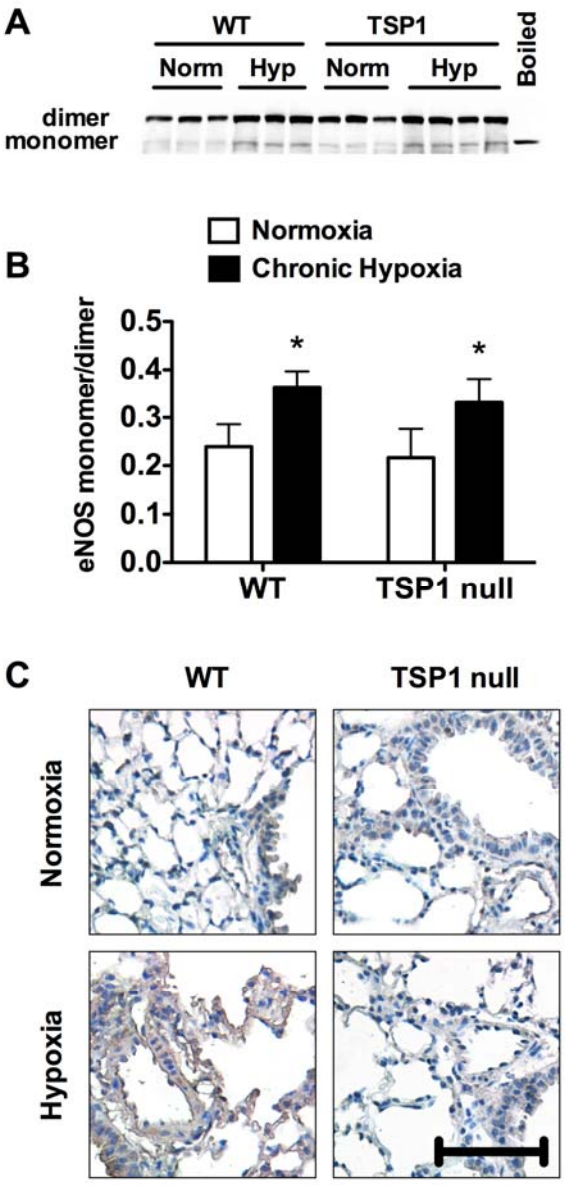

Figure 15. Loss of TSP1 prevents increased ROS production in hypoxic pulmonary hypertension

(A) Representative native gel electrophoresis probed against eNOS to determine eNOS monomer to dimer ratio in WT and TSP1 null mice after chronic hypoxia or room air. **(B)** Densitometry is presented as monomer to dimer ratio of eNOS expression ± S.D. (n = 4). **(C)** Representative photomicrographs of lung tissue from WT and TSP1 null mice exposed to chronic hypoxia or room air stained using antibodies against nitrotyrosine. Staining was performed on 2 sections from 4 mice in each group. Scale bar represents 100 μm.

4.3.6 TSP1 promotes Akt activation in hypoxic pulmonary hypertension

Activation of Akt drives eNOS activation in endothelial cells via phosphorylation of s1176 on eNOS . Also, Akt activation promotes the proliferation of vascular smooth muscle cells and thus contributes to vascular remodeling. Following chronic hypoxia total Akt expression was unchanged in wild type and TSP1 null lungs (Fig. 16A, B). Importantly, Akt phosphorylation was dramatically increased in wild type lungs (Fig. 16A, C). In contrast, TSP1 lung mice showed no change in Akt phosphorylation after hypoxic challenge. Densitometry was based on 4 animals per group. These data are consistent with both the observed changes in eNOS phosphorylation and histological evidence of decreased arterial muscularization in hypoxic TSP1 null lungs.

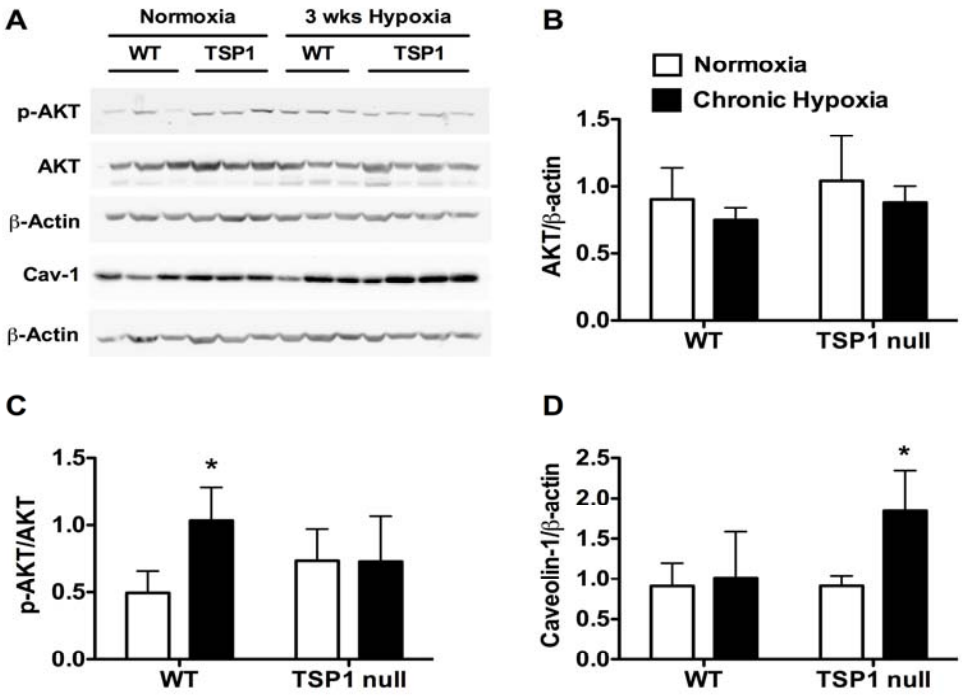

Figure 16. Effects of TSP1 on eNOS regulatory proteins in PH

(A) Representative Western blots of lung tissue from WT and TSP1 null mice exposed to chronic hypoxia or room air probed for AKT, phospho-serine 473 Akt, caveolin-1. and β-actin. **(B -D)** Densitometry is presented as ratio of **(B)** total AKT expression compared to β-actin (mean ± S.D. *n* = 4). and **(C)** phospho-AKT to total AKT(mean ± S.D. *n* = 4). **(D)** Densitometry presents ratio of caveolin-1 to β-actin expression ± S.D. (*n* = 4). * = statistically significant ($p < 0.05$) compared to WT normoxic.

4.3.7 Hypoxic TSP1 null mice show increased pulmonary Caveolin-1 expression

Besides phosphorylation, eNOS activity is also regulated through key protein-protein interactions [91, 97]. Caveolin-1 (Cav-1) binds to and inhibits eNOS and its expression is inversely related to eNOS activity. Recent data further demonstrate a role for caveolin-1 in limiting PH. Western blot reveals that lungs from TSP1 null mice express more Cav-1 protein after chronic hypoxia, whereas cav-1 expression remains unchanged in hypoxic wild type lungs (n=4 mice per group, Fig 16 A, D).

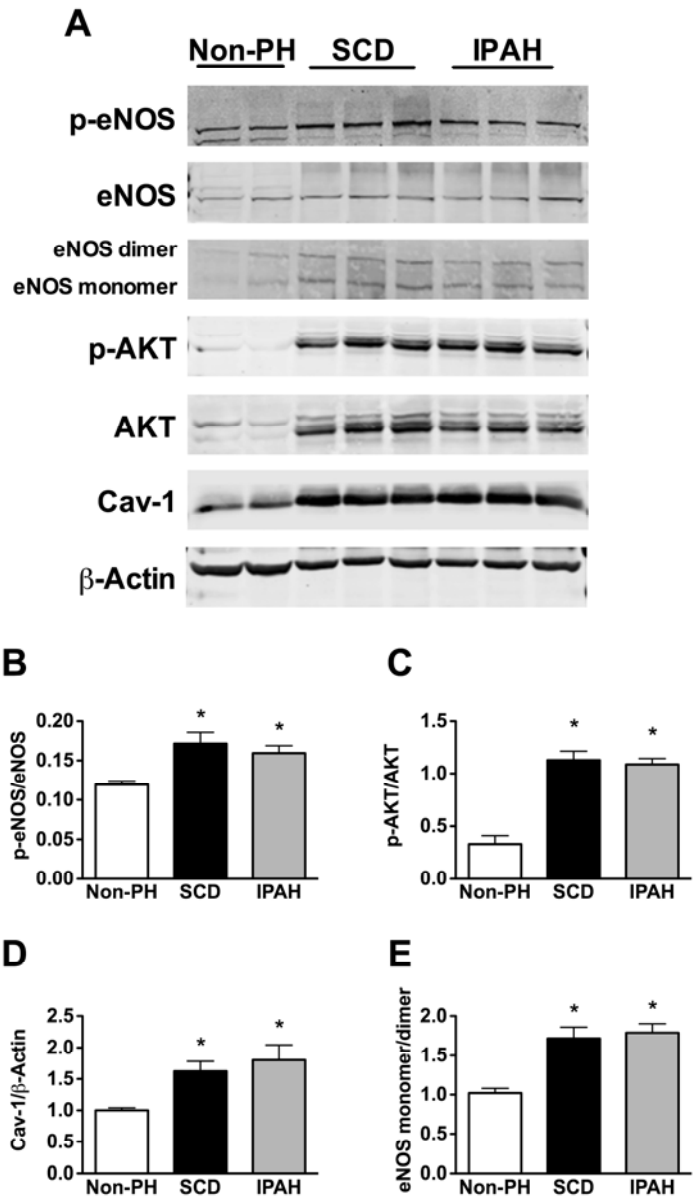

Figure 17. eNOS and AKT dysregulation in patients with PH

(A) Representative Western blots of lung tissue from non-PH, idiopathic PH or scleroderma associated PH patients probed for eNOS phosphoserine-1177 eNOS, Akt, phospho-Akt, caveolin-1 and β-Actin. **(B-E)** Quantitation of densitometric analysis of (B) mean ratio p-eNOS to total eNOS, (C) mean ratio of p-Akt to total Akt, (D) mean ratio of caveolin-1 to β-Actin, and mean ratio of eNOS monomer to eNOS dimer. All ratios represent mean ± S.D. and are the result of the total cohort (10 non-PH patients and 10 PH patients (5 idiopathic and 5 scleroderma PH). * = statistically significant ($p < 0.05$) compared to non-PH patients.

Hyperactive eNOS and AKT contribute to human pulmonary hypertension

Recent studies demonstrate that hyperactive eNOS may contribute to pulmonary hypertension. Consistent with this hypothesis, lung samples from patients with pulmonary hypertension demonstrated evidence of increased eNOS and Akt activation as shown by Western blot (Fig 17A-C). Additionally, eNOS monomer to dimer ratio was increased in samples from PH patients suggesting eNOS uncoupling (Fig 17A, D). These data were consistent with data from chronically hypoxic mice. Interestingly, in contrast to our findings in WT hypoxic mice we observed increased expression of Cav-1 in lung samples from patients with PH (Fig. 17 A, E). Densitrometric analysis of eNOS, Akt, and caveolin-1 expression was based on the total cohort of 10 non-PH patients and 10 PH patients (5=SCD, 5= IDAP).

4.4 DISCUSSION

The rationale for this study was based on two observations: 1) endothelial dysfunction is a key initiator of PH and 2) TSP1 inhibits the canonical NO pathway. We have shown previously that TSP1 in vascular cells can modulate normal vessel wall function and others have shown that increased TSP1 expression in hypoxia is linked to endothelial cell apoptosis and VSMC migration and proliferation. We show here for the first time that TSP1 expression is significantly elevated in a cohort of PH patients compared to non-PH patients. Interestingly, this increase was not just observed in patients diagnosed with idiopathic PH, but also in patients diagnosed with secondary PH. The mouse model of hypoxia-induced PH recapitulated our findings observed in patients by demonstrating a significant increase in TSP1 expression in WT hypoxic mice.

Importantly, the TSP1 null mice were protected from hypoxia-induced pulmonary hypertension. Compared to WT mice TSP1 null animals displayed significantly reduced RV systolic pressure and RV hypertrophy in conjunction with less hypertrophy of pulmonary arterioles. Since the lack of TSP1 shows protection from PH, our findings suggest that TSP1 exacerbates the development of the disease.

In order to gain mechanistic insight into the role of TSP1 in PH we explored the role of TSP1 in regard to eNOS. Under normoxic conditions, TSP1 null mice exhibited a substantial increase in eNOS phosphorylation at serine 1176 compared to WT mice. This increase in eNOS phosphorylation, and presumably activity, could be one mechanism by which the loss of TSP1 limits PH. These data also suggest that physiologic levels of TSP1 constantly limit eNOS activity *in vivo*. In the setting of hypoxia total NOS expression was increased two-fold in WT and TSP1 null animals. While we observed no increase in the ratio of phospho-eNOS to total eNOS in the WT hypoxic lungs compared to normoxia, the overall upregulation of eNOS suggests an increase in the total amount of active eNOS under hypoxia. In contrast, the ratio of phospho-s1176 eNOS to total eNOS was significantly decreased in hypoxic TSP1 null mice suggesting decreased eNOS activity in hypoxia. The difference in eNOS phosphorylation between these groups was likely due, in part, to increased expression of caveolin-1 in the TSP1 null hypoxic mice. These findings are relevant in light of recent reports that overactive eNOS, in the setting of caveolin-1 null mice, contributes to hypoxia-induced PH. In these studies, overactive eNOS was associated with increased ROS production in the lungs of the caveolin-1 null mice, which was suggested to occur in response to uncoupled eNOS.

In our experiments, hypoxia uniformly increased eNOS monomer in both wild type and TSP1 null mice. However, in contrast to wild type animals, null mice showed less evidence of

ROS in tissues consistent with a lack of superoxide production from uncoupled eNOS. Based on this current work and those demonstrating a protective role for cav-1 in PH, it is reasonable to speculate that TSP1 null mice enjoy tissue protection in part through the inhibition of uncoupled eNOS activity as a result of increased caveolin-1 expression.

The lack of increased phosphorylation of Akt in hypoxic TSP1 null mice compared to wild type mice correlates with several observations in this study. Firstly, Akt is known to phosphorylate eNOS on serine 1177 and the pattern of Akt phosphorylation closely resembles that of eNOS in this study. This suggests that, in addition to changes in Cav-1 expression, differences in Akt phosphorylation likely contribute to the differences seen in eNOS phosphorylation. Also, Akt is indirectly activated by ROS and thus the lack of Akt phosphorylation in the TSP1 null hypoxic mice correlates with decreased evidence of ROS in these mice. Finally, the Akt signaling pathway promotes vascular smooth muscle cell growth and survival and thus decreased Akt activation in the hypoxic TSP1 null mice is consistent with the observed decrease in vascular hypertrophy.

Similar to changes seen in hypoxic vs. normoxic WT mice, samples from PH patients exhibited both increased Akt and eNOS phosphorylation compared to non-PH samples. This suggests some similarity in mechanism between mouse and man. Interestingly, while we observed no change in caveolin-1 in WT hypoxic mice, samples from PH patients showed increased caveolin-1 expression. This differs dramatically from a recently published work that reported decreased caveolin-1 expression in both hypoxic WT mice and a cohort of 4 samples from PH patients. In mice, this discrepancy could be due to strain differences since the caveolin-1 null mice are on a mixed background compared to the TSP1 null mice which are on a C57Bl6/J background. In terms of the difference observed in human samples one can only speculate that

this may be due to differences in the stage of disease or perhaps in sample handling. However, as in TSP1 null mice, we would hypothesize that the upregulation of caveolin-1 in our human PH samples could be a potential protective mechanism since we observed a substantial increase in eNOS uncoupling in these same samples.

Taken together, the findings presented in this study suggest that TSP1 has a dual role in promoting hypoxia-driven PAH. Initially, by suppressing eNOS activation and later by promoting conditions leading to increased ROS. Targeting TSP1, resulting in enhancement of endogenous NO production and signaling and suppression of VSMC proliferation, may thus represent a novel therapeutic strategy for treating pulmonary hypertension.

5.0 CONCLUSIONS

5.1 TSP1 AND PULMONARY DISEASE

Pulmonary hypertension, a disease characterized by increased pulmonary pressures, is affecting an increasing number of people nationwide. There is no known cure for PH and the mortality rate remains high. While primary PH (familial or idiopathic) seems unpreventable at this point, secondary PH results from the progression of, among other diseases, interstitial lung disease, autoimmune disease, or portal hypertension. In the case of secondary PH the disease may arise from preventable causes. For example COPD and interstitial lung disease, has been attributed to environmental risk factors, including smoking, obesity, and/or air pollution.

The overall vasoconstrictive phenotype in the lung results from vascular remodeling leading to occlussion and thus hypoxic areas in the pulmonary microvasculature, elevated expression of vasoconstrictors, a decrease in vasodilatory molecules, and increased inflammation.

This dissertation presents evidence demonstrating that the soluble protein TSP1 exerts a continuously constrictive influence on the vasculature and thus blood pressure. Additionally, TSP1 levels are significantly elevated in patients suffering from PH leading to further aggravation of the disease. The data indicate that the lack of TSP1 significantly protects mice

from developing hypoxia-induce PH, as shown by vastly improved hemodynamics and decreased right ventricular and vascular hypertrophy.

It was previously shown by our group that TSP1 leads to direct inhibition of cGMP production, and thus negatively regulates the NO-mediated vasodilatory pathway. We show in this study that one mechanism by which TSP1 exerts its vasoconstrictive effect is due to direct inhibition of eNOS. These data suggest that therapies that target eNOS/NO pathway may be limited by the presence of endogenous TSP1. Thus, these discoveries may lead to better drug development that focus on TSP1, its necessary interaction with CD47, and its downstream inhibitory effect on eNOS.

5.2 TSP1 - A NOVEL DAMPER OF NO

Proper function of eNOS is critical in maintaining blood pressure. Its dilatory role in physiology has been well established and studied over the last two decades. It also is not surprising that acute release of constrictive agents shifts the balance established by eNOS towards hypertension. However, here we show that thrombospondin-1 which is endogenously and constitutively expressed as soluble protein in the blood, dampens the dilatory effect of eNOS under healthy steady state conditions.

It was previously shown by our group that addition of TSP1 to vascular cells, via its necessary interaction with the receptor CD47, results in decreased cGMP levels, a downstream product of the NO activated -dilatory pathway. In this thesis we present data demonstrating for the first time that levels of TSP1 that fall within the normal physiologic range observed in blood, inhibit the NO mediated-pathway upstream of cGMP production, at the level of eNOS. We

further show in isolated aortas of wild type mice that addition of TSP1 at these normal physiologic levels (2.2 nM) shifts the dose-response curve of endothelial dependent relaxation upwards (Fig.7A). Vessels treated with TSP1 thus require a higher dose of ACh to obtain the same level of endothelium-dependent relaxation as observed in untreated vessels. As proof of principle we further demonstrated that addition of TSP1 had no effect on vessels isolated from CD47 null mice (Fig.8C). In addition infusion of low levels of TSP1 (2.2nM) into anesthetized TSP1 null mice as well as wildtype mice significantly raised their blood pressure indicating that TSP1 functions as vasopressor by dampering NO production (Fig.10).

5.3 TPS1 AS NEGATIVE REGULATOR OF ENOS

The regulation of eNOS is complex and full activity of the enzyme is dependent on its phosphorylation at specific residues, interaction with other proteins, as well as cellular calcium and oxygen levels. *In vitro* studies in systemic human endothelial cells demonstrated that the interaction of TSP1 with CD47 inhibits eNOS at various levels. Treatment of endothelial cells with TSP1 resulted in drastically decreased enzyme phosphorylation at serine 1177, a well established phosphorylation site indicative of enzyme activity, in response to ACh (Fig.6B). We additionally checked for phosphorylation at threonine 495, a site known to mediate inhibition of eNOS. In our hands we did not observe any change in phosphorylation at that site (data not shown). Others have found similar difficulties observing phosphorylation events at that threonine to known inhibitors of eNOS (PM Bauer, Bill Sessa).

The interaction of a variety of proteins with eNOS influences its enzymatic activity as well. Activation of eNOS has been shown to coincide with dissociation of cav-1, increased

association with HSP90, and increased association with the calcium-dependent protein calmodulin. Pretreatment of endothelial cells with TSP1 resulted in an abrogation of the normal increase in HSP90/eNOS association in response to ACh. We were unable to detect changes in cav-1 association with eNOS after TSP1 exposure (data not shown). The regulation of eNOS is dynamic and our results do not exclude the possibility that changes in the interaction of eNOS with cav-1 could change over time or under different stimulatory conditions.

Interestingly, we observed that addition of TSP1 led to modulation of calcium flux in response to ACh (Fig. 5) in both cultured endothelial cells as well as the isolated mouse aorta. We initially assumed that this modulation of calcium flux would also translate to visible changes in the interaction of eNOS with the calcium-dependent protein calmodulin. However, we did not observe this under our conditions (data not shown). Further exploration of calcium's exact role and mechanism in the context of TSP1 will be interesting for future studies.

Independent of the exact dynamic changes occurring on eNOS itself due to exposure to TSP1, the overall outcome showed a significant decrease in enzyme activity. Ultimately decreased eNOS activity leads to decreased production of NO, decreased cGMP production (as previously shown by our group) and an overall increased vascular tone. Summarizing, we thus demonstrated for the first time that TSP1 inhibits eNOS activity and that the mechanism of inhibition occurs at multiple levels.

5.4 THE ROLE OF TSP1 IN PULMONARY HYPERTENSION

Analysis of lung tissues from patients with PH demonstrated a significant increase in TSP1 protein expression and led to our exploration of TSP1's role in this disease using the model of

hypoxia-induced pulmonary hypertension. We observed that TSP1 null mice exposed to chronic hypoxia were significantly protected from the development of PH. In comparison to WT mice with hypoxia-induced PH, TSP1 null mice displayed lower right ventricular systolic pressures, lower right ventricular hypertrophy as well as less arteriolar muscularization in the lung. We also observed their ability to thrive under hypoxic conditions by not losing body weight as compared to the WT mice (Supplemental Figures under Appendix A).

Further experiments focused on changes in eNOS regulation and revealed that cav-1 expression is increased in the hypoxic TSP1 null compared to the hypoxic WT mice. While both hypoxic groups experienced the same level of eNOS uncoupling and thus increased ROS production, this harmful effect is dampened by the overall inhibitory effect that cav-1 has on eNOS (Fig). Additionally nitrotyrosine staining of the pulmonary vasculature, characteristic of ROS production, was decreased in the hypoxic TSP1 null mice compared to the strong staining of the hypoxic WT mice.

One of the most commonly prescribed drugs to treat PH is sildenafil, a PDE5 inhibitor. By inhibiting enzymatic activity of PDE5, the breakdown of cGMP is slowed, increasing the overall cGMP levels and thus leading to increased vasodilation. Though widely prescribed, it has also been shown that many patients seem not to respond to PDE 5 inhibitors. This dissertation has demonstrated that 1) TSP1 inhibits eNOS directly and 2) that TSP1 levels are significantly increased in PH patients. It might thus be possible that drugs targeting this pathway downstream of eNOS will have less efficacy due to upstream inhibition of eNOS as well as inhibition of sGC and PKG.

Another group of drugs used to treat PH targets vasoconstrictors. Increased levels of vasoconstrictors have been observed in patients with PH and a variety of antagonists have been

developed. This dissertation demonstrates that TSP1 functions as pressor and thus can contribute to the overall increased vasoconstictive vascular tone in PH.

The development of drugs that target CD47 directly or TSP1 might therefore be able to treat two problems by developing one drug that can block the TSP1/CD47 interaction. It would lower the vasoconstrictive effect of TSP1 and would remove the inhibition of eNOS.

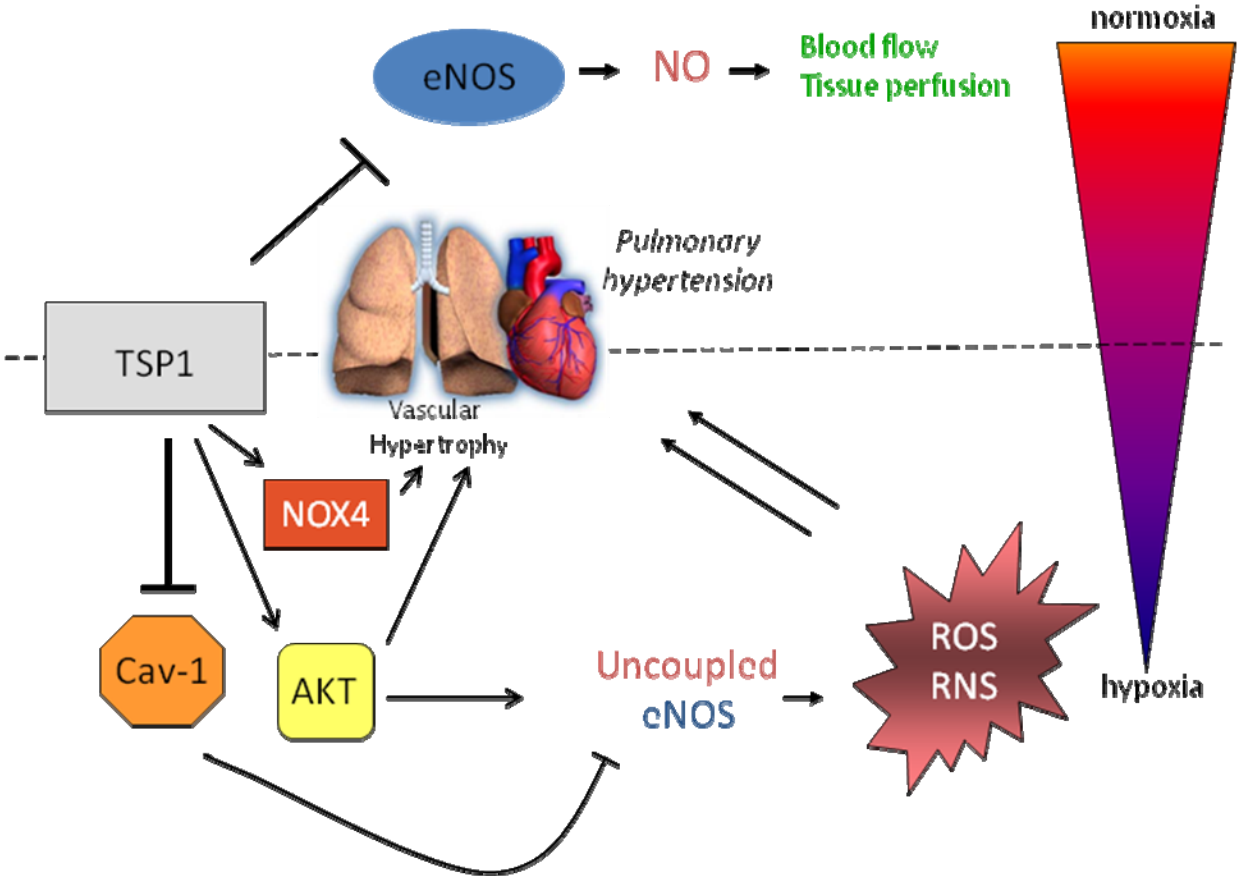

Figure 18. Schematic describing the proposed role of TSP1 in pulmonary hypertension.

TSP1 is proposed to play a dual role in the development of pulmonary hypertension. Initially, by limiting eNOS activation and downstream signaling, TSP1 may lead to loss of bioavailable eNOS and endothelial dysfunction. As the disease progresses TSP1 promotes conditions leading to increased superoxide production from uncoupled eNOS including increased Akt activation and suppression of caveolin-1 expression.

5.5 SUMMARY AND FUTURE DIRECTIONS

The studies herein illustrate two novel findings: first, addition of TSP1 to cells and isolated vessels and animals, inhibits the classical NO-mediated vasodilatory pathway by directly inhibiting eNOS activity. This effect of TSP1 is upstream of its previously shown inhibition at the cGMP and PKG level. Secondly, in the disease setting of pulmonary hypertension, TSP1 levels of patients are significantly elevated and, in an animal model, aggravate the progression of the disease. We further observed that the effect of TSP1 is associated with increased production of reactive oxygen species. Taken together, these studies demonstrate that TSP1 acts as novel negative regulator of the NO dilatory pathway and targets it at multiple levels. We further observed that TSP1 is intimately involved in vascular disease. In summary, as this new role of TSP1 in the vascular environment emerges, it creates new targets for the development of therapeutic drugs.

The main goal of this study was to shed light onto the role of TSP1 in a physiologic setting by focusing on the organism as a whole. Future studies therefore can further decipher the exact mechanisms involved that are regulated by TSP1 as demonstrated by us here. As such the modulation of calcium flux in response to TSP1 could lead into studies of G-protein coupled receptor signaling occurring possibly in parallel to the regulation of eNOS. Another question to be explored would be the potentially limiting effect of calcium flux on the ability of eNOS, a calcium dependent enzyme, to fully function. The regulation of eNOS is very complex, depending not only on certain phosphorylation sites but also several cofactors and interacting proteins. It would be beneficial to understand the temporal order of events leading to decreased eNOS activity to allow for more specific drug targets.

While this study focused on the role of TSP1 in pulmonary hypertension, it would be beneficial to extend this research to other vascular diseases of endothelial dysfunction, like atherosclerosis or diabetes. For the studies discussed here we focused on the endothelium. However, another unknown is the role of TSP1 on smooth muscle. In atherosclerosis the smooth muscle layer extends into the lumen of the vessel proliferating past the endothelium and thus is in direct contact with TSP1. All of these studies will help us to better understand disease and hopefully allow us to treat and ultimately prevent it.

APPENDIX A: SUPPLEMNTAL FIGURES

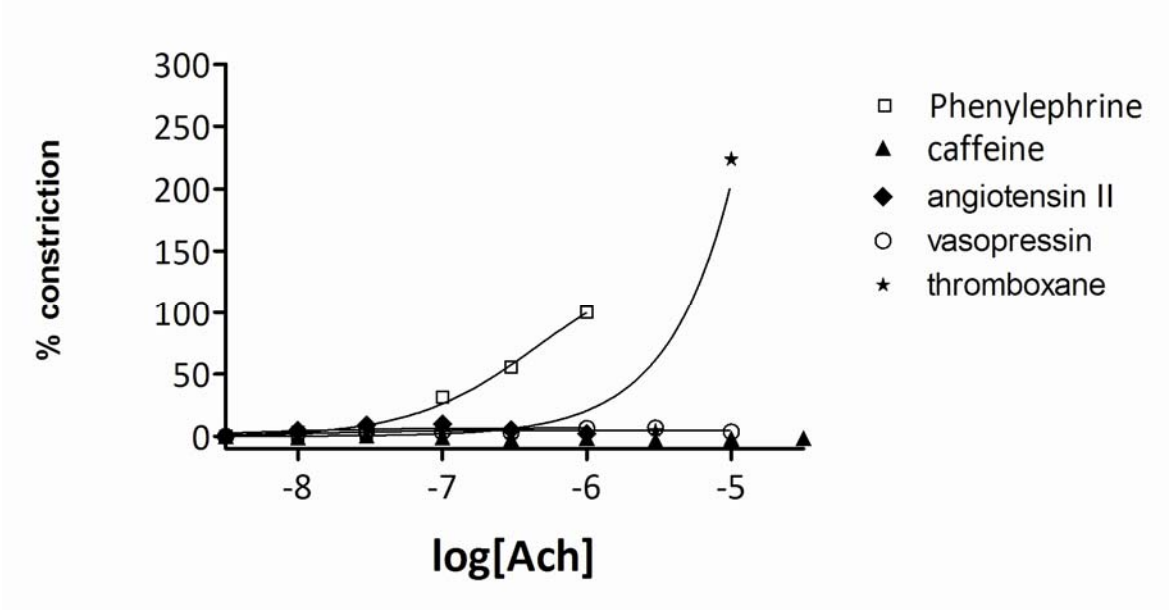

Figure 19. Myogenic response of CD47 null to a variety of vasoconstrictors

A variety of different vaso-constrictors was added sequentially to four aortic rings of one CD47 null mouse. The maximum response to PE was set to be 100 % and compared the other agonists. Interestingly these null vessels only responded to PE and thromboxane. However, even the PE response is significantly blunted when compared to a WT mouse.

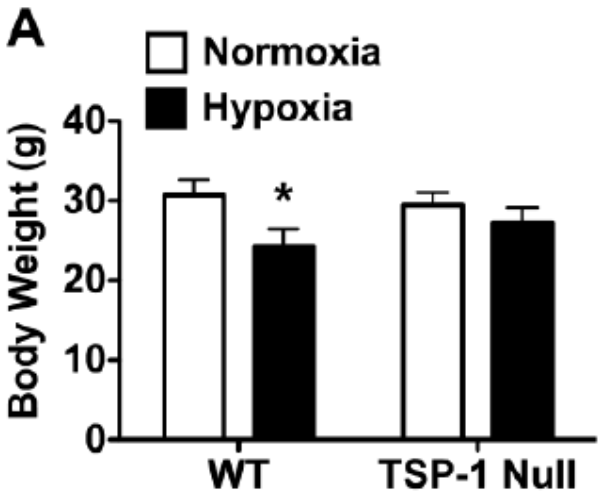

Figure 20. TSP1 null mice thrive under hypoxia

After 21 days of exposure to hypoxia, TSP1 null mice did not lose any significant amount of body weight compared to hypoxic WT mice. Taking body weight as an indicator of overall well being, the TSP1 null mice appeared to thrive compared to WT mice (n=8 per group, * = $p<0.05$significance)

APPENDIX B: ZINC-INDUCED ACTIVATION OF PKC-EPSILON MODULATES HYPOXIA INDUCED CONTRACTION OF PULMONARY ENDOTHELIUM

Eileen M. Bauer[1], Rong Cao[1], Jun Chen[2], Q. Jane Wang[2], Salony Maniar[1], Bruce R. Pitt[1] and Claudette M. St. Croix[1]Departments of Environmental and Occupational Health[1], University of Pittsburgh Graduate School of Public Health and Department of Pharmacology[2] University of Pittsburgh School of Medicine

Submitted for Publication

ABSTRACT

PKCepsilon (PKCε) is a novel calcium independent and zinc sensitive kinase that has been implicated in vascular contraction. Our lab has previously shown that acute hypoxic exposure induces nitric oxide (NO)-mediated increases in intracellular labile zinc in pulmonary endothelium which contribute to contraction of small intracinar arteries of the isolated perfused lung (IPL) [301].We now show that inhibition of PKC by Ro-31-8220, or infection with a herpes virus expressing dominant negative PKCε, significantly attenuated the hypoxia induced contraction of isolated pulmonary endothelial cells, and that pharmacologic inhibition of PKCε significantly decreased hypoxic pulmonary vasoconstriction (HPV) in the IPL. Cell fractionation andWestern blot analysis revealed that either hypoxia, or exogenously applied zinc, induced

translocation of PKCε from the cytosolic to the membrane fraction in isolated pulmonary vascular endothelial cells that were accompanied by NO-dependent increases in PKCε activity. Furthermore, zinc-induced phosphorylation of the contractile regulatory protein, myosin light chain (MLC) was shown to be PKC -dependent. Collectively, these data suggest that PKCε serves one effector molecule mediating zinc/hypoxia-induced constriction in the pulmonary microvasculature.

INTRODUCTION

Hypoxic pulmonary vasoconstriction (HPV) is a complex, multifactorial phenomenon resulting in the shunting of blood from areas of poor gas exchange to better ventilated regions of the lung [302]. As such, HPV is an important physiologic regulator of ventilation:perfusion matching in the lung; though sustained HPV is associated with vascular remodeling ultimately leading to pulmonary hypertension. While the precise mechanism underlying HPV remains unclear, it is thought that intrinsic properties of pulmonary vascular smooth muscle (oxygen sensing and coordination of ionic conductances) that are modulated by communication with endothelium (biosynthesis of vasoactive substances including NO) account for hypoxic mediated vasoconstriction of pulmonary arteries [303]. Our previous studies showed that zinc thiolate signaling is a component of acute hypoxia mediated NO biosynthesis and that this pathway contributes to hypoxic induced vasoconstriction within the pulmonary microcirculation [301].

The mechanism by which zinc can induce vasoconstriction in the pulmonary vasculature is not known. However, zinc-associated proteins account for a large part of mammalian proteome and many of these candidate targets are components of signaling and effector pathways in cellular contraction. Intracellular zinc concentrations have been shown to influence protein kinase C

(PKC) activity and processing [304-306]; and PKC is an important signaling molecule mediating contractile responses in both the systemic and pulmonary circulations [307-309]. While the roles of individual isoforms of PKC in the control of pulmonary vascular reactivity have not been clearly defined, PKCε has been implicated in contraction of the systemic vasculature [310] and is a critical mediator of ischemic preconditioning in the myocardium [311-312]. Pertinent to our studies of pulmonary vascular reactivity, wide-body deletion of PKCε was shown to blunt murine HPV leaving ANGII and KCl responses preserved [313]. We hypothesized that PKCε, a zinc sensitive signaling molecule in HPV transduces hypoxia mediated changes in zinc homeostasis to induce constriction of the pulmonary microvasculature.

METHODS

Chemicals and Materials: All reagents were purchased from Sigma-Aldrich (www.sigmaaldrich.com) unless otherwise noted. The GFP-dominant negative PKCε herpes simplex virus was provided by Joseph Glorioso [314].

Cell Culture: Cells were grown at 37°C with 5% CO_2. Details regarding the harvest and culture of sheep pulmonary artery endothelial cells (SPAEC) are described elsewhere [315]Rat pulmonary microvascular endothelial cells (RPMEC) and rat aortic endothelial cells (RAEC) were purchased from VEC Technologies (VEC Technologies Inc, Resselaer, NY) and grown in complete MCDB-131 (Lonza). Rat pulmonary artery endothelial cells (RPAEC) were grown in Dulbecco Modified Media (Fisher Scientific) with 10% fetal bovine serum, 2 mM glutamine, 100 U/ml penicillin/streptomycin.

For the zinc treatments described in subsequent sections, cells were incubated in 10 μM zinc in combination with the zinc ionophore, pyrithione (5 μM). Chelation of intracellular zinc

was achieved by preincubation of cells with N,N,N',N'-Tetrakis-(2-pyridylmethyl)-Ethylenediamine (TPEN,10 μM) for 30 m prior to any additional treatment.

Animals: Sprague Dawley rats were purchased from the Jackson Laboratories (Bar Harbor, ME) and housed in a pathogen free environment with ad libitum access to filtered water and standard rat chow. All studies were performed using protocols approved by the Institutional Animal Care and Use Committee (IACUC) at the University of Pittsburgh and following the guidelines of the American Physiological Society.

Cell Membrane Fractionation: Cells were lysed (100 mM Tris·HCl, pH 7.4, 1%, v/v Nonidet P-40, 10 mM NaF, 1 mM vanadate, 10 μg/ml of aprotinin, 10 μg/ml of leupeptin) and centrifuged for 10 m at 14000 rpm. The supernatant was further centrifuged at 43,000 x g for 30 m [316]. The resulting supernatant was then used as cytoplasmic fraction and the resuspended pellet as membrane fraction. Protein concentrations were determined using Lowry's assay to allow for equal gel loading and at least 15 μg total protein per fractions were used for Western blot analysis.

PKCε Immunoprecipitation and Enzyme Activity Assay: Cells were washed twice with PBS, and lysed in modified RIPA buffer (100 mM Tris·HCl, pH 7.4, 1%, v/v, Nonidet-P40 10 mM NaF, 1 mM vanadate, 10 μg/ml of aprotinin, 10 μg/ml of leupeptin). Insoluble material was removed by centrifugation and protein concentrations determined using the Bio-Rad DC protein assay. Equal amounts of protein were precleared with protein A-Sepharose and then incubated with monoclonal PKCε antibody for 2 h at 4 °C. The immune complexes were isolated with Protein A-Sepharose, washed and eluted. Equal amounts of immunocomplex were then subjected to PKCε kinase assay, as described previously [317] In brief, the assay was carried out by

coincubating 20 µl of immunoprecipitated PKCε with 50 µM ATP, 5 µg of phosphatidylserine, 40 µM PKCε substrate peptide (a preferred substrate of PKCε, Upstate Biotechnology, Lake Placid, NY), 0.2 µl of [^{32}P]ATP (Perkin Elmer Life and Analytical Sciences, Boston, MA) in a final volume of 50 µl. The reaction was allowed to proceed at 30°C for 10 min. An aliquot of the reaction mixture was then spotted on p81 paper, washed in 5% acetic acid, and counted in the scintillation counter.

Western Blot: Equal amounts of cytoplasmic and membrane fractions were separated by SDS–PAGE and transferred to nitrocellulose membranes. Membranes were blocked in TBST (Tris buffered saline, 0.1% Tween 20), 5% non-fat dry milk for 30 min, followed by incubation in primary antibody over night (mouse PKCε antibody, Santa Cruz; rabbit β-actin, BD Cell Signaling; rabbit phosphoMLC(18/19) Cell Signaling). Membranes were washed in TBST prior to incubation for 1 h with horseradish peroxidase-conjugated secondary antibodies. Membranes were washed and developed using enhanced chemiluminescence substrate (Pierce Biotechnology, Rockford, IL). The protein level of PKCε in each sample was normalized to the level of β-actin.

Isolated Perfuse Rat Lung: Male Sprague-Dawley rats (300-350g) were anesthetized i.p. with 0.8 ml pentobarbital (Nembutal, sodium solution, 50 mg/ ml). Following a tracheotomy rat lungs were ventilated (model 683, Harvard Apparatus, Holliston, MA) with humidified normoxic (20% O_2, 5% CO_2, 75% N_2) or humidified hypoxic (1.5% O_2, 5% CO_2, 75% N_2) air at 48 breaths/min, 2 cm positive end-expiratory pressure (PEEP) and with tidal volumes between 2.5-3 ml based on body weight. A thoracotomy was performed to expose heart and lungs, and 100 µl heparin (Abraxis Pharmaceutical Products, Schaumburg, IL) was injected in the right ventricle.

After cannulating the pulmonary artery and left atrium, flow was increased to 12 ml/min. Initial blood containing perfusate was discarded, and replaced with recirculating clean perfusate. The perfusion buffer was warmed Krebs-Henseleit buffer supplemented with 4% Ficoll, 3.1 μM meclofenamate and 2.8 mM $CaCl_2$ (pH 7.38). The pH was continuously monitored and adjusted by bubbling with 5% CO_2. Pressure was continuously monitored during pulmonary perfusion and recorded at constant flow (PowerLab, ADInstruments, Inc., Colorado Springs, CO). The preparation was allowed to equilibrate for 15 min followed by priming with 150 ng angiotensin II via bolus injection. The IPL was then exposed to three successive 5 min episodes of alveolar hypoxia separated by 10 min recovery. Ro-31-8220 was added to the perfusate (final concentration 2 μM) and after further perfusion with inhibitor for 10 min, the IPL was exposed to 2 successive 5 min hypoxic periods.

Cell contraction assay: RPMEC and SPAEC were seeded on 35 mm collagen coated glass bottom dishes (MatTek Corporation, Ashland, MA) and imaged in a closed, thermo-controlled (37ºC) stage insert (Tokai-Hit, Tokyo, Japan). Images were obtained using a Nikon TE2000E inverted microscope equipped with a 40X oil immersion objective (Nikon, CFI PlanFluor, NA 1.3) and Q-Imaging Retiga EXI camera (Burnaby, BC, Canada). MetaMetamorph (Molecular Devices, Downingtown, PA) was used to collect and analyze data and to drive the microscope. After collection of baseline images, cells were exposed to an anoxic gas mixture (5% CO_2, 95% N_2) that was shown to acutely reduce oxygen tension to13 ± 2 mmHg, as measured using a Clarke electrode. Contractile events due to changes in oxygen tension were determined by changes in cell surface area [301]. PKCε was inhibited pharmacologically in RPMECs by addition of Ro-31-8220 (1 μM) to the culture media 30 min prior to hypoxic stimulation. SPAECs were

infected with dominant negative PKCε using a replication deficient herpes simplex viral vector [314] 24 h prior to imaging.

Statistical Analysis: Results are given as mean ±SD. Data were analyzed using a one-way analysis of variance for multiple comparisons with post-hoc Tukey tests for pairwise comparisons. Significance was set at $P < 0.05$.

RESULTS

Inhibition of PKCε attenuates hypoxia-induced contraction of isolated pulmonary endothelial cells. We previously reported that: a) S-nitrosation of zinc sulfur clusters is an important component of NO signaling; and b) the heavy metal-binding protein, metallothionein (MT) is a critical link between NO and intracellular zinc homeostasis [318-319]. We further showed that zinc thiolate signaling is a component of the effects of acute hypoxia mediated NO biosynthesis and that this pathway contributes to constriction in pulmonary endothelium [301]. Likely participants in such signaling include PKC isoforms that are known to be tightly regulated by zinc and participate in HPV (i.e. PKCε). We examined a potential role of PKCε in mediating hypoxia-dependent contractile behavior at the level of the single cell using high resolution differential interference contract (DIC) imaging of changes in cell surface area in live rat pulmonary microvascular endothelial cells (RPMEC) and sheep pulmonary artery endothelial cells (SPAEC). A role for PKCε in mediating hypoxia-induced endothelial cell contraction was initially investigated using the PKC inhibitor Ro-31-8220 which has been shown to inhibit PKCε with an IC_{50} of 0.024 μM. Cellular contraction was assessed using measurement of cell surface area [301]. Figure 1A shows a representative field of cells at baseline (A, D), during hypoxia (at 30

min, B, E) and following the recovery period (30 min, C, F). The hypoxia induced decreases in surface area were significantly attenuated in the presence of the PKCε inhibitor, Ro 31-8220 (from 16 ± 7% to 4.5 ± 6% with Ro-31-8220, $P < 0.005$, Figure 1B). Due to concerns regarding the use of pharmacological inhibitors to individually target specific isoforms of PKC, we also adopted a dominant negative approach to study the role of PKCε in modulating hypoxia-induced endothelial cell contraction. SPAEC were infected with a GFP-tagged herpes simplex virus encoding dominant negative PKCε (Figure 2A) 24 hrs prior to hypoxic exposure. The infection efficiency was extremely low in the RPMEC, and thus, for these studies, they were replaced with SPAEC which have been shown to: 1) increase NO production when exposed to acute hypoxia [301]; 2) increase intracellular labile zinc in response to NO [315, 319]; and 3) contract in response to hypoxic exposure (Figure 2). We compared hypoxia-induced contractile responses between cells expressing the dominant negative PKCε construct (green) with uninfected cells within the same experiment. The 17.0 ± 5.5% decrease in area in the uninfected cells was significantly greater than the contraction observed in cells expressing PKCεDN (0.2 ± 7.0%, $P = 0.012$, Figure 2B). These data suggest that PKCε serves as one effector molecule mediating hypoxia-induced constriction in the pulmonary microvasculature.

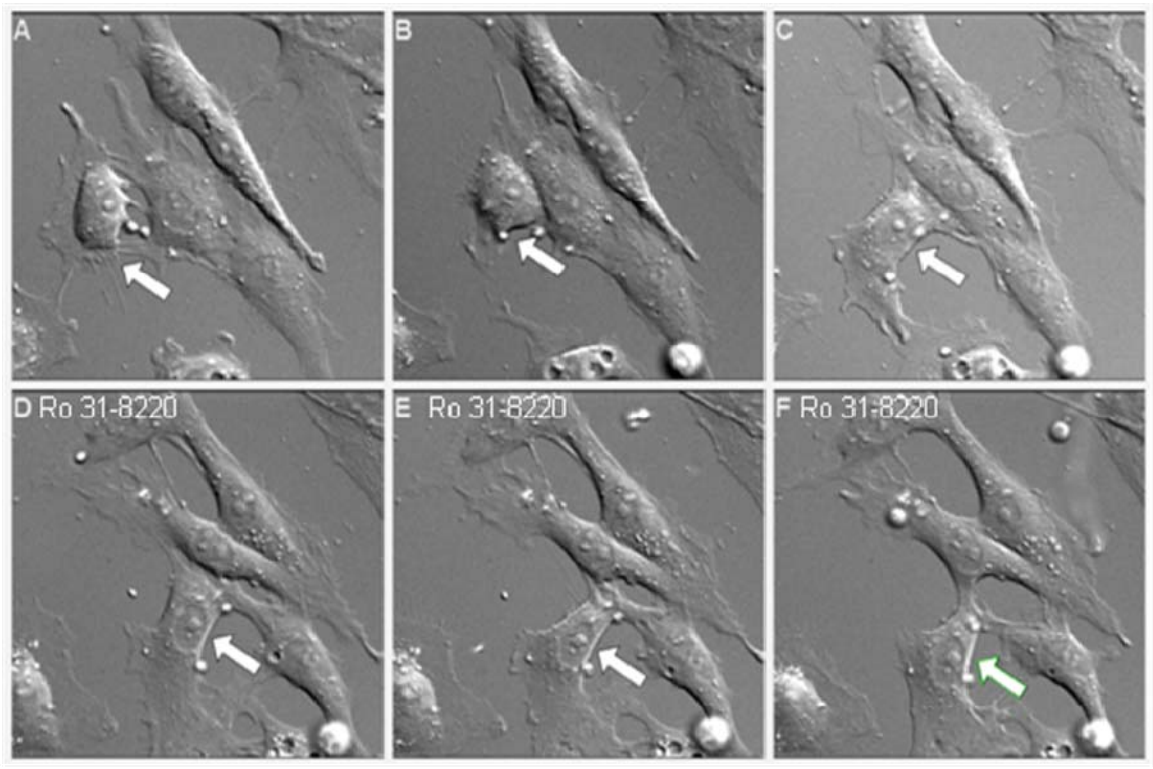

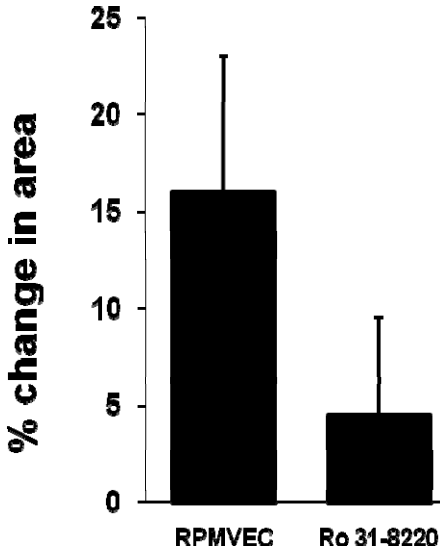

Figure 21.PKC inhibition attenuates hypoxia induced contraction in rat pulmonary microvascular endothelial cells (RPMEC).

The images show the same representative field of cells at baseline (A, D), during hypoxia (at 30 min, B, E) and following the recovery period (30 min, C, F). The hypoxia-induced contraction shown in panels A-C was

significantly attenuated in the presence of the PKCε inhibitor, Ro-31-8220 (1 μM, panels D-F). The mean data for 6 separate experiments (with 3-5 cells per experiment) is shown in the bar chart ($P < 0.05$).

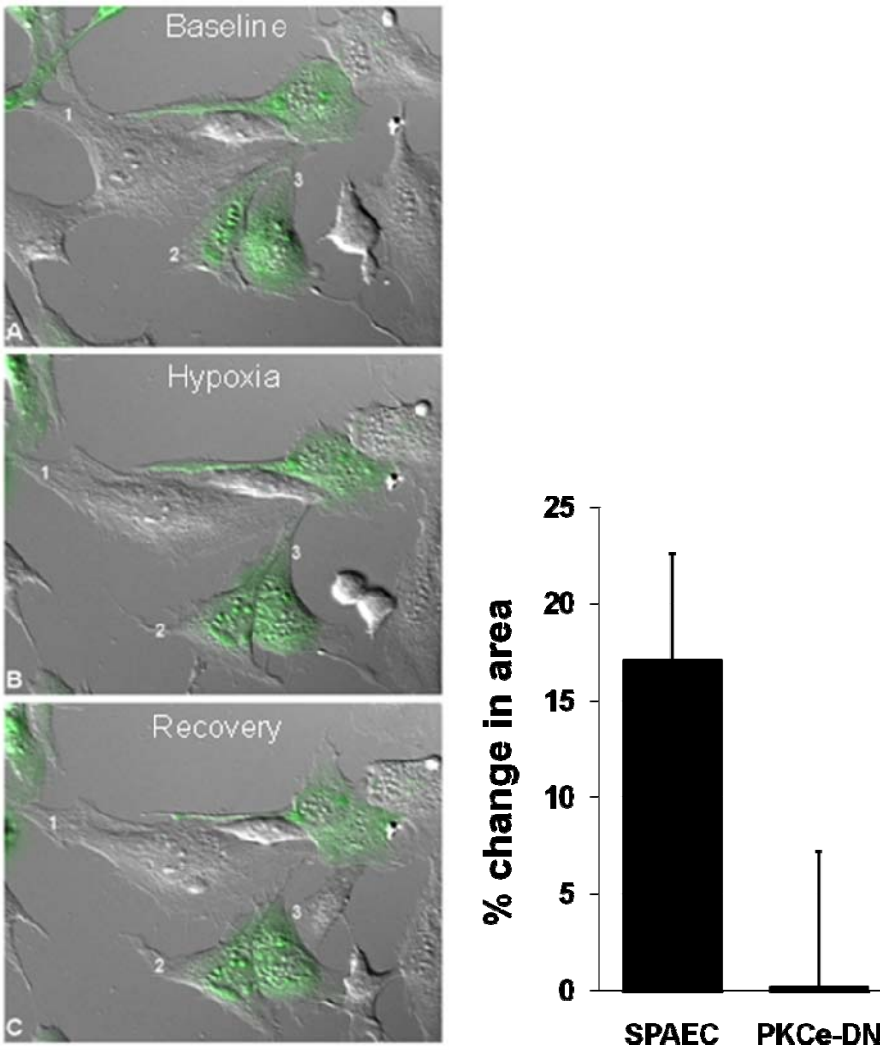

Figure 22. Dominant negative PKCε attenuates hypoxia induced contraction of sheep pulmonary artery endothelial cells (SPAEC)

The images show a representative field of cells at baseline (A), during hypoxia (at 30 min, B) and following the normoxic recovery period (30 min, C). The contractile responses of cells expressing the GFP-tagged PKCεDN construct (green) were compared to cells that were not infected. In the example shown, the uninfected cell (cell 1) shows 10% decrease in area as compared to cells expressing PKCεDN (cells 2 and 3). The mean data for 4 separate experiments (with 2-6 cells per group per experiment) are shown in the bar chart ($P < 0.05$).

Pharmacologic inhibition of PKC attenuates hypoxic pulmonary vasoconstriction (HPV) in the isolated perfused rat lung. We have reported previously that hypoxic vasoconstriction is blunted in IPL of $MT^{-/-}$ mice and in wild-type mice, or rats, treated with the zinc chelator, *N*,*N*,*N*',*N*'-tetrakis(2-pyridylmethyl)-ethylenediamine (TPEN), revealing a role for zinc in modulating HPV [301]. The data obtained in isolated cells (Figures 1 and 2) suggest that the zinc-sensitive kinase, PKCε, also contributes to hypoxia induced contraction of pulmonary endothelium. Before further delineation of this component of the NO-zinc signaling pathway, we confirmed a role for PKC in mediating hypoxia induced contraction at the level of the intact tissue. Figure 3A shows representative pulmonary artery pressure tracings from isolated and ventilated rat lungs which were perfused *in situ* using constant flow. After a 15 min equilibration period and a stimulatory bolus injection of 150 ng angiotensin II, the lungs were exposed to two rounds of hypoxic ventilation (5% oxygen). Ro-31-8220 (2 μM) was added to the perfusate during normoxia. After a 10 min equilibration period in the presence of the inhibitor, the IPL was exposed to 2 further periods of hypoxia. Inhibition of PKCε with Ro-31-8220 blunted hypoxia-induced increases in pulmonary perfusion pressure by 56.9 ± 20.0 % (Figure 3B, $P = 0.018$). While decreased HPV has also been observed in PKCε null mice [313], this response was attributed to adaptive effects of gene knockout and increased expression of Kv3.1 channel expression in pulmonary vascular smooth muscle, rather than a direct result of specific PKCε deletion. Our present data obtained using Ro-31-8220, are in agreement with previous reports showing that pharmacologic PKC inhibition (i.e phloretin) in rats, dogs, and rabbits blunts HPV [308, 320]. One advantage of using pharmacologic inhibitors to reveal a role for PKCε in mediating pulmonary vascular contraction is that such acute exposures (< 1 hour) would not be expected to alter expression patterns of hypoxia-sensitive ion channels.

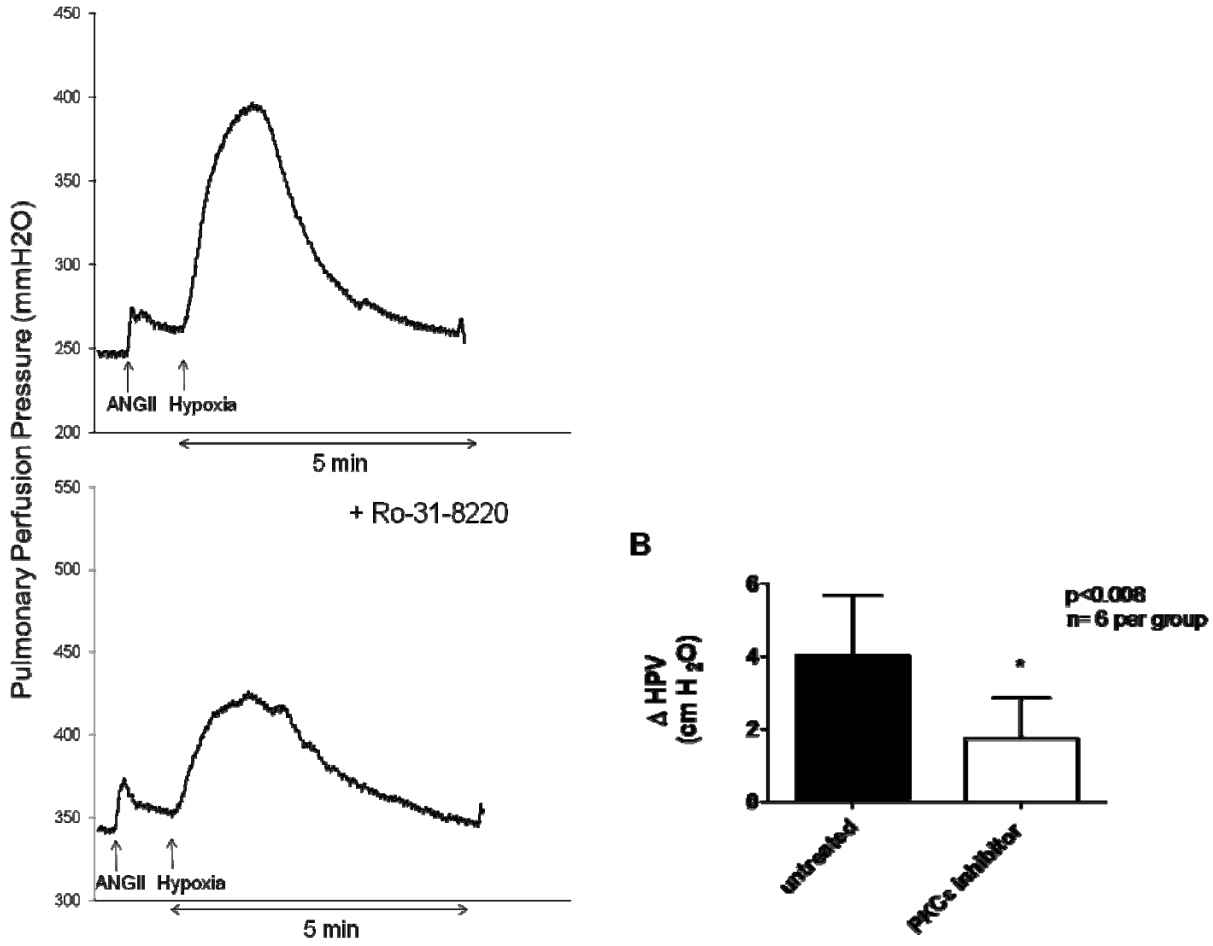

Figure 23. Pharmacological inhibition of PKC blunts hypoxic pulmonary vasoconstriction in the isolated perfused lung (IPL)

Representative pulmonary artery pressure tracings from the same rat showing the HPV response to hypoxia in the absence (A), and presence of Ro-31-8220 (B). PKC inhibition significantly blunted HPV (P <0.01, n=6).

Acute hypoxia induces zinc and nitric oxide (NO)-dependent increases in PKCε enzyme activity in pulmonary endothelium. We have previously shown that acute hypoxia induces an NO-mediated increase in FluoZin-3 detectable zinc in isolated pulmonary endothelial cells as well as in the isolated perfused lung [301]. We now hypothesize that hypoxia-induced zinc release can modulate contractile events in pulmonary endothelium via modulation of PKCε activity. PMA has been shown to activate PKC enzyme activity and cause physical translocation of the

enzyme from the cytosol to the membrane fraction in cells [312, 321]. We used cell fractionation via ultracentrifugation followed by Western blot analysis to confirm that PMA induced PKCε protein translocation between the membrane and cytosolic fractions in primary pulmonary artery endothelial cells isolated from rat (RPAEC, Figure 4A). When RPAEC were exposed to acute hypoxia (1.5% for 15, 30, 60 min) we observed a time-dependent decrease in PKCε protein levels in the cytosolic fraction ($P<0.05$, Figure 4B) and a corresponding increase in the appearance of the protein in the membrane fraction ($P<0.05$, Figure 4C). These hypoxia induced effects were reversed by addition of the zinc specific chelator TPEN (10 μM) (Figure 4B, $P<0.001$). Similar changes in PKCε localization were achieved by addition of exogenous zinc to the media during normoxia (Figure 4C,D, $P < 0.05$). Furthermore, exogenous zinc (10 μM) was shown to be associated with increases ($P < 0.05$) in PKCε enzyme activity which were reversed by addition of TPEN (10 μM) (Figure 5). Exposure of RPAEC to acute hypoxia was also associated with time-dependent increases in PKCε enzyme activity (Figure 5) that were reversed by the addition of the NOS inhibitor, L-Name (1mM, $P < 0.05$), or the zinc specific chelator TPEN (10 μM, $P < 0.001$). Collectively, these data suggest that the effects of hypoxic exposure on PKCε enzyme function in isolated pulmonary endothelial cells are regulated by NO-mediated changes in zinc homeostasis.

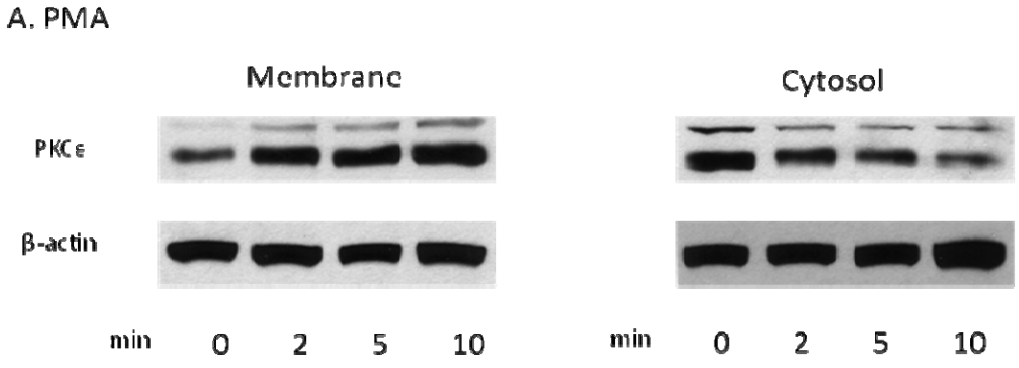

Fig. continued below

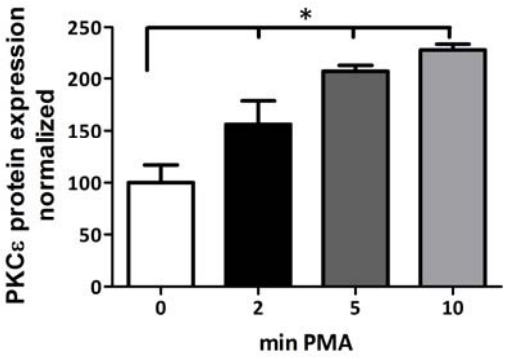

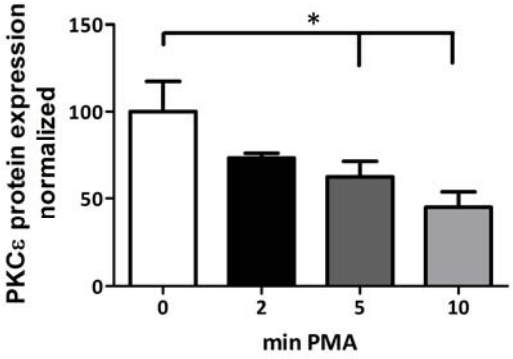

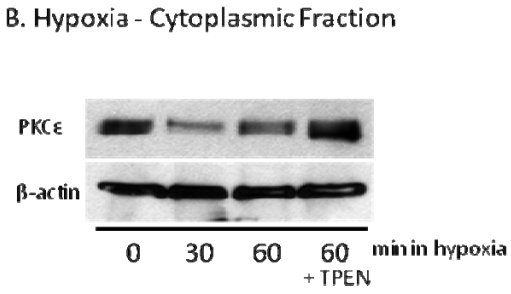

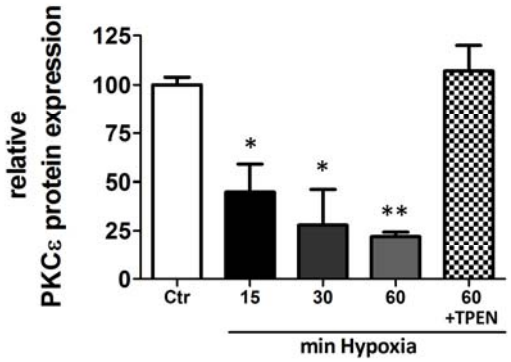

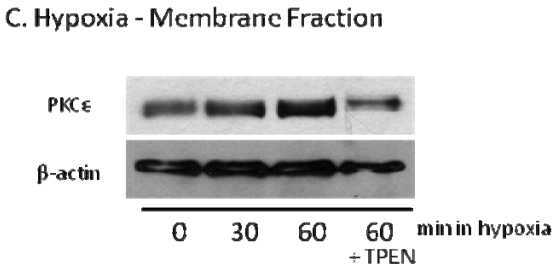

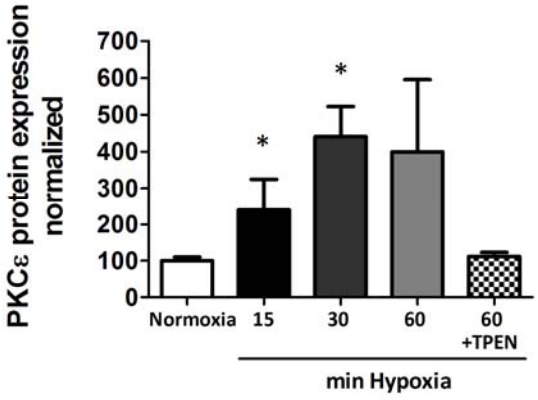

Fig. continued below

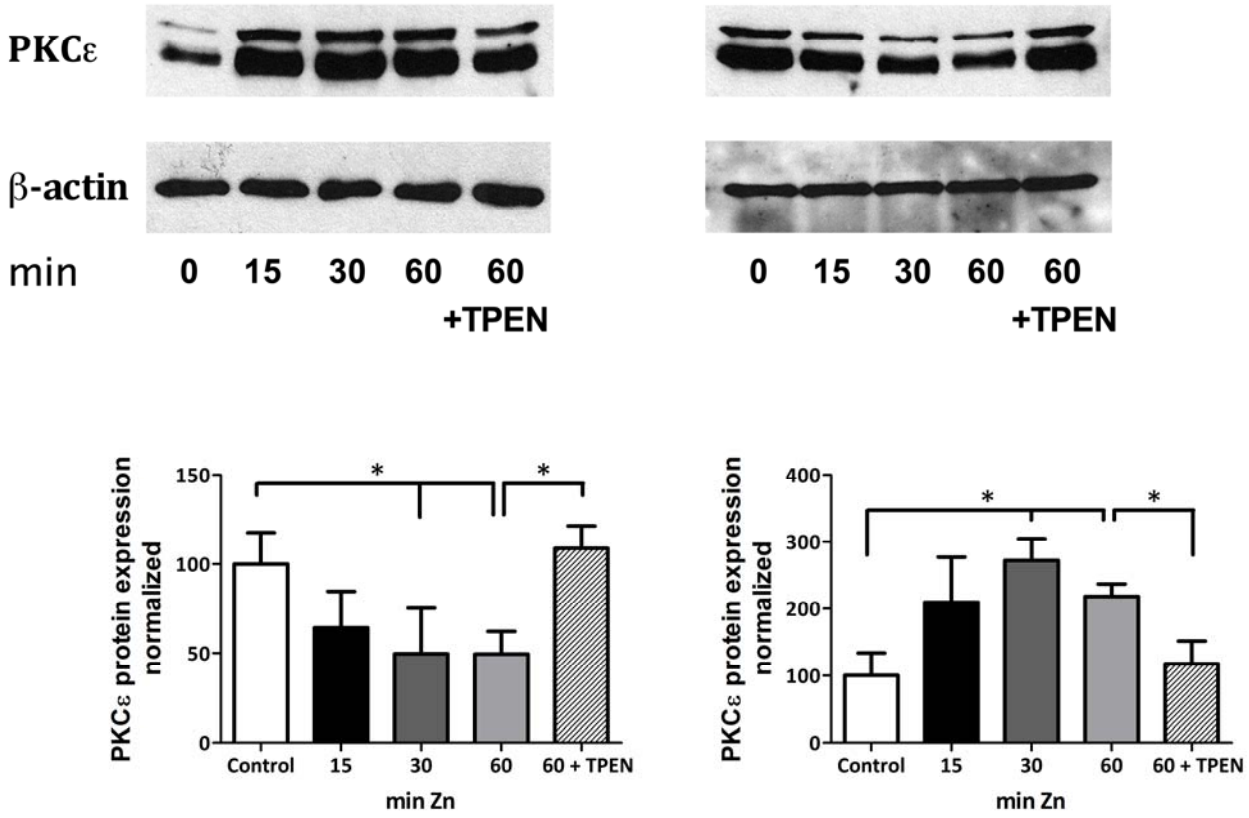

Figure 24. PKCε translocates from the cytosol to the membrane fraction in response to PMA, hypoxia, and zinc

RPAEC were incubated for 10 min with PMAand membrane and cytosolic fractions separated by ultracentrifugation followed by Western blot analysis against PKCε. Quantification of the intensity of bands showed a loss of PKCε protein in the cytoplasm and an increase in the membrane fraction following PMA treatment (A). Pulmonary endothelial cells were exposed to hypoxia (60 min) followed by fractionation and Western blot analysis against PKCε. Quantification of the intensity of bands showed a significant loss of PKCε protein in the cytoplasm (B), and increased accumulation in the membrane fraction in response to hypoxia (C). These changes were reversed by the addition of 10 μM TPEN. Treatment with exogenous zinc also resulted in a significant loss of PKCε protein in the cytoplasm and accumulation in the membrane fraction (D) which was reversed by TPEN (10 μM). For all blots intensity values were normalized by dividing each lane to the β-actin intensity value. Each Western is a representative blot and each graph is the result of at least 3 independent experiments (* $P < 0.05$, ** $P < 0.001$).

Exogenous zinc induces phosphorylation of the myosin regulatory light chain (MLC) at Thr18/Ser19. Force generation requires extensive remodeling of the actin cytoskeleton. As is the case in smooth muscle cells, changes in contractile force are accomplished *via* the regulation of the level of phosphorylation of the regulatory myosin light chain (MLC) [322]. We used immunoblotting to show that exogenous zinc (10 μM) can itself induce Thr18/Ser19 phosphorylation in isolated pulmonary endothelial cells (Figure 6). The zinc-induced phosphorylation of MLC was decreased almost to baseline by either zinc chelation (TPEN, 25 μM) or by PKC inhibition with Ro-31-8220. TPEN and Ro-31-8220 in combination reduced the phosphorylation event below baseline levels. In combination, these data suggest that PKC is one of the key signaling molecules transducing the effects of zinc on cellular contraction in pulmonary endothelium.

A. ZINC

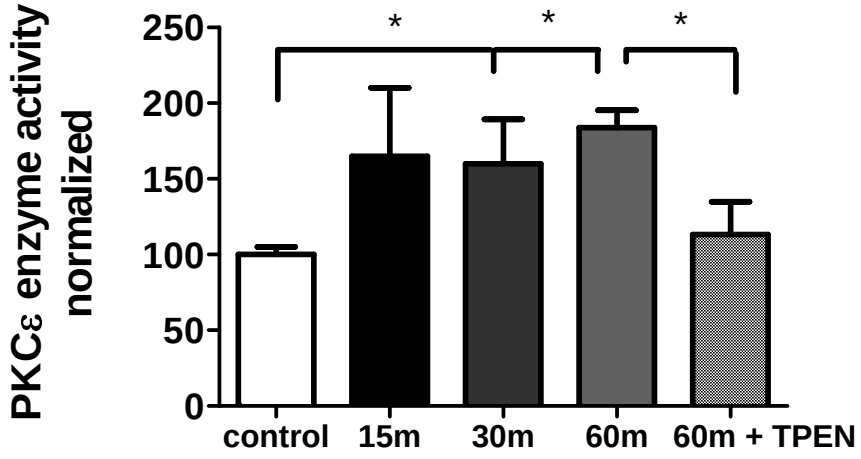

B. HYPOXIA

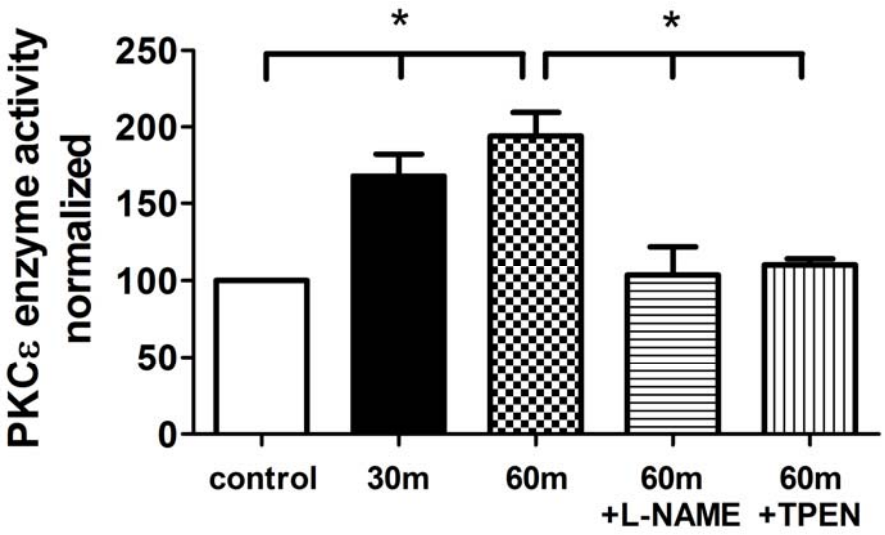

Figure 25. Hypoxia increases PKCε activity in rat pulmonary artery endothelial cells (RPAECs) in a NO and zinc dependent manner

Zinc-induced increases in PKCε activity (A) were reversed by TPEN (10 μM). The graph is the result of 3 independent experiments ($p<0.05$). Enzyme activity observed in normoxic cells was increased significantly by exposure to acute hypoxia (B). The changes were reversed by the competitive NOS inhibitor L-Name (1 mM) or the zinc-specific chelator, TPEN (10 μM). The graph is the result of 3 independent experiments ($p<0.05$).

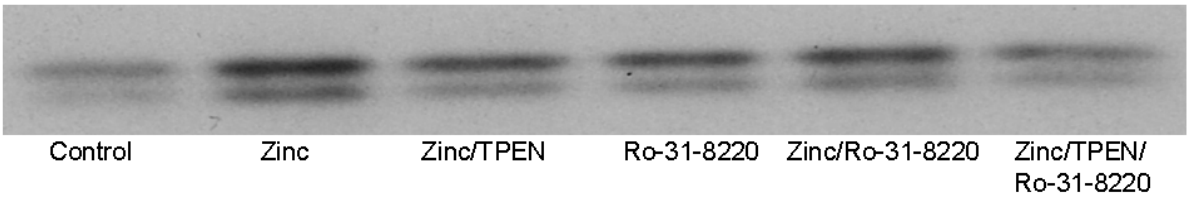

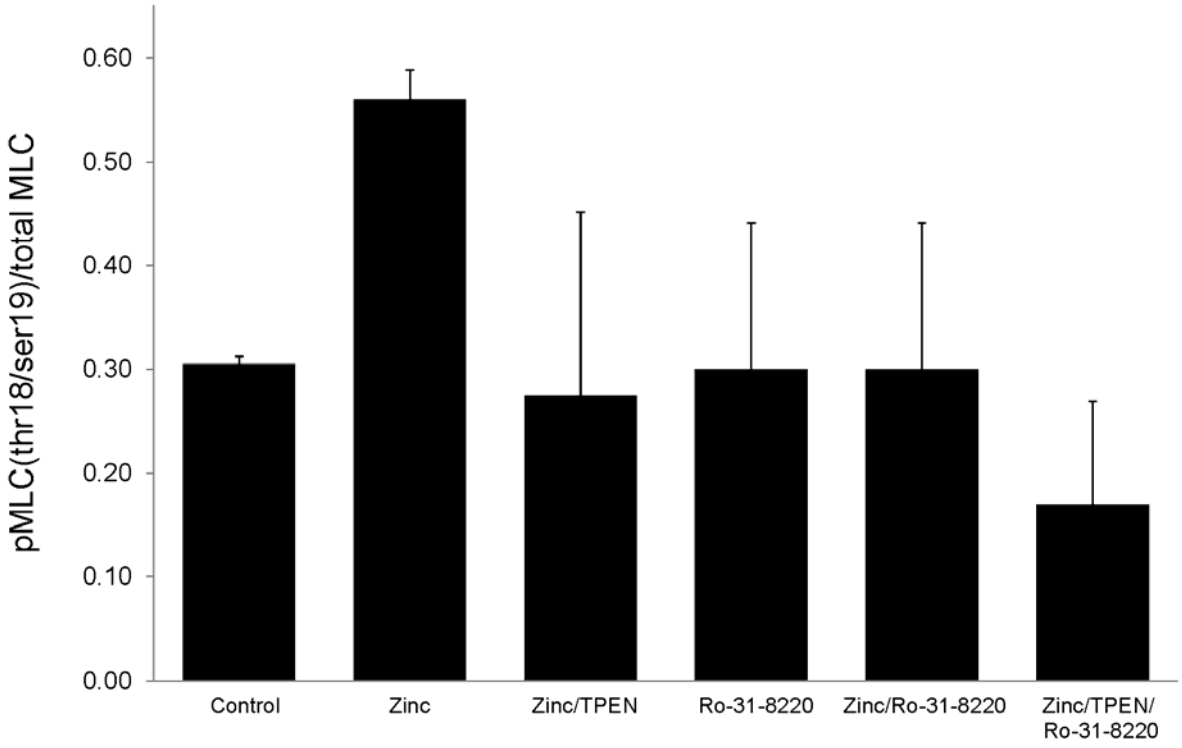

Figure 26. Exogenous zinc (10 μM) increases Thr18/Ser19 phosphorylation in rat pulmonary artery endothelial cells (RPAECs).

The zinc-induced phosphorylation of MLC was decreased almost to baseline by either zinc chelation (TPEN, 25 μM) or by PKC inhibition with Ro-31-8220. TPEN and Ro-31-8220 in combination reduced the phosphorylation event below baseline levels.

Discussion

We demonstrated that: 1) PKCε inhibition blunted hypoxia-induced contraction of isolated pulmonary endothelial cells, and attenuated HPV in the isolated perfused lung; 2) hypoxic exposure induced translocation of PKCε from the cytosolic to the membrane fraction, accompanied by NO- and zinc-dependent increases in PKCε activity, in primary cultures of pulmonary endothelial cells; and 3) under normoxic conditions, exogenous zinc caused increases in PKCε activity and resulted in PKC-dependent phosphorylation of myosin light chain, an

important signaling element mediating contractile activity in a number of cell types. Collectively, these data implicate PKCε as one target molecule regulating the effects of nitric oxide released zinc on contraction of pulmonary endothelium.

PKC activators, including mimicks of the natural ligand diacyglycerol (i.e. phorbol myristae acetate (PMA)) stimulate contraction, and potentiate HPV [308]; whereas PKC inhibitors decrease HPV[308, 320, 323]. However, investigating the involvement of PKCε in HPV is complicated by the lack of specificity of the pharmacological inhibitors and activators of individual PKC isoforms. Ro-31-8220 has an IC_{50} of 0.024 μM for PKCε, however at high concentrations it can also inhibit PKCα, PKCβII and PKCγ. The difficulties in using such inhibitors are further demonstrated by observations that Ro-31-8220 has been shown to be able to activate c-Jun expression and inhibit mitogen-activated protein kinase (MAP kinase) phosphatase-1 expression [324-325]. While it is possible that multiple isoforms of PKC contribute to the contraction of the pulmonary vasculature, and we cannot eliminate the possibility that these play a role in modulating the response to hypoxia observed in the IPL, the observation that the dominant negative approach to specifically inhibit PKCε also significantly attenuated the hypoxia-induced contraction of isolated cells confirmed the importance of the PKCε isoform in mediating contraction of pulmonary endothelium.

The specificity of the proposed PKCε pathway in mediating hypoxia induced contraction in the pulmonary vasculature is not known. We have previously shown that both hypoxia-induced changes in labile zinc and hypoxia-induced endothelial cell contraction [301] were unique to cells derived from lung in that aortic endothelium did not exhibit these responses to low PO_2. However, we do not anticipate that the tissue specificity of HPV is conferred by activation of PKCε in that PKC has been shown to be an important signaling molecule mediating contractile

responses in both the systemic and pulmonary circulation [307, 323]. The importance of PKC signal transduction pathways in the modulation of myogenic reactivity is well established [309]. Purported mechanisms include depolarization-induced voltage gated calcium channel activation, Ca^{2+} sensitization, and/or myosin light chain phosphatase inhibition[326-328].

Intracellular zinc concentrations are known to influence PKC activity and processing [304-306]. We recently observed that zinc contributed to tBH-induced necrosis, in part, via a PKC-dependent pathway, providing one potential link between zinc and PKC in pulmonary endothelium[329-330]. The diacylglycerol (DAG)-binding sites of PKC have been mapped to two pairs of Zn fingers in the regulatory domain. Each finger contains six cysteines that fold to form a structure that coordinates 2 Zn atoms [331-332]. While oxidative stress is thought to activate PKC by modifying zinc thiolate clusters of the regulatory domain of the NH_2 terminus, relieving autoinhibition and facilitating cofactor independent PKC activation [331], it has been suggested that changes in intracellular zinc affect PKC activity by targeting the enzyme's C1 domain which contains cysteine rich finger like motifs that bind zinc [304].

NO donors have been shown to induce activation, translocation, and nitration of PKCε in cardiac myocytes [330]. In fact, both eNOS and iNOS proteins are associated with PKCε in the heart [312], though data obtained in PKCe -/- mice suggest a role for PKCε in the regulation of eNOS expression during chronic hypoxic exposure rather than in the direct regulation of enzymatic activity [313]. The TPEN sensitivity of both PKC activation and MLC phosphorylation suggest that zinc is required for the hypoxia-induced regulation of pulmonary endothelial cell contraction.

It has been reported that increased production of reactive oxygen species (ROS) during hypoxia contributes to HPV [333-334]; and there is accumulating evidence that increases in ROS,

particularly superoxide, can activate PKCε in pulmonary smooth muscle [335-336]. In our hands, the hypoxia-induced changes we observed in PKCε activity were both L-NAME and TPEN sensitive arguing for a role for NO-induced changes in labile zinc in mediating enzyme function. Indeed, our data show that zinc itself can induce contraction (data not shown), PKCε activation as well as PKCε-dependent phosphorylation of MLC in pulmonary artery endothelial cells.

Endothelial cells contain all the molecular machinery required to generate contractile force via the actomyosin motor. Endothelial cell contraction is initiated by phosphorylation of the 20 kDa regulatory myosin light chain (MLC) at ser19/thr18 [337]. MLC phosphorylation is dependent upon a balance between the activities of calcium/calmodulin dependent MLC kinase (MLCK) and myosin light chain phosphatase (MLCP). Our data shows that the zinc induced phosphorylation event is significantly attenuated by PKC inhibition. One potential pathway by which PKC could indirectly cause increases in MLC20 phosphorylation is via inhibition of MLCP [328, 338]. Regulation of MLCP has been shown to involve the PKC substrate, CPI-17; a potent inhibitor of the phosphatase [339-341]. The PKC-CPI-17 pathway has been reported to be involved in the regulation of MLC phosphorylation, reorganization of microfilaments and focal adhesions, and histamine-induced barrier dysfunction in pulmonary endothelium [316].

Summary. Our data suggest a role for PKC in mediating the downstream effects of hypoxia-induced changes in intracellular zinc homeostasis to produce contraction of pulmonary endothelium. While data obtained using dominant negative approaches directly implicate the involvement of PKCε, we cannot eliminate the possibility that other isoforms of PKC also contribute to HPV and/or the generation of contractile force in isolated pulmonary endothelial cells.

BIBLIOGRAPHY

1. Carlson CB, Lawler J, Mosher DF. Structures of thrombospondins. Cell Mol Life Sci 2008;65:672-86.
2. Baenziger NL, Brodie GN, Majerus PW. Isolation and properties of a thrombin-sensitive protein of human platelets. J Biol Chem 1972;247:2723-31.
3. Hagen I, Olsen T, Solum NO. Studies on subcellular fractions of human platelets by the lactoperoxidase-iodination technique. Biochim Biophys Acta 1976;455:214-25.
4. Baenziger NL, Brodie GN, Majerus PW. A thrombin-sensitive protein of human platelet membranes. Proc Natl Acad Sci U S A 1971;68:240-3.
5. Liu A, Mosher DF, Murphy-Ullrich JE, Goldblum SE. The counteradhesive proteins, thrombospondin 1 and SPARC/osteonectin, open the tyrosine phosphorylation-responsive paracellular pathway in pulmonary vascular endothelia. Microvasc Res 2009;77:13-20.
6. Carlson CB, Bernstein DA, Annis DS, et al. Structure of the calcium-rich signature domain of human thrombospondin-2. Nat Struct Mol Biol 2005;12:910-4.
7. Tan K, Duquette M, Liu JH, et al. The structures of the thrombospondin-1 N-terminal domain and its complex with a synthetic pentameric heparin. Structure 2006;14:33-42.
8. McLaren KM. Immunohistochemical localisation of thrombospondin in human megakaryocytes and platelets. J Clin Pathol 1983;36:197-9.
9. McPherson J, Sage H, Bornstein P. Isolation and characterization of a glycoprotein secreted by aortic endothelial cells in culture. Apparent identity with platelet thrombospondin. J Biol Chem 1981;256:11330-6.
10. Mosher DF, Doyle MJ, Jaffe EA. Synthesis and secretion of thrombospondin by cultured human endothelial cells. J Cell Biol 1982;93:343-8.
11. Frazier WA. Thrombospondin: a modular adhesive glycoprotein of platelets and nucleated cells. J Cell Biol 1987;105:625-32.
12. Isenberg JS, Hyodo F, Matsumoto K, et al. Thrombospondin-1 limits ischemic tissue survival by inhibiting nitric oxide-mediated vascular smooth muscle relaxation. Blood 2007;109:1945-52.
13. Isenberg JS, Martin-Manso G, Maxhimer JB, Roberts DD. Regulation of nitric oxide signalling by thrombospondin 1: implications for anti-angiogenic therapies. Nat Rev Cancer 2009;9:182-94.
14. Isenberg JS, Qin Y, Maxhimer JB, et al. Thrombospondin-1 and CD47 regulate blood pressure and cardiac responses to vasoactive stress. Matrix Biol 2009;28:110-9.

15. Isenberg JS, Ridnour LA, Dimitry J, Frazier WA, Wink DA, Roberts DD. CD47 is necessary for inhibition of nitric oxide-stimulated vascular cell responses by thrombospondin-1. J Biol Chem 2006;281:26069-80.
16. Isenberg JS, Ridnour LA, Perruccio EM, Espey MG, Wink DA, Roberts DD. Thrombospondin-1 inhibits endothelial cell responses to nitric oxide in a cGMP-dependent manner. Proc Natl Acad Sci U S A 2005;102:13141-6.
17. Isenberg JS, Romeo MJ, Yu C, et al. Thrombospondin-1 stimulates platelet aggregation by blocking the antithrombotic activity of nitric oxide/cGMP signaling. Blood 2008;111:613-23.
18. Isenberg JS, Shiva S, Gladwin M. Thrombospondin-1-CD47 blockade and exogenous nitrite enhance ischemic tissue survival, blood flow and angiogenesis via coupled NO-cGMP pathway activation. Nitric Oxide 2009;21:52-62.
19. Isenberg JS, Wink DA, Roberts DD. Thrombospondin-1 antagonizes nitric oxide-stimulated vascular smooth muscle cell responses. Cardiovasc Res 2006;71:785-93.
20. Silverstein RL, Febbraio M. CD36, a scavenger receptor involved in immunity, metabolism, angiogenesis, and behavior. Sci Signal 2009;2:re3.
21. Gerrard JM, Phillips DR, Rao GH, et al. Biochemical studies of two patients with the gray platelet syndrome. Selective deficiency of platelet alpha granules. J Clin Invest 1980;66:102-9.
22. Chung J, Gao AG, Frazier WA. Thrombspondin acts via integrin-associated protein to activate the platelet integrin alphaIIbbeta3. J Biol Chem 1997;272:14740-6.
23. Chung J, Wang XQ, Lindberg FP, Frazier WA. Thrombospondin-1 acts via IAP/CD47 to synergize with collagen in alpha2beta1-mediated platelet activation. Blood 1999;94:642-8.
24. Dorahy DJ, Thorne RF, Fecondo JV, Burns GF. Stimulation of platelet activation and aggregation by a carboxyl-terminal peptide from thrombospondin binding to the integrin-associated protein receptor. J Biol Chem 1997;272:1323-30.
25. Wang XQ, Lindberg FP, Frazier WA. Integrin-associated protein stimulates alpha2beta1-dependent chemotaxis via Gi-mediated inhibition of adenylate cyclase and extracellular-regulated kinases. J Cell Biol 1999;147:389-400.
26. Lamy L, Foussat A, Brown EJ, Bornstein P, Ticchioni M, Bernard A. Interactions between CD47 and thrombospondin reduce inflammation. J Immunol 2007;178:5930-9.
27. Lindberg FP, Gresham HD, Schwarz E, Brown EJ. Molecular cloning of integrin-associated protein: an immunoglobulin family member with multiple membrane-spanning domains implicated in alpha v beta 3-dependent ligand binding. J Cell Biol 1993;123:485-96.
28. Giancotti FG, Ruoslahti E. Integrin signaling. Science 1999;285:1028-32.
29. Schwartz MA, Baron V. Interactions between mitogenic stimuli, or, a thousand and one connections. Curr Opin Cell Biol 1999;11:197-202.
30. Wang XQ, Frazier WA. The thrombospondin receptor CD47 (IAP) modulates and associates with alpha2 beta1 integrin in vascular smooth muscle cells. Mol Biol Cell 1998;9:865-74.
31. Brown EJ, Frazier WA. Integrin-associated protein (CD47) and its ligands. Trends Cell Biol 2001;11:130-5.
32. Kosfeld MD, Frazier WA. Identification of active peptide sequences in the carboxyl-terminal cell binding domain of human thrombospondin-1. J Biol Chem 1992;267:16230-6.
33. Jiang P, Lagenaur CF, Narayanan V. Integrin-associated protein is a ligand for the P84 neural adhesion molecule. J Biol Chem 1999;274:559-62.

34. Fujioka Y, Matozaki T, Noguchi T, et al. A novel membrane glycoprotein, SHPS-1, that binds the SH2-domain-containing protein tyrosine phosphatase SHP-2 in response to mitogens and cell adhesion. Mol Cell Biol 1996;16:6887-99.
35. Neel BG, Gu H, Pao L. The 'Shp'ing news: SH2 domain-containing tyrosine phosphatases in cell signaling. Trends Biochem Sci 2003;28:284-93.
36. Timms JF, Swanson KD, Marie-Cardine A, et al. SHPS-1 is a scaffold for assembling distinct adhesion-regulated multi-protein complexes in macrophages. Curr Biol 1999;9:927-30.
37. Hatherley D, Harlos K, Dunlop DC, Stuart DI, Barclay AN. The structure of the macrophage signal regulatory protein alpha (SIRPalpha) inhibitory receptor reveals a binding face reminiscent of that used by T cell receptors. J Biol Chem 2007;282:14567-75.
38. Nakaishi A, Hirose M, Yoshimura M, et al. Structural insight into the specific interaction between murine SHPS-1/SIRP alpha and its ligand CD47. J Mol Biol 2008;375:650-60.
39. Ohnishi H, Kaneko Y, Okazawa H, et al. Differential localization of Src homology 2 domain-containing protein tyrosine phosphatase substrate-1 and CD47 and its molecular mechanisms in cultured hippocampal neurons. J Neurosci 2005;25:2702-11.
40. Oldenborg PA. Role of CD47 in erythroid cells and in autoimmunity. Leuk Lymphoma 2004;45:1319-27.
41. Lindberg FP, Bullard DC, Caver TE, Gresham HD, Beaudet AL, Brown EJ. Decreased resistance to bacterial infection and granulocyte defects in IAP-deficient mice. Science 1996;274:795-8.
42. Manna PP, Dimitry J, Oldenborg PA, Frazier WA. CD47 augments Fas/CD95-mediated apoptosis. J Biol Chem 2005;280:29637-44.
43. Koshimizu H, Araki T, Takai S, et al. Expression of CD47/integrin-associated protein induces death of cultured cerebral cortical neurons. J Neurochem 2002;82:249-57.
44. Blystone SD, Lindberg FP, LaFlamme SE, Brown EJ. Integrin beta 3 cytoplasmic tail is necessary and sufficient for regulation of alpha 5 beta 1 phagocytosis by alpha v beta 3 and integrin-associated protein. J Cell Biol 1995;130:745-54.
45. Porter JC, Hogg N. Integrins take partners: cross-talk between integrins and other membrane receptors. Trends Cell Biol 1998;8:390-6.
46. Landry Y, Niederhoffer N, Sick E, Gies JP. Heptahelical and other G-protein-coupled receptors (GPCRs) signaling. Curr Med Chem 2006;13:51-63.
47. Malinski T, Taha Z. Nitric oxide release from a single cell measured in situ by a porphyrinic-based microsensor. Nature 1992;358:676-8.
48. Furchgott RF, Zawadzki JV. The obligatory role of endothelial cells in the relaxation of arterial smooth muscle by acetylcholine. Nature 1980;288:373-6.
49. Hobbs AJ. Soluble guanylate cyclase: the forgotten sibling. Trends Pharmacol Sci 1997;18:484-91.
50. Friebe A, Koesling D. The function of NO-sensitive guanylyl cyclase: what we can learn from genetic mouse models. Nitric Oxide 2009;21:149-56.
51. Evgenov OV, Pacher P, Schmidt PM, Hasko G, Schmidt HH, Stasch JP. NO-independent stimulators and activators of soluble guanylate cyclase: discovery and therapeutic potential. Nat Rev Drug Discov 2006;5:755-68.
52. Hathaway DR, March KL, Lash JA, Adam LP, Wilensky RL. Vascular smooth muscle. A review of the molecular basis of contractility. Circulation 1991;83:382-90.
53. Ignarro LJ. Signal transduction mechanisms involving nitric oxide. Biochem Pharmacol 1991;41:485-90.

54. Waldman SA, Murad F. Cyclic GMP synthesis and function. Pharmacol Rev 1987;39:163-96.
55. Boolell M, Allen MJ, Ballard SA, et al. Sildenafil: an orally active type 5 cyclic GMP-specific phosphodiesterase inhibitor for the treatment of penile erectile dysfunction. Int J Impot Res 1996;8:47-52.
56. Lucas KA, Pitari GM, Kazerounian S, et al. Guanylyl cyclases and signaling by cyclic GMP. Pharmacol Rev 2000;52:375-414.
57. Conti M. Phosphodiesterases and cyclic nucleotide signaling in endocrine cells. Mol Endocrinol 2000;14:1317-27.
58. Rubbo H, Darley-Usmar V, Freeman BA. Nitric oxide regulation of tissue free radical injury. Chem Res Toxicol 1996;9:809-20.
59. Beckman JS, Koppenol WH. Nitric oxide, superoxide, and peroxynitrite: the good, the bad, and ugly. Am J Physiol 1996;271:C1424-37.
60. Clempus RE, Griendling KK. Reactive oxygen species signaling in vascular smooth muscle cells. Cardiovasc Res 2006;71:216-25.
61. Ferder L, Inserra F, Martinez-Maldonado M. Inflammation and the metabolic syndrome: role of angiotensin II and oxidative stress. Curr Hypertens Rep 2006;8:191-8.
62. Inoguchi T, Nawata H. NAD(P)H oxidase activation: a potential target mechanism for diabetic vascular complications, progressive beta-cell dysfunction and metabolic syndrome. Curr Drug Targets 2005;6:495-501.
63. Rabelink TJ, Luscher TF. Endothelial nitric oxide synthase: host defense enzyme of the endothelium? Arterioscler Thromb Vasc Biol 2006;26:267-71.
64. Dinerman JL, Lowenstein CJ, Snyder SH. Molecular mechanisms of nitric oxide regulation. Potential relevance to cardiovascular disease. Circ Res 1993;73:217-22.
65. Kerwin JF, Jr., Lancaster JR, Jr., Feldman PL. Nitric oxide: a new paradigm for second messengers. J Med Chem 1995;38:4343-62.
66. Moncada S, Palmer RM, Higgs EA. Nitric oxide: physiology, pathophysiology, and pharmacology. Pharmacol Rev 1991;43:109-42.
67. Lundberg JO, Weitzberg E, Gladwin MT. The nitrate-nitrite-nitric oxide pathway in physiology and therapeutics. Nat Rev Drug Discov 2008;7:156-67.
68. Zweier JL, Wang P, Samouilov A, Kuppusamy P. Enzyme-independent formation of nitric oxide in biological tissues. Nat Med 1995;1:804-9.
69. de F, Sanchez de Miguel L, Farre J, et al. Expression of an endothelial-type nitric oxide synthase isoform in human neutrophils: modification by tumor necrosis factor-alpha and during acute myocardial infarction. J Am Coll Cardiol 2001;37:800-7.
70. Kleinbongard P, Schulz R, Rassaf T, et al. Red blood cells express a functional endothelial nitric oxide synthase. Blood 2006;107:2943-51.
71. Lowenstein CJ, Michel T. What's in a name? eNOS and anaphylactic shock. J Clin Invest 2006;116:2075-8.
72. Dudzinski DM, Igarashi J, Greif D, Michel T. The regulation and pharmacology of endothelial nitric oxide synthase. Annu Rev Pharmacol Toxicol 2006;46:235-76.
73. Dudzinski DM, Michel T. Life history of eNOS: partners and pathways. Cardiovasc Res 2007;75:247-60.
74. Pollock JS, Forstermann U, Mitchell JA, et al. Purification and characterization of particulate endothelium-derived relaxing factor synthase from cultured and native bovine aortic endothelial cells. Proc Natl Acad Sci U S A 1991;88:10480-4.

75. Arnal JF, Clamens S, Pechet C, et al. Ethinylestradiol does not enhance the expression of nitric oxide synthase in bovine endothelial cells but increases the release of bioactive nitric oxide by inhibiting superoxide anion production. Proc Natl Acad Sci U S A 1996;93:4108-13.
76. Baydoun AR, Emery PW, Pearson JD, Mann GE. Substrate-dependent regulation of intracellular amino acid concentrations in cultured bovine aortic endothelial cells. Biochem Biophys Res Commun 1990;173:940-8.
77. Masters BS, McMillan K, Sheta EA, Nishimura JS, Roman LJ, Martasek P. Neuronal nitric oxide synthase, a modular enzyme formed by convergent evolution: structure studies of a cysteine thiolate-liganded heme protein that hydroxylates L-arginine to produce NO. as a cellular signal. FASEB J 1996;10:552-8.
78. Alderton WK, Cooper CE, Knowles RG. Nitric oxide synthases: structure, function and inhibition. Biochem J 2001;357:593-615.
79. Narhi LO, Fulco AJ. Identification and characterization of two functional domains in cytochrome P-450BM-3, a catalytically self-sufficient monooxygenase induced by barbiturates in Bacillus megaterium. J Biol Chem 1987;262:6683-90.
80. Gorren AC, Mayer B. Tetrahydrobiopterin in nitric oxide synthesis: a novel biological role for pteridines. Curr Drug Metab 2002;3:133-57.
81. Crane BR, Arvai AS, Ghosh DK, et al. Structure of nitric oxide synthase oxygenase dimer with pterin and substrate. Science 1998;279:2121-6.
82. Fischmann TO, Hruza A, Niu XD, et al. Structural characterization of nitric oxide synthase isoforms reveals striking active-site conservation. Nat Struct Biol 1999;6:233-42.
83. Li H, Raman CS, Glaser CB, et al. Crystal structures of zinc-free and -bound heme domain of human inducible nitric-oxide synthase. Implications for dimer stability and comparison with endothelial nitric-oxide synthase. J Biol Chem 1999;274:21276-84.
84. Raman CS, Li H, Martasek P, Kral V, Masters BS, Poulos TL. Crystal structure of constitutive endothelial nitric oxide synthase: a paradigm for pterin function involving a novel metal center. Cell 1998;95:939-50.
85. Griffith OW, Stuehr DJ. Nitric oxide synthases: properties and catalytic mechanism. Annu Rev Physiol 1995;57:707-36.
86. Sessa WC. eNOS at a glance. J Cell Sci 2004;117:2427-9.
87. Sessa WC. Regulation of endothelial derived nitric oxide in health and disease. Mem Inst Oswaldo Cruz 2005;100 Suppl 1:15-8.
88. Brown DA, London E. Structure of detergent-resistant membrane domains: does phase separation occur in biological membranes? Biochem Biophys Res Commun 1997;240:1-7.
89. Shaul PW. Regulation of endothelial nitric oxide synthase: location, location, location. Annu Rev Physiol 2002;64:749-74.
90. Shaul PW, Anderson RG. Role of plasmalemmal caveolae in signal transduction. Am J Physiol 1998;275:L843-51.
91. Shaul PW, Smart EJ, Robinson LJ, et al. Acylation targets emdothelial nitric-oxide synthase to plasmalemmal caveolae. J Biol Chem 1996;271:6518-22.
92. Fujimoto T, Nakade S, Miyawaki A, Mikoshiba K, Ogawa K. Localization of inositol 1,4,5-trisphosphate receptor-like protein in plasmalemmal caveolae. J Cell Biol 1992;119:1507-13.
93. Bauer PM, Fulton D, Boo YC, et al. Compensatory phosphorylation and protein-protein interactions revealed by loss of function and gain of function mutants of multiple serine phosphorylation sites in endothelial nitric-oxide synthase. J Biol Chem 2003;278:14841-9.

94. Chen ZP, Mitchelhill KI, Michell BJ, et al. AMP-activated protein kinase phosphorylation of endothelial NO synthase. FEBS Lett 1999;443:285-9.
95. Dimmeler S, Fleming I, Fisslthaler B, Hermann C, Busse R, Zeiher AM. Activation of nitric oxide synthase in endothelial cells by Akt-dependent phosphorylation. Nature 1999;399:601-5.
96. Fleming I, Fisslthaler B, Dimmeler S, Kemp BE, Busse R. Phosphorylation of Thr(495) regulates Ca(2+)/calmodulin-dependent endothelial nitric oxide synthase activity. Circ Res 2001;88:E68-75.
97. Fulton D, Gratton JP, Sessa WC. Post-translational control of endothelial nitric oxide synthase: why isn't calcium/calmodulin enough? J Pharmacol Exp Ther 2001;299:818-24.
98. Gallis B, Corthals GL, Goodlett DR, et al. Identification of flow-dependent endothelial nitric-oxide synthase phosphorylation sites by mass spectrometry and regulation of phosphorylation and nitric oxide production by the phosphatidylinositol 3-kinase inhibitor LY294002. J Biol Chem 1999;274:30101-8.
99. McCabe TJ, Fulton D, Roman LJ, Sessa WC. Enhanced electron flux and reduced calmodulin dissociation may explain "calcium-independent" eNOS activation by phosphorylation. J Biol Chem 2000;275:6123-8.
100. Michell BJ, Chen Z, Tiganis T, et al. Coordinated control of endothelial nitric-oxide synthase phosphorylation by protein kinase C and the cAMP-dependent protein kinase. J Biol Chem 2001;276:17625-8.
101. Erwin PA, Lin AJ, Golan DE, Michel T. Receptor-regulated dynamic S-nitrosylation of endothelial nitric-oxide synthase in vascular endothelial cells. J Biol Chem 2005;280:19888-94.
102. Erwin PA, Mitchell DA, Sartoretto J, Marletta MA, Michel T. Subcellular targeting and differential S-nitrosylation of endothelial nitric-oxide synthase. J Biol Chem 2006;281:151-7.
103. Ravi K, Brennan LA, Levic S, Ross PA, Black SM. S-nitrosylation of endothelial nitric oxide synthase is associated with monomerization and decreased enzyme activity. Proc Natl Acad Sci U S A 2004;101:2619-24.
104. Hess DT, Matsumoto A, Kim SO, Marshall HE, Stamler JS. Protein S-nitrosylation: purview and parameters. Nat Rev Mol Cell Biol 2005;6:150-66.
105. Drab M, Verkade P, Elger M, et al. Loss of caveolae, vascular dysfunction, and pulmonary defects in caveolin-1 gene-disrupted mice. Science 2001;293:2449-52.
106. Feron O, Balligand JL. Caveolins and the regulation of endothelial nitric oxide synthase in the heart. Cardiovasc Res 2006;69:788-97.
107. Head BP, Insel PA. Do caveolins regulate cells by actions outside of caveolae? Trends Cell Biol 2007;17:51-7.
108. Parat MO, Fox PL. Palmitoylation of caveolin-1 in endothelial cells is post-translational but irreversible. J Biol Chem 2001;276:15776-82.
109. Rothberg KG, Heuser JE, Donzell WC, Ying YS, Glenney JR, Anderson RG. Caveolin, a protein component of caveolae membrane coats. Cell 1992;68:673-82.
110. Arthur HM, Ure J, Smith AJ, et al. Endoglin, an ancillary TGFbeta receptor, is required for extraembryonic angiogenesis and plays a key role in heart development. Dev Biol 2000;217:42-53.
111. Jerkic M, Rivas-Elena JV, Prieto M, et al. Endoglin regulates nitric oxide-dependent vasodilatation. FASEB J 2004;18:609-11.

112. Sorensen LK, Brooke BS, Li DY, Urness LD. Loss of distinct arterial and venous boundaries in mice lacking endoglin, a vascular-specific TGFbeta coreceptor. Dev Biol 2003;261:235-50.
113. Toporsian M, Gros R, Kabir MG, et al. A role for endoglin in coupling eNOS activity and regulating vascular tone revealed in hereditary hemorrhagic telangiectasia. Circ Res 2005;96:684-92.
114. Fontana J, Fulton D, Chen Y, et al. Domain mapping studies reveal that the M domain of hsp90 serves as a molecular scaffold to regulate Akt-dependent phosphorylation of endothelial nitric oxide synthase and NO release. Circ Res 2002;90:866-73.
115. Sato K, Balla J, Otterbein L, et al. Carbon monoxide generated by heme oxygenase-1 suppresses the rejection of mouse-to-rat cardiac transplants. J Immunol 2001;166:4185-94.
116. Takahashi S, Mendelsohn ME. Calmodulin-dependent and -independent activation of endothelial nitric-oxide synthase by heat shock protein 90. J Biol Chem 2003;278:9339-44.
117. Takahashi S, Mendelsohn ME. Synergistic activation of endothelial nitric-oxide synthase (eNOS) by HSP90 and Akt: calcium-independent eNOS activation involves formation of an HSP90-Akt-CaM-bound eNOS complex. J Biol Chem 2003;278:30821-7.
118. Wei Q, Xia Y. Roles of 3-phosphoinositide-dependent kinase 1 in the regulation of endothelial nitric-oxide synthase phosphorylation and function by heat shock protein 90. J Biol Chem 2005;280:18081-6.
119. Martinez-Ruiz A, Villanueva L, Gonzalez de Orduna C, et al. S-nitrosylation of Hsp90 promotes the inhibition of its ATPase and endothelial nitric oxide synthase regulatory activities. Proc Natl Acad Sci U S A 2005;102:8525-30.
120. Li H, Wallerath T, Forstermann U. Physiological mechanisms regulating the expression of endothelial-type NO synthase. Nitric Oxide 2002;7:132-47.
121. Marsden PA, Heng HH, Scherer SW, et al. Structure and chromosomal localization of the human constitutive endothelial nitric oxide synthase gene. J Biol Chem 1993;268:17478-88.
122. Venema RC, Nishida K, Alexander RW, Harrison DG, Murphy TJ. Organization of the bovine gene encoding the endothelial nitric oxide synthase. Biochim Biophys Acta 1994;1218:413-20.
123. Balligand JL, Feron O, Dessy C. eNOS activation by physical forces: from short-term regulation of contraction to chronic remodeling of cardiovascular tissues. Physiol Rev 2009;89:481-534.
124. Brouet A, Sonveaux P, Dessy C, Balligand JL, Feron O. Hsp90 ensures the transition from the early Ca2+-dependent to the late phosphorylation-dependent activation of the endothelial nitric-oxide synthase in vascular endothelial growth factor-exposed endothelial cells. J Biol Chem 2001;276:32663-9.
125. Busse R, Mulsch A. Induction of nitric oxide synthase by cytokines in vascular smooth muscle cells. FEBS Lett 1990;275:87-90.
126. Gelinas DS, Bernatchez PN, Rollin S, Bazan NG, Sirois MG. Immediate and delayed VEGF-mediated NO synthesis in endothelial cells: role of PI3K, PKC and PLC pathways. Br J Pharmacol 2002;137:1021-30.
127. Gerber HP, McMurtrey A, Kowalski J, et al. Vascular endothelial growth factor regulates endothelial cell survival through the phosphatidylinositol 3'-kinase/Akt signal transduction pathway. Requirement for Flk-1/KDR activation. J Biol Chem 1998;273:30336-43.
128. Thakker GD, Hajjar DP, Muller WA, Rosengart TK. The role of phosphatidylinositol 3-kinase in vascular endothelial growth factor signaling. J Biol Chem 1999;274:10002-7.

129. Michel T, Vanhoutte PM. Cellular signaling and NO production. Pflugers Arch 2010.
130. Galligan JJ. Focus on: "G protein-dependent activation of smooth muscle eNOS via natriuretic peptide clearance receptor". Am J Physiol 1998;275:C1407-8.
131. Phelan MW, Faller DV. Hypoxia decreases constitutive nitric oxide synthase transcript and protein in cultured endothelial cells. J Cell Physiol 1996;167:469-76.
132. Shaul PW, North AJ, Brannon TS, et al. Prolonged in vivo hypoxia enhances nitric oxide synthase type I and type III gene expression in adult rat lung. Am J Respir Cell Mol Biol 1995;13:167-74.
133. Xue C, Rengasamy A, Le Cras TD, Koberna PA, Dailey GC, Johns RA. Distribution of NOS in normoxic vs. hypoxic rat lung: upregulation of NOS by chronic hypoxia. Am J Physiol 1994;267:L667-78.
134. Perrella MA, Hildebrand FL, Jr., Margulies KB, Burnett JC, Jr. Endothelium-derived relaxing factor in regulation of basal cardiopulmonary and renal function. Am J Physiol 1991;261:R323-8.
135. Rees DD, Palmer RM, Moncada S. Role of endothelium-derived nitric oxide in the regulation of blood pressure. Proc Natl Acad Sci U S A 1989;86:3375-8.
136. Stamler JS, Loh E, Roddy MA, Currie KE, Creager MA. Nitric oxide regulates basal systemic and pulmonary vascular resistance in healthy humans. Circulation 1994;89:2035-40.
137. Vallance P, Collier J, Moncada S. Effects of endothelium-derived nitric oxide on peripheral arteriolar tone in man. Lancet 1989;2:997-1000.
138. Fiscus RR. Molecular mechanisms of endothelium-mediated vasodilation. Semin Thromb Hemost 1988;14 Suppl:12-22.
139. Ignarro LJ. Biological actions and properties of endothelium-derived nitric oxide formed and released from artery and vein. Circ Res 1989;65:1-21.
140. Rubanyi GM, Romero JC, Vanhoutte PM. Flow-induced release of endothelium-derived relaxing factor. Am J Physiol 1986;250:H1145-9.
141. Papini AM. The use of post-translationally modified peptides for detection of biomarkers of immune-mediated diseases. J Pept Sci 2009;15:621-8.
142. MacNaul KL, Hutchinson NI. Differential expression of iNOS and cNOS mRNA in human vascular smooth muscle cells and endothelial cells under normal and inflammatory conditions. Biochem Biophys Res Commun 1993;196:1330-4.
143. Aji W, Ravalli S, Szabolcs M, et al. L-arginine prevents xanthoma development and inhibits atherosclerosis in LDL receptor knockout mice. Circulation 1997;95:430-7.
144. Boger RH, Bode-Boger SM, Brandes RP, et al. Dietary L-arginine reduces the progression of atherosclerosis in cholesterol-fed rabbits: comparison with lovastatin. Circulation 1997;96:1282-90.
145. Forstermann U, Mugge A, Bode SM, Frolich JC. Response of human coronary arteries to aggregating platelets: importance of endothelium-derived relaxing factor and prostanoids. Circ Res 1988;63:306-12.
146. Hattori Y, Hattori S, Wang X, Satoh H, Nakanishi N, Kasai K. Oral administration of tetrahydrobiopterin slows the progression of atherosclerosis in apolipoprotein E-knockout mice. Arterioscler Thromb Vasc Biol 2007;27:865-70.
147. Kojda G, Husgen B, Hacker A, et al. Impairment of endothelium-dependent vasorelaxation in experimental atherosclerosis is dependent on gender. Cardiovasc Res 1998;37:738-47.

148. Otsuji S, Nakajima O, Waku S, et al. Attenuation of acetylcholine-induced vasoconstriction by L-arginine is related to the progression of atherosclerosis. Am Heart J 1995;129:1094-100.
149. Tiefenbacher CP, Bleeke T, Vahl C, Amann K, Vogt A, Kubler W. Endothelial dysfunction of coronary resistance arteries is improved by tetrahydrobiopterin in atherosclerosis. Circulation 2000;102:2172-9.
150. Balakumar P, Chakkarwar VA, Krishan P, Singh M. Vascular endothelial dysfunction: a tug of war in diabetic nephropathy? Biomed Pharmacother 2009;63:171-9.
151. Nakagawa T. A new mouse model resembling human diabetic nephropathy: uncoupling of VEGF with eNOS as a novel pathogenic mechanism. Clin Nephrol 2009;71:103-9.
152. Durante W, Sen AK, Sunahara FA. Impairment of endothelium-dependent relaxation in aortae from spontaneously diabetic rats. Br J Pharmacol 1988;94:463-8.
153. Williams SB, Cusco JA, Roddy MA, Johnstone MT, Creager MA. Impaired nitric oxide-mediated vasodilation in patients with non-insulin-dependent diabetes mellitus. J Am Coll Cardiol 1996;27:567-74.
154. Alp NJ, Mussa S, Khoo J, et al. Tetrahydrobiopterin-dependent preservation of nitric oxide-mediated endothelial function in diabetes by targeted transgenic GTP-cyclohydrolase I overexpression. J Clin Invest 2003;112:725-35.
155. Heitzer T, Brockhoff C, Mayer B, et al. Tetrahydrobiopterin improves endothelium-dependent vasodilation in chronic smokers : evidence for a dysfunctional nitric oxide synthase. Circ Res 2000;86:E36-41.
156. Hong HJ, Hsiao G, Cheng TH, Yen MH. Supplemention with tetrahydrobiopterin suppresses the development of hypertension in spontaneously hypertensive rats. Hypertension 2001;38:1044-8.
157. Huang PL, Huang Z, Mashimo H, et al. Hypertension in mice lacking the gene for endothelial nitric oxide synthase. Nature 1995;377:239-42.
158. Wagenseil JE, Mecham RP. Vascular extracellular matrix and arterial mechanics. Physiol Rev 2009;89:957-89.
159. Berry CL, Looker T, Germain J. The growth and development of the rat aorta. I. Morphological aspects. J Anat 1972;113:1-16.
160. Gerrity RG, Adams EP, Cliff WJ. The aortic tunica media of the developing rat. II. Incorporation by medial cells 3-H-proline into collagen and elastin: autoradiographic and chemical studies. Lab Invest 1975;32:601-9.
161. Wolinsky H, Glagov S. A lamellar unit of aortic medial structure and function in mammals. Circ Res 1967;20:99-111.
162. Burton AC. Relation of structure to function of the tissues of the wall of blood vessels. Physiol Rev 1954;34:619-42.
163. Schulze-Bauer CA, Regitnig P, Holzapfel GA. Mechanics of the human femoral adventitia including the high-pressure response. Am J Physiol Heart Circ Physiol 2002;282:H2427-40.
164. Stenmark KR, Davie N, Frid M, Gerasimovskaya E, Das M. Role of the adventitia in pulmonary vascular remodeling. Physiology (Bethesda) 2006;21:134-45.
165. Hall JE. Integration and regulation of cardiovascular function. Am J Physiol 1999;277:S174-86.
166. Badeer HS. Hemodynamics for medical students. Adv Physiol Educ 2001;25:44-52.

167. Vane JR, Anggard EE, Botting RM. Regulatory functions of the vascular endothelium. N Engl J Med 1990;323:27-36.
168. Feletou M, Vanhoutte PM. EDHF: an update. Clin Sci (Lond) 2009;117:139-55.
169. Feletou M, Vanhoutte PM. Endothelial dysfunction: a multifaceted disorder (The Wiggers Award Lecture). Am J Physiol Heart Circ Physiol 2006;291:H985-1002.
170. Moncada S, Vane JR. Pharmacology and endogenous roles of prostaglandin endoperoxides, thromboxane A2, and prostacyclin. Pharmacol Rev 1978;30:293-331.
171. Chataigneau T, Feletou M, Duhault J, Vanhoutte PM. Epoxyeicosatrienoic acids, potassium channel blockers and endothelium-dependent hyperpolarization in the guinea-pig carotid artery. Br J Pharmacol 1998;123:574-80.
172. Fleming I. Cytochrome P450 epoxygenases as EDHF synthase(s). Pharmacol Res 2004;49:525-33.
173. Miyata N, Roman RJ. Role of 20-hydroxyeicosatetraenoic acid (20-HETE) in vascular system. J Smooth Muscle Res 2005;41:175-93.
174. Cosentino F, Barker JE, Brand MP, et al. Reactive oxygen species mediate endothelium-dependent relaxations in tetrahydrobiopterin-deficient mice. Arterioscler Thromb Vasc Biol 2001;21:496-502.
175. Cosentino F, Katusic ZS. Tetrahydrobiopterin and dysfunction of endothelial nitric oxide synthase in coronary arteries. Circulation 1995;91:139-44.
176. Edwards DH, Li Y, Griffith TM. Hydrogen peroxide potentiates the EDHF phenomenon by promoting endothelial Ca2+ mobilization. Arterioscler Thromb Vasc Biol 2008;28:1774-81.
177. Ellis A, Triggle CR. Endothelium-derived reactive oxygen species: their relationship to endothelium-dependent hyperpolarization and vascular tone. Can J Physiol Pharmacol 2003;81:1013-28.
178. Larsen BT, Bubolz AH, Mendoza SA, Pritchard KA, Jr., Gutterman DD. Bradykinin-induced dilation of human coronary arterioles requires NADPH oxidase-derived reactive oxygen species. Arterioscler Thromb Vasc Biol 2009;29:739-45.
179. Liu Y, Zhao H, Li H, Kalyanaraman B, Nicolosi AC, Gutterman DD. Mitochondrial sources of H2O2 generation play a key role in flow-mediated dilation in human coronary resistance arteries. Circ Res 2003;93:573-80.
180. Shimokawa H, Matoba T. Hydrogen peroxide as an endothelium-derived hyperpolarizing factor. Pharmacol Res 2004;49:543-9.
181. Takaki A, Morikawa K, Murayama Y, et al. Roles of endothelial oxidases in endothelium-derived hyperpolarizing factor responses in mice. J Cardiovasc Pharmacol 2008;52:510-7.
182. Takaki A, Morikawa K, Tsutsui M, et al. Crucial role of nitric oxide synthases system in endothelium-dependent hyperpolarization in mice. J Exp Med 2008;205:2053-63.
183. Wu L, Wang R. Carbon monoxide: endogenous production, physiological functions, and pharmacological applications. Pharmacol Rev 2005;57:585-630.
184. Szabo C. Hydrogen sulphide and its therapeutic potential. Nat Rev Drug Discov 2007;6:917-35.
185. Wang R. Two's company, three's a crowd: can H2S be the third endogenous gaseous transmitter? FASEB J 2002;16:1792-8.
186. Lipez-Miranda V, Herradon E, Martin MI. Vasorelaxation caused by cannabinoids: mechanisms in different vascular beds. Curr Vasc Pharmacol 2008;6:335-46.

187. Humbert M, Morrell NW, Archer SL, et al. Cellular and molecular pathobiology of pulmonary arterial hypertension. J Am Coll Cardiol 2004;43:13S-24S.
188. Mandegar M, Fung YC, Huang W, Remillard CV, Rubin LJ, Yuan JX. Cellular and molecular mechanisms of pulmonary vascular remodeling: role in the development of pulmonary hypertension. Microvasc Res 2004;68:75-103.
189. Michelakis ED. Spatio-temporal diversity of apoptosis within the vascular wall in pulmonary arterial hypertension: heterogeneous BMP signaling may have therapeutic implications. Circ Res 2006;98:172-5.
190. Michelakis ED, Wilkins MR, Rabinovitch M. Emerging concepts and translational priorities in pulmonary arterial hypertension. Circulation 2008;118:1486-95.
191. Voelkel NF, Cool C, Lee SD, Wright L, Geraci MW, Tuder RM. Primary pulmonary hypertension between inflammation and cancer. Chest 1998;114:225S-30S.
192. Welsh DJ, Harnett M, MacLean M, Peacock AJ. Proliferation and signaling in fibroblasts: role of 5-hydroxytryptamine2A receptor and transporter. Am J Respir Crit Care Med 2004;170:252-9.
193. D'Alonzo GE, Barst RJ, Ayres SM, et al. Survival in patients with primary pulmonary hypertension. Results from a national prospective registry. Ann Intern Med 1991;115:343-9.
194. Rubin LJ. Primary pulmonary hypertension. N Engl J Med 1997;336:111-7.
195. Simonneau G, Galie N, Rubin LJ, et al. Clinical classification of pulmonary hypertension. J Am Coll Cardiol 2004;43:5S-12S.
196. Simonneau G, Robbins IM, Beghetti M, et al. Updated clinical classification of pulmonary hypertension. J Am Coll Cardiol 2009;54:S43-54.
197. Morris CR, Kato GJ, Poljakovic M, et al. Dysregulated arginine metabolism, hemolysis-associated pulmonary hypertension, and mortality in sickle cell disease. Jama 2005;294:81-90.
198. Giaid A, Saleh D. Reduced expression of endothelial nitric oxide synthase in the lungs of patients with pulmonary hypertension. N Engl J Med 1995;333:214-21.
199. Giaid A, Saleh D, Yanagisawa M, Forbes RD. Endothelin-1 immunoreactivity and mRNA in the transplanted human heart. Transplantation 1995;59:1308-13.
200. Humbert M, Sitbon O, Simonneau G. Treatment of pulmonary arterial hypertension. N Engl J Med 2004;351:1425-36.
201. Jeffery TK, Morrell NW. Molecular and cellular basis of pulmonary vascular remodeling in pulmonary hypertension. Prog Cardiovasc Dis 2002;45:173-202.
202. Saleh D, Furukawa K, Tsao MS, et al. Elevated expression of endothelin-1 and endothelin-converting enzyme-1 in idiopathic pulmonary fibrosis: possible involvement of proinflammatory cytokines. Am J Respir Cell Mol Biol 1997;16:187-93.
203. Macchia A, Marchioli R, Marfisi R, et al. A meta-analysis of trials of pulmonary hypertension: a clinical condition looking for drugs and research methodology. Am Heart J 2007;153:1037-47.
204. Mandegar M, Remillard CV, Yuan JX. Ion channels in pulmonary arterial hypertension. Prog Cardiovasc Dis 2002;45:81-114.
205. Mandegar M, Yuan JX. Role of K+ channels in pulmonary hypertension. Vascul Pharmacol 2002;38:25-33.
206. Sweeney M, Yuan JX. Hypoxic pulmonary vasoconstriction: role of voltage-gated potassium channels. Respir Res 2000;1:40-8.

207. Wang J, Juhaszova M, Rubin LJ, Yuan XJ. Hypoxia inhibits gene expression of voltage-gated K+ channel alpha subunits in pulmonary artery smooth muscle cells. J Clin Invest 1997;100:2347-53.
208. Yuan XJ, Wang J, Juhaszova M, Gaine SP, Rubin LJ. Attenuated K+ channel gene transcription in primary pulmonary hypertension. Lancet 1998;351:726-7.
209. Badesch DB, Abman SH, Ahearn GS, et al. Medical therapy for pulmonary arterial hypertension: ACCP evidence-based clinical practice guidelines. Chest 2004;126:35S-62S.
210. Hoeper MM, Galie N, Simonneau G, Rubin LJ. New treatments for pulmonary arterial hypertension. Am J Respir Crit Care Med 2002;165:1209-16.
211. Thenappan T, Shah SJ, Rich S, Gomberg-Maitland M. A USA-based registry for pulmonary arterial hypertension: 1982-2006. Eur Respir J 2007;30:1103-10.
212. Butrous G, Ghofrani HA, Grimminger F. Pulmonary vascular disease in the developing world. Circulation 2008;118:1758-66.
213. Dorfmuller P, Perros F, Balabanian K, Humbert M. Inflammation in pulmonary arterial hypertension. Eur Respir J 2003;22:358-63.
214. Palevsky HI, Schloo BL, Pietra GG, et al. Primary pulmonary hypertension. Vascular structure, morphometry, and responsiveness to vasodilator agents. Circulation 1989;80:1207-21.
215. Rubin LJ. Pulmonary arterial hypertension. Proc Am Thorac Soc 2006;3:111-5.
216. Adnot S, Raffestin B, Eddahibi S, Braquet P, Chabrier PE. Loss of endothelium-dependent relaxant activity in the pulmonary circulation of rats exposed to chronic hypoxia. J Clin Invest 1991;87:155-62.
217. Celermajer DS, Cullen S, Deanfield JE. Impairment of endothelium-dependent pulmonary artery relaxation in children with congenital heart disease and abnormal pulmonary hemodynamics. Circulation 1993;87:440-6.
218. Dinh Xuan AT, Higenbottam TW, Clelland C, Pepke-Zaba J, Cremona G, Wallwork J. Impairment of pulmonary endothelium-dependent relaxation in patients with Eisenmenger's syndrome. Br J Pharmacol 1990;99:9-10.
219. Dinh-Xuan AT, Pepke-Zaba J, Butt AY, Cremona G, Higenbottam TW. Impairment of pulmonary-artery endothelium-dependent relaxation in chronic obstructive lung disease is not due to dysfunction of endothelial cell membrane receptors nor to L-arginine deficiency. Br J Pharmacol 1993;109:587-91.
220. Mathew R, Gloster ES, Sundararajan T, Thompson CI, Zeballos GA, Gewitz MH. Role of inhibition of nitric oxide production in monocrotaline-induced pulmonary hypertension. J Appl Physiol 1997;82:1493-8.
221. Mathew R, Zeballos GA, Tun H, Gewitz MH. Role of nitric oxide and endothelin-1 in monocrotaline-induced pulmonary hypertension in rats. Cardiovasc Res 1995;30:739-46.
222. Steinhorn RH, Russell JA, Lakshminrusimha S, Gugino SF, Black SM, Fineman JR. Altered endothelium-dependent relaxations in lambs with high pulmonary blood flow and pulmonary hypertension. Am J Physiol Heart Circ Physiol 2001;280:H311-7.
223. Sperling RT, Creager MA. Nitric oxide and pulmonary hypertension. Coron Artery Dis 1999;10:287-94.
224. Fagan KA, Fouty BW, Tyler RC, et al. The pulmonary circulation of homozygous or heterozygous eNOS-null mice is hyperresponsive to mild hypoxia. J Clin Invest 1999;103:291-9.
225. Han RN, Stewart DJ. Defective lung vascular development in endothelial nitric oxide synthase-deficient mice. Trends Cardiovasc Med 2006;16:29-34.

226. Fulton D, Fontana J, Sowa G, et al. Localization of endothelial nitric-oxide synthase phosphorylated on serine 1179 and nitric oxide in Golgi and plasma membrane defines the existence of two pools of active enzyme. J Biol Chem 2002;277:4277-84.
227. Fulton D, Gratton JP, McCabe TJ, et al. Regulation of endothelium-derived nitric oxide production by the protein kinase Akt. Nature 1999;399:597-601.
228. Kone BC. Protein-protein interactions controlling nitric oxide synthases. Acta Physiol Scand 2000;168:27-31.
229. Michel JB, Feron O, Sase K, Prabhakar P, Michel T. Caveolin versus calmodulin. Counterbalancing allosteric modulators of endothelial nitric oxide synthase. J Biol Chem 1997;272:25907-12.
230. Michel T, Feron O. Nitric oxide synthases: which, where, how, and why? J Clin Invest 1997;100:2146-52.
231. Resta TC, Gonzales RJ, Dail WG, Sanders TC, Walker BR. Selective upregulation of arterial endothelial nitric oxide synthase in pulmonary hypertension. Am J Physiol 1997;272:H806-13.
232. Xue C, Johns RA. Upregulation of nitric oxide synthase correlates temporally with onset of pulmonary vascular remodeling in the hypoxic rat. Hypertension 1996;28:743-53.
233. Murata T, Sato K, Hori M, Ozaki H, Karaki H. Decreased endothelial nitric-oxide synthase (eNOS) activity resulting from abnormal interaction between eNOS and its regulatory proteins in hypoxia-induced pulmonary hypertension. J Biol Chem 2002;277:44085-92.
234. Achcar RO, Demura Y, Rai PR, et al. Loss of caveolin and heme oxygenase expression in severe pulmonary hypertension. Chest 2006;129:696-705.
235. Stenmark KR, Meyrick B, Galie N, Mooi WJ, McMurtry IF. Animal models of pulmonary arterial hypertension: the hope for etiological discovery and pharmacological cure. Am J Physiol-Lung C 2009;297:L1013-L32.
236. Pietra GG, Edwards WD, Kay JM, et al. Histopathology of primary pulmonary hypertension. A qualitative and quantitative study of pulmonary blood vessels from 58 patients in the National Heart, Lung, and Blood Institute, Primary Pulmonary Hypertension Registry. Circulation 1989;80:1198-206.
237. Overbeek MJ, Vonk MC, Boonstra A, et al. Pulmonary arterial hypertension in limited cutaneous systemic sclerosis: a distinctive vasculopathy. Eur Respir J 2009;34:371-9.
238. Tuder RM. Pathology of pulmonary arterial hypertension. Semin Respir Crit Care Med 2009;30:376-85.
239. Bull TM, Coldren CD, Geraci MW, Voelkel NF. Gene expression profiling in pulmonary hypertension. Proc Am Thorac Soc 2007;4:117-20.
240. Tada Y, Laudi S, Harral J, et al. Murine pulmonary response to chronic hypoxia is strain specific. Exp Lung Res 2008;34:313-23.
241. Estrada KD, Chesler NC. Collagen-related gene and protein expression changes in the lung in response to chronic hypoxia. Biomech Model Mechanobiol 2009;8:263-72.
242. Tuchscherer HA, Vanderpool RR, Chesler NC. Pulmonary vascular remodeling in isolated mouse lungs: effects on pulsatile pressure-flow relationships. J Biomech 2007;40:993-1001.
243. Mukhopadhyay S, Xu F, Sehgal PB. Aberrant cytoplasmic sequestration of eNOS in endothelial cells after monocrotaline, hypoxia, and senescence: live-cell caveolar and cytoplasmic NO imaging. Am J Physiol Heart Circ Physiol 2007;292:H1373-89.

244. Wilson DM, Perkins SN, Thomas JA, et al. Effects of elevated serum insulinlike growth factor-II on growth hormone and insulinlike growth factor-I mRNA and secretion. Metabolism 1989;38:57-62.
245. Wilson DW, Segall HJ, Pan LC, Dunston SK. Progressive inflammatory and structural changes in the pulmonary vasculature of monocrotaline-treated rats. Microvasc Res 1989;38:57-80.
246. Meyrick BO, Reid LM. Crotalaria-induced pulmonary hypertension. Uptake of 3H-thymidine by the cells of the pulmonary circulation and alveolar walls. Am J Pathol 1982;106:84-94.
247. Tanaka Y, Schuster DP, Davis EC, Patterson GA, Botney MD. The role of vascular injury and hemodynamics in rat pulmonary artery remodeling. J Clin Invest 1996;98:434-42.
248. Okada K, Tanaka Y, Bernstein M, Zhang W, Patterson GA, Botney MD. Pulmonary hemodynamics modify the rat pulmonary artery response to injury. A neointimal model of pulmonary hypertension. Am J Pathol 1997;151:1019-25.
249. Taraseviciene-Stewart L, Kasahara Y, Alger L, et al. Inhibition of the VEGF receptor 2 combined with chronic hypoxia causes cell death-dependent pulmonary endothelial cell proliferation and severe pulmonary hypertension. FASEB J 2001;15:427-38.
250. Landmesser U, Hornig B, Drexler H. Endothelial function: a critical determinant in atherosclerosis? Circulation 2004;109:II27-33.
251. Sauzeau V, Le Jeune H, Cario-Toumaniantz C, et al. Cyclic GMP-dependent protein kinase signaling pathway inhibits RhoA-induced Ca2+ sensitization of contraction in vascular smooth muscle. J Biol Chem 2000;275:21722-9.
252. Isenberg JS, Frazier WA, Krishna MC, Wink DA, Roberts DD. Enhancing cardiovascular dynamics by inhibition of thrombospondin-1/CD47 signaling. Curr Drug Targets 2008;9:833-41.
253. Kao KJ, Klein PA. A monoclonal antibody-based enzyme-linked immunosorbent assay for quantitation of plasma thrombospondin. Am J Clin Pathol 1986;86:317-23.
254. Tan BK, Syed F, Lewandowski KC, O'Hare JP, Randeva HS. Circadian oscillation of circulating prothrombotic thrombospondin-1: ex vivo and in vivo regulation by insulin. J Thromb Haemost 2008.
255. Figueroa XF, Gonzalez DR, Martinez AD, Duran WN, Boric MP. ACh-induced endothelial NO synthase translocation, NO release and vasodilatation in the hamster microcirculation in vivo. J Physiol 2002;544:883-96.
256. Fulton D, Ruan L, Sood SG, Li C, Zhang Q, Venema RC. Agonist-stimulated endothelial nitric oxide synthase activation and vascular relaxation. Role of eNOS phosphorylation at Tyr83. Circ Res 2008;102:497-504.
257. Kuhlmann CR, Schafer M, Li F, et al. Modulation of endothelial Ca(2+)-activated K(+) channels by oxidized LDL and its contribution to endothelial proliferation. Cardiovasc Res 2003;60:626-34.
258. Miller RC, Schoeffter P, Stoclet JC. Insensitivity of calcium-dependent endothelial stimulation in rat isolated aorta to the calcium entry blocker, flunarizine. Br J Pharmacol 1985;85:481-7.
259. Fleming I, Busse R. Signal transduction of eNOS activation. Cardiovasc Res 1999;43:532-41.
260. Danthuluri NR, Cybulsky MI, Brock TA. ACh-induced calcium transients in primary cultures of rabbit aortic endothelial cells. Am J Physiol 1988;255:H1549-53.

261. Ghigo D, Alessio P, Foco A, et al. Nitric oxide synthesis is impaired in glutathione-depleted human umbilical vein endothelial cells. Am J Physiol 1993;265:C728-32.
262. Suh SH, Vennekens R, Manolopoulos VG, et al. Characterisation of explanted endothelial cells from mouse aorta: electrophysiology and Ca2+ signalling. Pflugers Arch 1999;438:612-20.
263. Gentile MT, Vecchione C, Maffei A, et al. Mechanisms of soluble beta-amyloid impairment of endothelial function. J Biol Chem 2004;279:48135-42.
264. Chatterjee A, Black SM, Catravas JD. Endothelial nitric oxide (NO) and its pathophysiologic regulation. Vascul Pharmacol 2008;49:134-40.
265. Miike T, Shirahase H, Kanda M, Kunishiro K, Kurahashi K. Regional heterogeneity of substance P-induced endothelium-dependent contraction, relaxation, and -independent contraction in rabbit pulmonary arteries. Life Sci 2008;83:810-4.
266. Marin J, Sanchez-Ferrer CF. Role of endothelium-formed nitric oxide on vascular responses. Gen Pharmacol 1990;21:575-87.
267. Volpert OV, Lawler J, Bouck NP. A human fibrosarcoma inhibits systemic angiogenesis and the growth of experimental metastases via thrombospondin-1. Proc Natl Acad Sci U S A 1998;95:6343-8.
268. Bayraktar M, Dundar S, Kirazli S, Teletar F. Platelet factor 4, beta-thromboglobulin and thrombospondin levels in type I diabetes mellitus patients. J Int Med Res 1994;22:90-4.
269. Lutz J, Huwiler KG, Fedczyna T, et al. Increased plasma thrombospondin-1 (TSP-1) levels are associated with the TNF alpha-308A allele in children with juvenile dermatomyositis. Clin Immunol 2002;103:260-3.
270. Macko RF, Gelber AC, Young BA, et al. Increased circulating concentrations of the counteradhesive proteins SPARC and thrombospondin-1 in systemic sclerosis (scleroderma). Relationship to platelet and endothelial cell activation. J Rheumatol 2002;29:2565-70.
271. Browne P, Shalev O, Hebbel RP. The molecular pathobiology of cell membrane iron: the sickle red cell as a model. Free Radic Biol Med 1998;24:1040-8.
272. Cheung DW, Chen G. Calcium activation of hyperpolarization response to acetylcholine in coronary endothelial cells. J Cardiovasc Pharmacol 1992;20 Suppl 12:S120-3.
273. Fukao M, Hattori Y, Kanno M, Sakuma I, Kitabatake A. Sources of Ca2+ in relation to generation of acetylcholine-induced endothelium-dependent hyperpolarization in rat mesenteric artery. Br J Pharmacol 1997;120:1328-34.
274. Moncada S, Higgs EA. Molecular mechanisms and therapeutic strategies related to nitric oxide. FASEB J 1995;9:1319-30.
275. Schwartz MA, Brown EJ, Fazeli B. A 50-kDa integrin-associated protein is required for integrin-regulated calcium entry in endothelial cells. J Biol Chem 1993;268:19931-4.
276. Morgan AJ, Jacob R. Ionomycin enhances Ca2+ influx by stimulating store-regulated cation entry and not by a direct action at the plasma membrane. Biochem J 1994;300 (Pt 3):665-72.
277. Neylon CB, Irvine RF. Thrombin attenuates the stimulatory effect of histamine on Ca2+ entry in confluent human umbilical vein endothelial cell cultures. J Biol Chem 1991;266:4251-6.
278. Jow F, Numann R. Fluid flow modulates calcium entry and activates membrane currents in cultured human aortic endothelial cells. J Membr Biol 1999;171:127-39.
279. Li YS, Haga JH, Chien S. Molecular basis of the effects of shear stress on vascular endothelial cells. J Biomech 2005;38:1949-71.

280. Freyberg MA, Kaiser D, Graf R, Buttenbender J, Friedl P. Proatherogenic flow conditions initiate endothelial apoptosis via thrombospondin-1 and the integrin-associated protein. Biochem Biophys Res Commun 2001;286:141-9.
281. Crews DE, Williams SR. Molecular aspects of blood pressure regulation. Hum Biol 1999;71:475-503.
282. Joyner MJ, Charkoudian N, Wallin BG. A sympathetic view of the sympathetic nervous system and human blood pressure regulation. Exp Physiol 2008;93:715-24.
283. Sakai K, Hirooka Y, Matsuo I, et al. Overexpression of eNOS in NTS causes hypotension and bradycardia in vivo. Hypertension 2000;36:1023-8.
284. Swislocki A, Eason T, Kaysen GA. Oral administration of the nitric oxide biosynthesis inhibitor, N-nitro-L-arginine methyl ester (L-NAME), causes hypertension, but not glucose intolerance or insulin resistance, in rats. Am J Hypertens 1995;8:1009-14.
285. Kosugi T, Heinig M, Nakayama T, et al. Lowering blood pressure blocks mesangiolysis and mesangial nodules, but not tubulointerstitial injury, in diabetic eNOS knockout mice. Am J Pathol 2009;174:1221-9.
286. Liu Z, Zhao Q, Han Q, Gao M, Zhang N. Serum thrombospondin-1 is altered in patients with hemorrhagic fever with renal syndrome. J Med Virol 2008;80:1799-803.
287. Gladwin MT, Sachdev V, Jison ML, et al. Pulmonary hypertension as a risk factor for death in patients with sickle cell disease. N Engl J Med 2004;350:886-95.
288. Khoo JP, Zhao L, Alp NJ, et al. Pivotal role for endothelial tetrahydrobiopterin in pulmonary hypertension. Circulation 2005;111:2126-33.
289. Konduri GG, Ou J, Shi Y, Pritchard KA, Jr. Decreased association of HSP90 impairs endothelial nitric oxide synthase in fetal lambs with persistent pulmonary hypertension. Am J Physiol Heart Circ Physiol 2003;285:H204-11.
290. Lakshminrusimha S, Wiseman D, Black SM, et al. The role of nitric oxide synthase-derived reactive oxygen species in the altered relaxation of pulmonary arteries from lambs with increased pulmonary blood flow. Am J Physiol Heart Circ Physiol 2007;293:H1491-7.
291. Ignarro LJ, Buga GM, Wood KS, Byrns RE, Chaudhuri G. Endothelium-derived relaxing factor produced and released from artery and vein is nitric oxide. Proc Natl Acad Sci U S A 1987;84:9265-9.
292. Palmer RM, Ferrige AG, Moncada S. Nitric oxide release accounts for the biological activity of endothelium-derived relaxing factor. Nature 1987;327:524-6.
293. Garg UC, Hassid A. Nitric oxide-generating vasodilators and 8-bromo-cyclic guanosine monophosphate inhibit mitogenesis and proliferation of cultured rat vascular smooth muscle cells. J Clin Invest 1989;83:1774-7.
294. Ignarro LJ, Buga GM, Wei LH, Bauer PM, Wu G, del Soldato P. Role of the arginine-nitric oxide pathway in the regulation of vascular smooth muscle cell proliferation. Proc Natl Acad Sci U S A 2001;98:4202-8.
295. Cirino G, Fiorucci S, Sessa WC. Endothelial nitric oxide synthase: the Cinderella of inflammation? Trends Pharmacol Sci 2003;24:91-5.
296. Isenberg JS, Hyodo F, Pappan LK, et al. Blocking thrombospondin-1/CD47 signaling alleviates deleterious effects of aging on tissue responses to ischemia. Arterioscler Thromb Vasc Biol 2007;27:2582-8.
297. Isenberg JS, Maxhimer JB, Powers P, Tsokos M, Frazier WA, Roberts DD. Treatment of liver ischemia-reperfusion injury by limiting thrombospondin-1/CD47 signaling. Surgery 2008;144:752-61.

298. Isenberg JS, Pappan LK, Romeo MJ, et al. Blockade of thrombospondin-1-CD47 interactions prevents necrosis of full thickness skin grafts. Ann Surg 2008;247:180-90.
299. Maier KG, Han X, Sadowitz B, Gentile KL, Middleton FA, Gahtan V. Thrombospondin-1: A proatherosclerotic protein augmented by hyperglycemia. J Vasc Surg 2010.
300. Moura R, Tjwa M, Vandervoort P, Van Kerckhoven S, Holvoet P, Hoylaerts MF. Thrombospondin-1 deficiency accelerates atherosclerotic plaque maturation in ApoE-/- mice. Circ Res 2008;103:1181-9.
301. Bernal PJ, Leelavanichkul K, Bauer E, et al. Nitric-oxide-mediated zinc release contributes to hypoxic regulation of pulmonary vascular tone. Circ Res 2008;102:1575-83.
302. Von Euler GL. Observations on the pulmonary arterial blood pressure in the cat. Acta Physiologica Scandinavica 1946;12:19.
303. Ward JP, Aaronson PI. Mechanisms of hypoxic pulmonary vasoconstriction: can anyone be right? Respir Physiol 1999;115:261-71.
304. Chou SS, Clegg MS, Momma TY, et al. Alterations in protein kinase C activity and processing during zinc-deficiency-induced cell death. Biochem J 2004;383:63-71.
305. Csermely P, Szamel M, Resch K, Somogyi J. Zinc can increase the activity of protein kinase C and contributes to its binding to plasma membranes in T lymphocytes. J Biol Chem 1988;263:6487-90.
306. Murakami K, Whiteley MK, Routtenberg A. Regulation of protein kinase C activity by cooperative interaction of Zn2+ and Ca2+. J Biol Chem 1987;262:13902-6.
307. Rasmussen H, Barrett P, Takuwa Y, Apfeldorf W. Calcium in the regulation of aldosterone secretion and vascular smooth muscle contraction. Hypertension 1987;10:I23-6.
308. Orton EC, Raffestin B, McMurtry IF. Protein kinase C influences rat pulmonary vascular reactivity. Am Rev Respir Dis 1990;141:654-8.
309. Davis MJ, Hill MA. Signaling mechanisms underlying the vascular myogenic response. Physiol Rev 1999;79:387-423.
310. Horowitz A, Clement-Chomienne O, Walsh MP, Morgan KG. Epsilon-isoenzyme of protein kinase C induces a Ca(2+)-independent contraction in vascular smooth muscle. Am J Physiol 1996;271:C589-94.
311. Baines CP, Zhang J, Wang GW, et al. Mitochondrial PKCepsilon and MAPK form signaling modules in the murine heart: enhanced mitochondrial PKCepsilon-MAPK interactions and differential MAPK activation in PKCepsilon-induced cardioprotection. Circ Res 2002;90:390-7.
312. Ping P, Takano H, Zhang J, et al. Isoform-selective activation of protein kinase C by nitric oxide in the heart of conscious rabbits: a signaling mechanism for both nitric oxide-induced and ischemia-induced preconditioning. Circ Res 1999;84:587-604.
313. Littler CM, Morris KG, Jr., Fagan KA, McMurtry IF, Messing RO, Dempsey EC. Protein kinase C-epsilon-null mice have decreased hypoxic pulmonary vasoconstriction. Am J Physiol Heart Circ Physiol 2003;284:H1321-31.
314. Srinivasan R, Wolfe D, Goss J, et al. Protein kinase C epsilon contributes to basal and sensitizing responses of TRPV1 to capsaicin in rat dorsal root ganglion neurons. Eur J Neurosci 2008;28:1241-54.
315. St Croix CM, Wasserloos KJ, Dineley KE, Reynolds IJ, Levitan ES, Pitt BR. Nitric oxide-induced changes in intracellular zinc homeostasis are mediated by metallothionein/thionein. Am J Physiol Lung Cell Mol Physiol 2002;282:L185-92.

316. Kolosova IA, Ma SF, Adyshev DM, et al. Role of CPI-17 in the regulation of endothelial cytoskeleton. Am J Physiol Lung Cell Mol Physiol 2004;287:L970-80.
317. Bandyopadhyay G, Standaert ML, Zhao L, et al. Activation of protein kinase C (alpha, beta, and zeta) by insulin in 3T3/L1 cells. Transfection studies suggest a role for PKC-zeta in glucose transport. J Biol Chem 1997;272:2551-8.
318. Pearce LL, Gandley RE, Han W, et al. Role of metallothionein in nitric oxide signaling as revealed by a green fluorescent fusion protein. Proc Natl Acad Sci U S A 2000;97:477-82.
319. St Croix CM, Stitt MS, Leelavanichkul K, Wasserloos KJ, Pitt BR, Watkins SC. Nitric oxide-induced modification of protein thiolate clusters as determined by spectral fluorescence resonance energy transfer in live endothelial cells. Free Radic Biol Med 2004;37:785-92.
320. Barman SA. Potassium channels modulate canine pulmonary vasoreactivity to protein kinase C activation. Am J Physiol 1999;277:L558-65.
321. Takayama M, Ebihara Y, Tani M. Differences in the expression of protein kinase C isoforms and its translocation after stimulation with phorbol ester between young-adult and middle-aged ventricular cardiomyocytes isolated from Fischer 344 rats. Jpn Circ J 2001;65:1071-6.
322. Somlyo AP, Somlyo AV. Ca2+ sensitivity of smooth muscle and nonmuscle myosin II: modulated by G proteins, kinases, and myosin phosphatase. Physiol Rev 2003;83:1325-58.
323. Weissmann N, Voswinckel R, Hardebusch T, et al. Evidence for a role of protein kinase C in hypoxic pulmonary vasoconstriction. Am J Physiol 1999;276:L90-5.
324. Beltman J, McCormick F, Cook SJ. The selective protein kinase C inhibitor, Ro-31-8220, inhibits mitogen-activated protein kinase phosphatase-1 (MKP-1) expression, induces c-Jun expression, and activates Jun N-terminal kinase. J Biol Chem 1996;271:27018-24.
325. Alessi DR, Caudwell FB, Andjelkovic M, Hemmings BA, Cohen P. Molecular basis for the substrate specificity of protein kinase B; comparison with MAPKAP kinase-1 and p70 S6 kinase. FEBS Lett 1996;399:333-8.
326. Yeon DS, Kim JS, Ahn DS, et al. Role of protein kinase C- or RhoA-induced Ca(2+) sensitization in stretch-induced myogenic tone. Cardiovasc Res 2002;53:431-8.
327. Korzick DH, Laughlin MH, Bowles DK. Alterations in PKC signaling underlie enhanced myogenic tone in exercise-trained porcine coronary resistance arteries. J Appl Physiol 2004;96:1425-32.
328. Buus CL, Aalkjaer C, Nilsson H, Juul B, Moller JV, Mulvany MJ. Mechanisms of Ca2+ sensitization of force production by noradrenaline in rat mesenteric small arteries. J Physiol 1998;510 (Pt 2):577-90.
329. Tang ZL, Wasserloos K, St Croix CM, Pitt BR. Role of zinc in pulmonary endothelial cell response to oxidative stress. Am J Physiol Lung Cell Mol Physiol 2001;281:L243-9.
330. Balafanova Z, Bolli R, Zhang J, et al. Nitric oxide (NO) induces nitration of protein kinase Cepsilon (PKCepsilon), facilitating PKCepsilon translocation via enhanced PKCepsilon - RACK2 interactions: a novel mechanism of no-triggered activation of PKCepsilon. J Biol Chem 2002;277:15021-7.
331. Gopalakrishna R, Jaken S. Protein kinase C signaling and oxidative stress. Free Radic Biol Med 2000;28:1349-61.
332. Shindo M, Irie K, Fukuda H, Ohigashi H. Analysis of the non-covalent interaction between metal ions and the cysteine-rich domain of protein kinase C eta by electrospray ionization mass spectrometry. Bioorg Med Chem 2003;11:5075-82.

333. Moudgil R, Michelakis ED, Archer SL. Hypoxic pulmonary vasoconstriction. J Appl Physiol 2005;98:390-403.
334. Waypa GB, Chandel NS, Schumacker PT. Model for hypoxic pulmonary vasoconstriction involving mitochondrial oxygen sensing. Circ Res 2001;88:1259-66.
335. Rathore R, Zheng YM, Li XQ, et al. Mitochondrial ROS-PKCepsilon signaling axis is uniquely involved in hypoxic increase in [Ca2+]i in pulmonary artery smooth muscle cells. Biochem Biophys Res Commun 2006;351:784-90.
336. Rathore R, Zheng YM, Niu CF, et al. Hypoxia activates NADPH oxidase to increase [ROS]i and [Ca2+]i through the mitochondrial ROS-PKCepsilon signaling axis in pulmonary artery smooth muscle cells. Free Radic Biol Med 2008;45:1223-31.
337. Goeckeler ZM, Wysolmerski RB. Myosin light chain kinase-regulated endothelial cell contraction: the relationship between isometric tension, actin polymerization, and myosin phosphorylation. J Cell Biol 1995;130:613-27.
338. Masuo M, Reardon S, Ikebe M, Kitazawa T. A novel mechanism for the Ca(2+)-sensitizing effect of protein kinase C on vascular smooth muscle: inhibition of myosin light chain phosphatase. J Gen Physiol 1994;104:265-86.
339. Eto M, Ohmori T, Suzuki M, Furuya K, Morita F. A novel protein phosphatase-1 inhibitory protein potentiated by protein kinase C. Isolation from porcine aorta media and characterization. J Biochem 1995;118:1104-7.
340. Kitazawa T, Takizawa N, Ikebe M, Eto M. Reconstitution of protein kinase C-induced contractile Ca2+ sensitization in triton X-100-demembranated rabbit arterial smooth muscle. J Physiol 1999;520 Pt 1:139-52.
341. Li L, Eto M, Lee MR, Morita F, Yazawa M, Kitazawa T. Possible involvement of the novel CPI-17 protein in protein kinase C signal transduction of rabbit arterial smooth muscle. J Physiol 1998;508 (Pt 3):871-81.